TENSILE PROPERTIES AND FATIGUE BEHAVIOR OF GEOPOLYMER MATRIX COMPOSITES WITH CARBON FIBER REINFORCEMENT AT ELEVATED TEMPERATURE

THESIS

Steffan M.L. Wilcox, Captain, USAF

AFIT-ENY-MS-18-M-304

DEPARTMENT OF THE AIR FORCE
AIR UNIVERSITY

AIR FORCE INSTITUTE OF TECHNOLOGY

Wright-Patterson Air Force Base, Ohio

AFIT-ENY-MS-18-M-304

TENSILE PROPERTIES AND FATIGUE BEHAVIOR OF GEOPOLYMER MATRIX COMPOSITES WITH CARBON FIBER REINFORCEMENT AT ELEVATED TEMPERATURE

THESIS

Presented to the Faculty

Department of Aeronautics and Astronautics

Graduate School of Engineering and Management

Air Force Institute of Technology

Air University

Air Education and Training Command

In Partial Fulfillment of the Requirements for the

Degree of Master of Science in Materials Science

Steffan M.L. Wilcox, B.S.M.E.

Captain, USAF

March 2018

AFIT-ENY-MS-18-M-304

TENSILE PROPERTIES AND FATIGUE BEHAVIOR OF GEOPOLYMER MATRIX COMPOSITES WITH CARBON FIBER REINFORCEMENT AT ELEVATED TEMPERATURE

Steffan M.L. Wilcox, B.S.M.E
Captain, USAF

Committee Membership:

Dr. Marina Ruggles-Wrenn
Chair

Dr. Thomas Eason
Member

Michael Falugi
Member

Abstract

The tensile stress-strain and tension-tension fatigue of geopolymer matrix composites reinforced with 0/90 carbon fibers was investigated at 23 and 300°C in laboratory air. Geopolymers are inorganic polymeric materials composed of alumina, silica, and alkali metal oxides. Because geopolymers are synthesized as a fluid mixture or particles and liquid, they can be cast into a desired shape, and cured at only slightly elevated temperatures. The relative ease of synthesis and low processing temperatures make geopolymers an attractive choice as a matrix material for composite materials. Geopolymers also offer resistance to heat and oxidizing environments. Currently, geopolymer matrix composites are being considered as possible replacements for ceramic matrix composites and high-temperature polymer matrix composites. In this work composites with two different types of geopolymer matrix were evaluated: (1) composite with a sodium-based geopolymer matrix (NaGP) and (2) composite with a potassium-based geopolymer matrix (KGP). Experimental results revealed a degrading effect of elevated temperature on tensile stress-strain behavior and tensile properties. Tension-tension fatigue tests were conducted at 300°C. Fatigue run-out was set to $2x10^5$ cycles. Fatigue run-out was only achieved at a low maximum stress of 30% UTS. Test specimens were examined before and after testing using an optical microscope. Examinations revealed severe degradation of the geopolymer matrix due to elevated temperature as well as due to mechanical loading. Profuse cracking and comminution of the geopolymer matrix occurred early in all tests. As a result further mechanical response of the

composite was governed by the carbon fibers. The best mechanical performance was obtained for a panel of the KGP-matrix composite. Further development of the KGP-matrix composites can build on the synthesis method used to fabricate this particular panel.

Acknowledgments

Many thanks to my advisor Dr. Marina Ruggles-Wrenn, for the great amount of time and patience she has invested in my academic journey here at AFIT. I particularly thank her for my remedial kindergarten education on integration constants, tensor notation, the Boltzmann Superposition Principle, and Laplace Transforms. Thanks to Mike Falugi (AFRL/RQVS), this research was made possible by arranging the testing material, supporting the research, and being part of the committee. Thanks to Dr. Thomas Eason (AFRL/RQHF) for participating in the thesis committee as well. I thank Dr. Larry Burggraf for expanding my knowledge on chemistry and physics, and revealing some of the mysteries of quantum mechanics just enough to make me feel better about my decision to approach phenomena on a more macro level. I would also like to thank the lab technician team, in particular Mike Ranft, who were always there to help me get the job done.

Steffan M.L. Wilcox

Table of Contents

Page

Abstract ..... **iv**

Acknowledgments ..... **vi**

Table of Contents ..... **vii**

List of Figures ..... **ix**

List of Tables ..... **xiii**

I. Introduction **1**

1.1 Motivation 1

1.2 Problem Statement 3

1.3 Methodology 4

1.4 Summary 5

II. Literature Review **6**

2.1 Composite Basics 6

2.2 Heat Resistance of Composites 8

2.3 Geopolymer Matrix Materials 11

2.4 Reinforcing Carbon Fibers 13

2.5 Carbon Fiber Geopolymer Matrix Composites – Previous Work 13

2.6 Matrix Additives 14

III. Material and Test Specimens **16**

3.1 Research Material 16

3.2 Test Specimen Design and Preparation 20

IV. Experimental Setup and Testing Procedures **23**

4.1 Experimental Equipment 23

4.2 Temperature Calibration 25

4.3 Mechanical Testing Procedures....25
4.3.1 Room Temperature Modulus Measurements....25
4.3.2 Monotonic Tensile Tests....26
4.3.3 Tension-tension Fatigue Tests....26
4.4 Material Characterization....27
V. Results and Discussion....29
5.1 Monotonic Tension at 23°C – Pilot Tests....29
5.2 Room-temperature Modulus Testing....31
5.3 Monotonic Tension at 23°C....36
5.4 Thermal Exposure and Dimpling Effects....41
5.5 Monotonic Tension at 300°C....53
5.6 Tension-Tension Fatigue at 23°C....58
5.7 Tension-Tension Fatigue at 300°C....61
VI. Conclusions and Recommendations....74
Appendix....76
Bibliography....83

List of Figures

Page

Figure 1. Schematic of a unidirectional fiber composite ply. 7

Figure 2. Schematic of a composite with a 0/90 cross-ply plain weave fabric. 8

Figure 3. Schematic of retained Strength/Weight Ratio at Temperature, adapted from [15] 10

Figure 4. An example of a polysialate geopolymer molecular structure, with Na as the alkali metal component [18]..... 12

Figure 5. Panel 5-7-C-1, dark areas correspond to less presence of matrix on the surface. 18

Figure 6. Surfaces of panels 3-14-C-1 (top) and 3-20-C (bottom) 19

Figure 7. Dog bone shaped tensile specimen drawing, dimensions in mm. 20

Figure 8. As-machined specimen from panel 3-20-C. 21

Figure 9. Test specimen with fiberglass tabs, from panel 12-5-C. 21

Figure 10. Contact end of ceramic high-temperature extensometer rods. 24

Figure 11. High-temperature test setup. 24

Figure 12. Tension-Tension Fatigue Test Procedure. 27

Figure 13. Zeiss Discover V12 Stereoscopic optical microscope..... 28

Figure 14. Tensile stress-strain curves obtained at 23°C for specimens from panels 5-9-C and 5-10-C. 30

Figure 15. Reconstructed 5-10-C-1 curve compared with later 5-10-C-2- test. 31

Figure 16. Elastic modulus vs cross-sectional area of Type 1 panels. 34

Figure 17. Elastic modulus vs cross-sectional area of Type 2 panels. 35

Figure 18. Elastic modulus vs thickness per ply of all panels tested. 36

Figure 19. Tensile stress-strain curves obtained at 23°C for specimens 5-9-C-1 and 5-7-C-1-3 of the composite with Type 2 geopolymer matrix. 37

Figure 20. Tensile stress-strain curves obtained at 23°C for the composite with Type 2 geopolymer matrix. 38

Figure 21. Tensile stress-strain curves obtained at 23°C for the composite with Type 1 geopolymer matrix. 39

Figure 22. Specimen 5-7-C-1-3, failed in tension test at 23°C. 41

Figure 23. Strain vs. time curve obtained for specimen 5-9-C-7 during temperature increase from 23 to 300°C under zero load. 42

Figure 24. Strain vs. time behavior observed for geopolymer matrix composite specimens during temperature rise from 23 to 300°C under zero load. Strain behavior is erratic. Strain measurements vary widely even for specimens cut from the same composite panel. 43

Figure 25. Strain vs. time behavior observed for geopolymer matrix composite specimens from panel 3-14-C-1 during temperature rise from 23 to 300°C under zero load. Specimens were not dimpled prior to thermal exposure. 45

Figure 26. 3-14-C-1-2 gage section before thermal exposure (top) and after thermal exposure (bottom). Dimples (dark depressions) can be seen on left and right hand side of frame. 47

Figure 27. Microcracking of matrix on surface of 5-7-C-14 Type 2 geopolymer matrix specimen before thermal exposure (left) and after (right). 47

Figure 28. Strain vs. time behavior observed for composite specimens with geopolymer matrix of Type 1 during second temperature exposure. 49

Figure 29. Strain vs. time behavior observed for composite specimens with geopolymer matrix of Type 2 during second temperature exposure. 50

Figure 30. Cracks on the side of a specimen appear from dimpling and grow from re-dimpling. 52

Figure 31. Tensile stress-strain curve obtained at 300°C for specimen 5-9-C-7 of the composite with Type 2 geopolymer matrix. 53

Figure 32. Schematic depicting straightening of reinforcing fibers with increasing strain. 54

Figure 33. Tensile stress-strain curved obtained at 300°C for specimen 5-9-C-7 and 5-9-C-2 of the composite with Type 2 geopolymer matrix. 55

Figure 34. Tensile stress-strain curved obtained at 300°C for composite panels 5-7-C-1 and 5-7-C-2 with Type 2 geopolymer matrix. 56

Figure 35. Voids in the matrix located at fiber cross-overs on the surface of the composite specimen 5-7-C-2-3 with Type 2 geopolymer matrix. 57

Figure 36. Tensile stress-strain curved obtained at 300°C for composite with Type 1 geopolymer matrix. 57

Figure 37. Stress-strain hysteresis response of composite specimen 3-14-C-2-4 with Type 1 geopolymer matrix in a tension-tension fatigue test performed at 23°C. Due to extensometer slippage, the cycles with an asterisk (*) are separated arbitrarily to show hysteresis curve evolution..... 59

Figure 38. Tensile stress-strain curve obtained for composite specimen 3-14-C-2-4 with Type 1 geopolymer matrix following 210,000 tension-tension fatigue cycles at 23°C. 60

Figure 39. Evolution of stress-strain hysteresis response of specimen 3-14-C-2-1 with Type 1 geopolymer matrix in a tension-tension fatigue test performed at 300°C. 63

Figure 40. Maximum stress vs. cycles to failure (S-N) curves obtained for geopolymer matrix composites in tension-tension fatigue tests at 300°C. 64

Figure 41. Maximum stress vs. cycles to failure (S-N) curves obtained for composites with Type 1 geopolymer matrix in tension-tension fatigue tests at 300°C. There is no trend line for 3-14-C-2 due to only one data point..... 65

Figure 42. Maximum stress vs. cycles to failure (S-N) curves obtained for composites with Type 2 geopolymer matrix in tension-tension fatigue tests at 300°C. Trend line for 5-7-C-1 does not account for the specimen which failed at 50 cycles. 66

Figure 43. Evolution of stress-strain hysteresis response of composite specimen 5-7-C-1-1 with Type 2 geopolymer matrix in a tension-tension fatigue test performed at 300°C..... 67

Figure 44. Evolution of stress-strain hysteresis response of composite specimen 5-7-C-1-6 with Type 2 geopolymer matrix in a tension-tension fatigue test performed at 300°C..... 68

Figure 45. Evolution of stress-strain hysteresis response of composite specimen 5-7-C-1-2 with Type 2 geopolymer matrix in a tension-tension fatigue test performed at 300°C. Cycle 200,000 with the asterisk is arbitrarily shifted right due to extensometer slipping. 69

Figure 46. Maximum load per unit length per ply vs. cycles to failure obtained at 300°C. 70

Figure 47. Tensile stress-strain curve obtained at 300°C for composite specimens achieving runout condition of 200,000 cycles at 300°C. 72

Figure 48. Failed fatigue runout specimen from tension testing. 72

Figure 49. Modulus results for Type 1 geopolymer matrix specimens. 76

Figure 50. Modulus results for Type 2 geopolymer matrix specimens (continued next page). 77

Figure 51. Modulus results for Type 2 geopolymer matrix specimens (continued). 78

Figure 52. Initial exposure of 3-14-C-1 specimens. 79

Figure 53. Initial thermal exposure of 5-10-C fatigue specimens. 79

Figure 54. Initial thermal exposure of 5-7-C-1 fatigue specimens. 80

Figure 55. Initial thermal exposure of 5-9-C fatigue specimens. 80

Figure 56. "Front" side of panel 5-7-C-1. 81

Figure 57. "Back" side of panel 5-7-C-1. 82

List of Tables

Page

Table 1. Geopolymer Compositions as reported by Metna Co. 16

Table 2. Panel information reported by Metna Co. 17

Table 3. Tensile strength of geopolymer matrix/carbon fiber composites from pilot tests. Estimated strength is compared with the experimental UTS values. 29

Table 4. Average Values of elastic modulus obtained for composite panels at 23°C. 32

Table 5. Tensile properties obtained for geopolymer-matrix/carbon-fiber composites at 23°C in laboratory air. 40

Table 6. Through-thickness swelling and mass loss due to thermal exposure. 51

Table 7. Summary of fatigue results obtained for geopolymer matrix composites at 23 and 300°C in laboratory air. 61

Table 8. Comparison of 3-14-C-2 specimens subject to tension-tension fatigue. 62

Table 9. Retained properties of the geopolymer-matrix composite specimens subjected to prior fatigue in laboratory air at 300°C. 71

TENSILE PROPERTIES AND FATIGUE BEHAVIOR OF GEOPOLYMER MATRIX COMPOSITES WITH CARBON FIBER REINFORCEMENT AT ELEVATED TEMPERATURE

I. Introduction

1.1 Motivation

There is a demand for engineering materials that can operate in harsh environments. To meet this need, new materials must be stronger, lighter, and able to withstand higher temperatures than current material systems. High-temperature environments are demanding on material systems, exposing the material to effects such as corrosion, oxidation, creep, and phase transformations, which are not experienced at room temperature. These detrimental effects need to be understood for a material system to succeed in an engineering application in a high-temperature environment.

Engineering materials designed to operate in high-temperature environments have a history of development. Metal alloy systems have been developed largely to their potential and are strong, but also have high density, which leads to high weight. Recently, the Air Force has been looking for material systems, which can offer a higher strength-to-weight ratio than metals. Structural ceramics and composites can satisfy this requirement.

Polymer matrix composites (PMCs) are an important class of light-weight structural materials [1]. Polymers intended for elevated temperature applications (such as PMR-15, PMR-II-50 and HFPE-II) have been successfully tested and shown to perform at temperatures up to and including 315ºC [2-4]. However, the polymer matrix resins rapidly deteriorate above these temperatures as they near their glass transition

temperatures, T_g. The undesirable effect of combustion can also occur in PMC materials, due to the carbon chemistry of the matrix resin of the material, which combusts in the atmosphere at sufficiently high temperature. Ceramic matrix composites (CMCs) have excellent high-temperature properties, but they also have lower toughness compared to metals. Carbon/carbon composite is a very strong material system, yet "a typical carbon/carbon composite oxidizes at 400 ºC" [5].

A new type of composites using an inorganic, geopolymer matrix can potentially be an alternative to CMCs and PMCs. Examples of a geopolymer matrix are aluminosilicates, primarily composed of silicon, aluminum, and oxygen bonded together in a polymer chain. Compared to polymer matrices, geopolymer matrices are much more fire-resistant, as they lack carbon and other easily combustible parts because of their inorganic chemistry, making them entirely non-combustible [6]. This allows geopolymer matrix based composites to perform better at elevated temperatures where other polymer matrix materials have the potential to combust as well as mechanically and chemically degrade.

Geopolymer matrix composites can be tailored to bridge the gap between PMCs and CMCs. A geopolymer matrix composite can be designed to combine the mechanical properties and manufacturability of PMCs with the higher-temperature capability of ceramics. Fire resistance is offered by geopolymer matrix materials at a low to moderate cost [6], making geopolymer matrix composites a potentially viable option compared to CMCs. Geopolymer matrices are easy to manufacture, as they are initially liquid and can be cast into any desired shape [7]. Geopolymer matrix composites can potentially perform effectively and economically, and as such are worth investigating.

1.2 Problem Statement

The purpose of this study is to experimentally evaluate mechanical properties and behavior of geopolymer matrix composite panels fabricated by Metna Co. at elevated temperature (300 ℃). The composite panels consist of woven carbon fiber plies in an alkali aluminosilicate geopolymer matrix. The alkali components of the aluminosilicate geopolymer are either sodium or potassium, depending on the panel. The panels are of various thickness and contain different additives to the geopolymer matrix to enhance performance, such as graphene nanoplatelets (GNPs), carbon nanotubes (CNTs), superplasticizer and sodium tetraborate (borax).

Additives such as graphene nanoplatelets (GNPs) which possess high stiffness and strength are known to increase the strength and toughness of cements [8]. Adding the GNPs to a geopolymer matrix may have a similar effect on the matrix properties, thus improving performance of a geopolymer matrix composite. Superplasticizer is known to improve the workability of the material [9], while borax improves the flash setting time [10].

Carbon fiber is used as reinforcement for various types of composites. Carbon fiber has a very high strength to weight ratio and is chemically stable. However, carbon fiber oxidizes at sufficiently high temperatures unless adequate environmental protection is provided [5]. A strong refractory fiber may replace the carbon fiber in developing geopolymer matrix composites that achieve higher temperatures. Basalt fiber is a possible choice, if the objective is to select a cost-effective option [11].

The first step in determining the suitability of a material system for structural application is to evaluate basic material properties via standard mechanical tests. This

approach is adopted in the current effort to evaluate the specific material systems developed by Metna Co. The basic methods and procedures for testing the geopolymer matrix composites are based on testing procedures from previous students under Dr. Ruggles-Wrenn [12-14]. As in previous work, dog-bone shaped tensile specimens are utilized such that failure of the specimens occurs in the specimen gage section.

1.3 Methodology

This effort aims to assess the suitability of the geopolymer matrix composites fabricated by Metna Co. for structural applications at temperatures up to 300°C. Basic tensile stress-strain behavior, tensile properties, and tension-tension fatigue response were of particular interest. Two tensile tests at room temperature (23°C) were initially performed to obtain a rough understanding of the material performance and basic tensile properties. Since the tensile strength obtained in experiments exceeded strength estimates provided by the material manufacturer, further testing and study of the materials fabricated by Metna Co. was warranted. Then, the elastic modulus of each test specimen was measured at 23°C. After obtaining modulus measurements, some panels were set aside because of high specimen-to-specimen variability. For the panels not set aside, at least one specimen from each panel was tested in tension to failure at elevated temperature (300°C). The values of the ultimate tensile strength (UTS) obtained in these tests were used to determine maximum fatigue stresses for subsequent tension-tension fatigue testing at 300°C. Prior to testing several specimens from each panel were examined with an optical microscope to assess manufacturing flaws and defects that may be present in the material. After testing, the failed specimens were also examined using

an optical microscope in order to assess the damage and failure modes. Understanding the damage and failure modes is critical to improving the material. Results of the experimental effort can inform and guide the material manufacturer, who in turn can change the material processing or material composition and design.

The experimental results together with the information collected from microscopy were used to characterize the potential of each composite variant to deliver adequate mechanical performance at 300°C. Based on these results a decision can be reached as to which composite variants are worthy of further study and development. If a particular material performs well, then further tests would be necessary to gain a sound statistical understanding of the material behavior.

1.4 Summary

This research aims to evaluate the several material systems developed by Metna Co. and to identify, if possible, a material system that can bridge a gap in thermo-mechanical performance between CMCs and PMCs. This study is concerned with basic mechanical properties. The objective is to gain a basic understanding of the mechanical response of several variants of the geopolymer matrix composite under monotonic tension and tension-tension fatigue at 300°C.

II. Literature Review

This chapter discusses the basic principles behind composites, presents the reasons for interest in a geopolymer as a matrix material for a composite, and offers a brief literature review of geopolymer matrix composites.

2.1 Composite Basics

A composite material consists of at least two different materials combined into one effective material. In the context of modern technology, this is typically accomplished by having a matrix material, which acts as a binder to keep the composite together, and a reinforcement material, which adds strength to the composite.

Perhaps the simplest composite system is a unidirectional composite ply, shown in Figure 1. A rule of mixtures approach can be used to evaluate basic properties of the composite ply from basic properties of the fiber and matrix constituents. Typically a perfect bond between the fiber and the matrix is assumed. The composite performance is thus a sum of the fraction of each material property. Of course, this idealization does not always match reality, but underlies the basic concept of combining two materials to take advantage of their properties and to obtain a new material with specially tailored properties and performance.

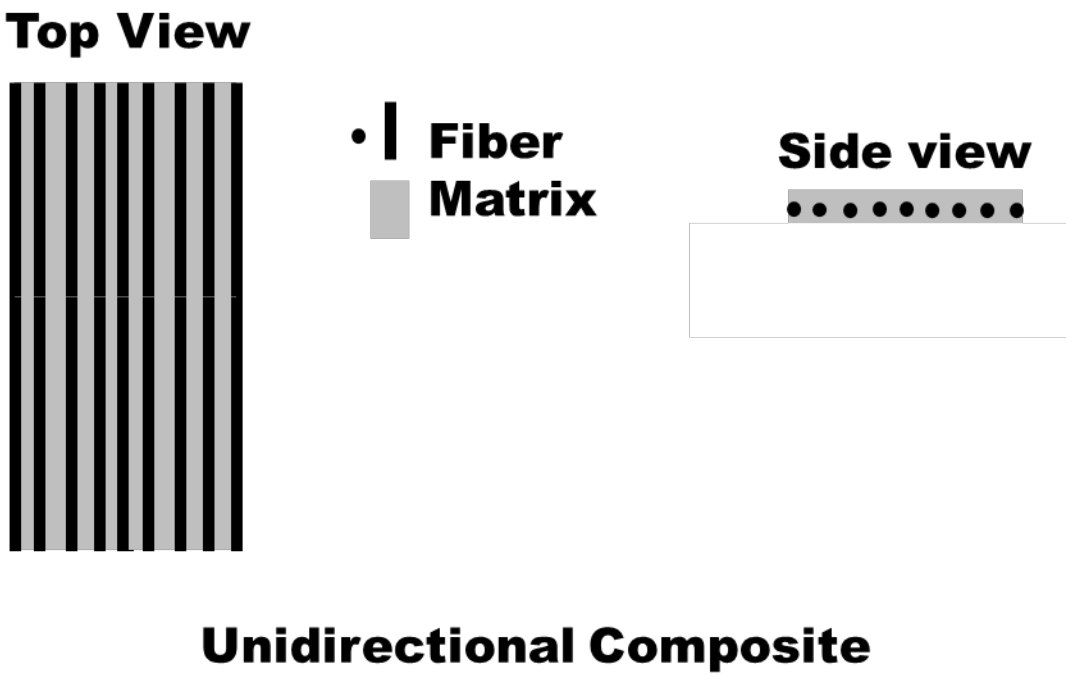

Figure 1. Schematic of a unidirectional fiber composite ply.

A unidirectional composite ply exhibits lower strength and stiffness in the transverse direction than the longitudinal direction. The fibers are not reinforcing the composite in the transverse direction, thus the transverse performance is dominated by the matrix properties. Additional fibers can be placed at 90º to the original fibers to increase strength and stiffness in the transverse direction. However, if the fiber volume fraction remains unchanged, orienting some fibers along the transvers (90°) direction decreases the reinforcement of the longitudinal (0º) direction. In many cases this is not detrimental to the composite performance, since the 90º fibers significantly improve properties and performance in the transverse direction. It is of note that this basic 0/90 cross-ply material is not isotropic. Therefore, performance of the composite depends on loading direction.

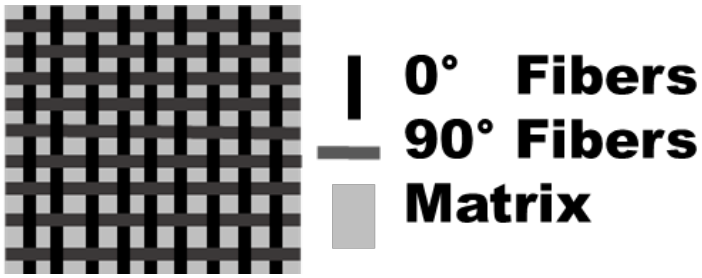

Figure 2. Schematic of a composite with a 0/90 cross-ply plain weave fabric.

A practical issue of assembling composites should be considered. It is difficult to perform hand laying of composites at any scale, if one is handling each individual fiber separately. Therefore, it is commonly found that fibers are woven into fabrics, which combine both the 0º and 90º fibers. These cross-ply fabrics provide an easy way to hand lay a composite (Figure 2). Additionally woven fabric plies also provide a good balance of properties for the longitudinal and transverse directions.

A composite consisting of a single lamina or ply would not be a structurally sound material. Such a material would be too thin to carry a significant load. Therefore, composite laminates are typically made with multiple layers (or laminae) to achieve sufficient thickness to bear the load.

2.2 Heat Resistance of Composites

As mentioned in Section 1.2, this research is focused on the performance of geopolymer matrix composites at 300ºC. When selecting reinforcing fibers and a matrix material for a composite material, the mechanical properties of each constituent must be carefully considered. The constituent materials must be chemically compatible and suitable for the environment to which the composite will be exposed. To understand

material performance at high temperatures, it is important to differentiate between fire resistance and heat resistance.

Fire resistance is the ability of a material to resist catching fire, as the name implies. Since fires need fuel, oxygen and a source of heat, heat resistance should be regarded separately from fire resistance, as a material could be in a non-combustible atmosphere or otherwise have non-combustible chemistry. Davidovits can lend some initial understanding of what heat resistance is: “The heat resistance of a material is a function, in the first place, of at least two parameters – the temperature and the time.”[5] Heat resistance then, in the context of this study, is defined as the ability of the material to maintain its mechanical properties and structural integrity at elevated temperature for a given duration.

In general, the ability to resist heat sets the CMCs and the PMCs far apart. Ceramic matrix composites are strong and can withstand high temperatures, but they are brittle and have lower toughness than metal alloys. Polymer matrix composites are strong at temperatures up to 315°C, but cannot withstand temperatures much higher than 315°C.

At lower temperatures PMCs possess excellent strength-to-weight ratio, a good example being carbon fiber PMCs (see Figure 3). The main weakness of PMC systems stems from lack of heat resistance and flame resistance. Due to the organic nature of PMC systems with their carbon chemistry, they are likely to catch on fire if exposed to enough heat. As can be seen in Figure 3, PMCs quickly lose strength as the temperature increases, making PMCs not a viable option for use at temperatures exceeding 315ºC.

For use at elevated temperatures CMCs are a viable option. Ceramic matrix composites have far better heat resistance than PMCs, with their strength not significantly

degraded until around 1550ºC. However, CMCs have a poor strength-to-weight ratio, due to the dense nature of ceramics, and there are other factors to consider for using CMCs. Davidovits mentions how CMCs are "limited to high end use because of their high cost and special processing requirements." [5] CMCs have been demonstrated to perform well at elevated temperature, but their high cost make them less attractive, if given a suitable alternative.

We define a large difference between the strength-temperature characteristics of the PMCs and CMCs as the thermo-mechanical gap (see the shaded region in Figure 3). To fill this thermo-mechanical gap, we need a composite with the right combination of reinforcing fiber and inorganic matrix. Geopolymer matrix composites may be able to bridge this gap.

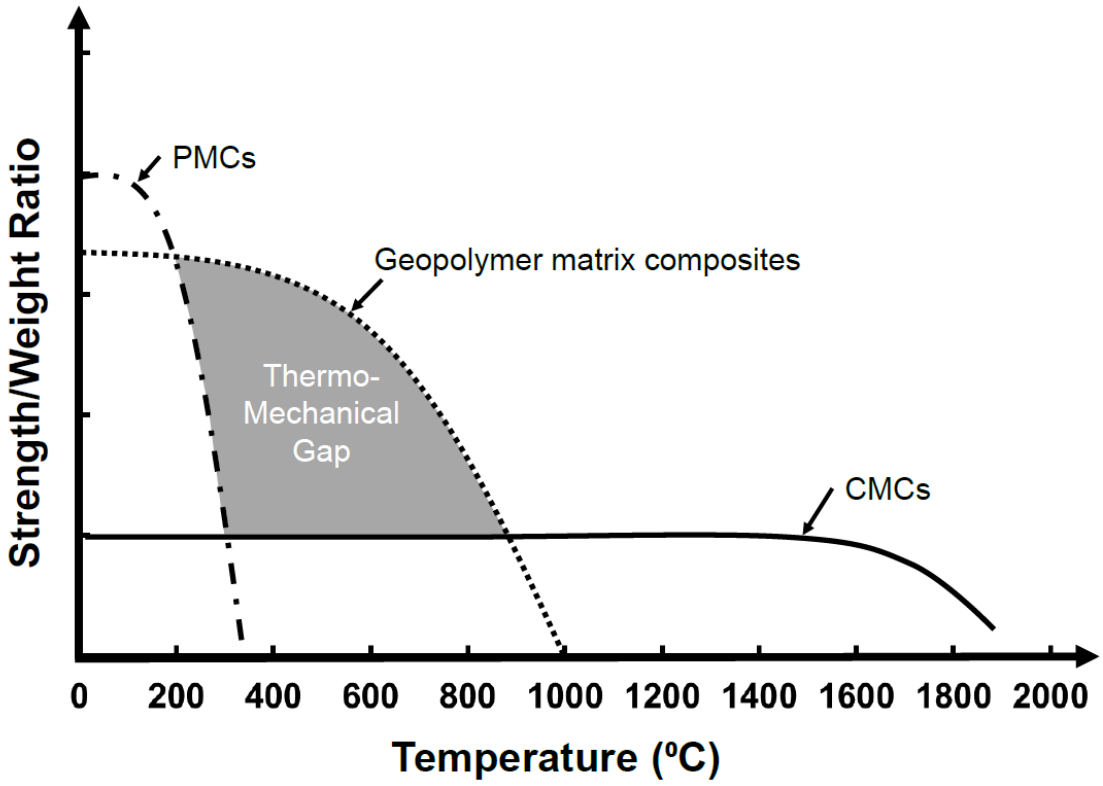

Figure 3. Schematic of retained Strength/Weight Ratio at Temperature, adapted from [15]

Due to their inorganic nature and fire-resistant properties geopolymers are a potentially suitable matrix material for composites designed for high temperature applications. Davidovits described the fire resistance of geopolymer as “the essence of all mineral geopolymers” [5]. Additionally, geopolymers offer processing advantages over CMCs, which lead to lower composite fabrication cost. Typical processing temperatures for CMCs are 1200-1500 ºC [16], whereas geopolymers can be processed at low temperatures [5]. Geopolymer matrix composites may offer low density and adequate performance at high temperature combined with a lower cost. These considerations make geopolymer matrix composites worthy of research and development.

2.3 Geopolymer Matrix Materials

Lukey, Deventer, and Duxson state: “‘Geopolymer’ is the name that since the late 1970s has been applied to a wide range of alkaline- or alkali-silicate-activated aluminosilicate binders of composition $M_2O \cdot mAl_2O_3 \cdot nSiO_2$, usually with $m \approx 1$ and $2 \leq n \leq 6$, and where M represents one or more alkali metals.” [17] The typical alkali metals chosen Na or K, with Na, K, and Cs investigated in [16]. These geopolymers can be thought of having either a covalent or ionic character. They are mostly thought of as being covalent, as discussed in Davidovits’ book [5].

Depending on the Si:Al ratio, these geopolymers consist of networks of molecular structures which can be classified as follows: (i) Si:Al = 1:1 is a sialate, (ii) Si:Al = 2:1 is a sialate-siloxo, (iii) Si:Al = 3:1 is a sialate-disiloxo, and (iv) Si:Al > 3:1 is a sialate link [5]. An example of an overall geopolymer structure for a polysialate composed of sialate

components can be seen in Figure 4. Note the clustering of the water (H_2O), with the alkali component (sodium in this example).

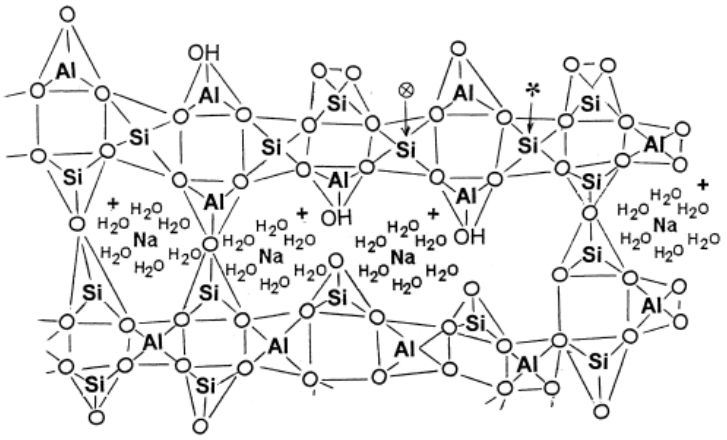

Figure 4. An example of a polysialate geopolymer molecular structure, with Na as the alkali metal component [18] *Reprinted from International Journal of Inorganic Materials, Vol 2, Valeria F.F Barbosa, MacKenzie K. and Clelio Thaumaturgo, Synthesis and characterization of materials based on inorganic polymers of alumina and silica: sodium polysialate polymers, 309-317, Copyright (2000), with permission from Elsevier.

For the composites studied in this work, Metna Co. reported Si:Al ratio of 6.1 and 7.73 for the sodium based geopolymer matrix materials. The reported Si:AL ratio was 9.46 for the potassium based geopolymer matrix materials. Therefore, the molecular structure of the geopolymer matrix materials in this study can be classified as consisting of sialate links.

Interestingly, geopolymers can adhere well to metals. A geopolymer matrix carbon fiber reinforced composite adheres well to titanium, and fails not on the adhesive bond, but on the carbon fiber [5]. If geopolymer matrix composites perform well for a chosen application, then the design engineer is presented with additional opportunities from the bonding phenomenon.

As mentioned earlier, geopolymer matrix composites are the subject of this study because of their high temperature properties. As other researchers put it: “Geopolymers have created significant interest as high-temperature materials due to their outstanding thermal stability and ability to be used both as a binder in carbon-fibre composites, and also as an additive in epoxy-based systems.” [17]

2.4 Reinforcing Carbon Fibers

Carbon fiber is a widely-used reinforcement for high-strength, high-performance composites. Due to the strength of the carbon atoms bonding with each other, carbon fiber exhibits high strength and high stiffness. Carbon fiber also has a low weight. The high strength and low weight lead to a high strength-to-weight ratio.

However, carbon fiber does poorly, when exposed to an atmosphere containing oxygen above 400 ºC. However, carbon fiber is not a bad choice of reinforcement for the geopolymer matrix composites fabricated by Metna Co. Due to shrinkage of geopolymer matrix when curing, there are some problems using fiberglass or SiC as a reinforcement material, but with carbon fiber there is little or no adherence to the matrix [5]. Therefore, compromising this material system with residual stresses should not be an issue with using carbon fibers.

2.5 Carbon Fiber Geopolymer Matrix Composites – Previous Work

Previous work from Lyon in 1995 has demonstrated the fire resistance of geopolymer matrix composites over PMCs when exposed to heat [6]. Papakonstantinou and Balaguru [19] compared flexural fatigue performance of geopolymer matrix-carbon fiber composites with other materials. A K-nano-sialate/carbon composite exhibited a

50% stress range capacity at 10^5 cycles [19]. Such stress range capacity is similar to that exhibited by PMCs, and higher than the 20% stress range capacity of 2024-T3 aluminum [19]. Lyon et al [20] studied mechanical properties of K-nano-sialate/carbon fiber composites. Lyon et al reported room temperature tensile strength of ~245 MPa and a modulus of ~45 GPA. However, strength and stiffness obtained at 600°C were half of the respective room-temperature values [20]. These tests have demonstrated that geopolymer matrix composites are a potentially viable material.

2.6 Matrix Additives

Additives are used to modify chemical or physical properties of the matrix material and those of the composite. Ideally, such additives enhance performance of the matrix and of the composite. The carbon nanotubes should act as reinforcement and are expected to toughen the geopolymer-matrix composite as well as make it stiffer, as is demonstrated for concrete with carbon nanofibers and nanoplatelets [8]. It was demonstrated the addition of sodium tetraborate (borax) increased the flash setting time of the geopolymer with high calcium oxide content [10]. It is not entirely clear why Metna Co. added the borax to the sodium based geopolymer when fabricating composites studied in this work. One possible objective is to increase the setting time to help with fabrication. The addition of superplasticizer is known to increase the workability of geopolymer paste without compromising the strength of the final product [9]. While these additives are not the main focus of this study, the additives used to fabricate composites for this study must be mentioned. Recognizing what additives were used to fabricate different variants of the composite studied in this work may help explain significant

differences in mechanical response of the different material variants, should such differences be observed.

III. Material and Test Specimens

This chapter describes the materials studied in this work. Design and processing of tensile specimens used in the experiments is also discussed.

3.1 Research Material

Composites studied in this work were fabricated by Metna Co. All composites were reinforced with carbon fiber fabric (Toray carbon T300B-40B), with 0.012-in. thickness (0.3048 mm) and 3K tow. The 0/90 plies of carbon fiber were woven in a plain weave. The density of carbon fiber is 5.7 oz./yd^2 (193.3 g/m^2). The geopolymer matrix composites supplied by Metna Co. had two different types of geopolymer matrix. Type 1 was a sodium based geopolymer (NaGP) and Type 2 was a potassium based geopolymer (KGP). Geopolymer chemistry for Type 1 and Type 2 matrix materials is summarized in Table 1.

Table 1. Geopolymer Compositions as reported by Metna Co.

Type	Alkali component	Si:Al Ratio	Alkali: Alumina Ratio	Alkali:Silica Ratio
1a	Na	6.1	1.7	0.27
1b	Na	7.73	2.03	0.29
2	K	9.46	2.4	0.25

Table 2 displays the reported matrix type, matrix additives, fiber architecture, fiber volume fraction, and estimates tensile strength for each composite variant supplied by Metna Co.

Table 2. Panel information reported by Metna Co.

Panel	Type	Matrix Additive	Carbon Fiber Layers	Estimated Fiber Volume Fraction	Estimated Tensile Strength (MPa)
3-14-C-1	1a	None	11	25%	150-180
3-14-C-2	1a	1 wt.% GNP	11	25%	150-180
3-20-C	1b	5 wt.% sodium tetraborate (borax)	13	40%	200
5-10-C	1b	5 wt.% sodium tetraborate (borax)	14	41%	145
5-6-C-1	1b	5 wt.% sodium tetraborate (borax)	9	35%	200
5-6-C-2	1b	5 wt.% sodium tetraborate (borax)	9	33%	200
5-7-C-1	2	Geopolymer w/0.1 wt% CNT and 0.5 wt.% superplasticizer	14	35%	300
5-7-C-2	2	Geopolymer w/0.1 wt% CNT and 0.5 wt.% superplasticizer	14	35%	200
5-9-C	2	Geopolymer w/0.1 wt% CNT and 0.5 wt.% superplasticizer	14	40%	250
12-C-3	2	Geopolymer w/0.1 wt% CNT and 0.5 wt.% superplasticizer	14	40%	250
12-5-C	2	Geopolymer w/0.1 wt% CNT and 0.5 wt.% superplasticizer	14	36%	250
13-1-C	2	Geopolymer w/0.1 wt% CNT and 0.5 wt.% superplasticizer	14	33.4%	250

The as-received composite panels had multiple processing flaws and defects on the surfaces. Some panels, such as panel 5-7-C-1, appeared to have better overall quality, although matrix infiltration into the composite panel is questionable in some areas (Figure 5). Several panels, such as panel 3-14-C-1 (Figure 6), have excess matrix material pooled on the panel surface. Defects of this type look like wrinkles or can otherwise be described as “elephant skin” in appearance. Several panels, such as panel 3-20-C were slightly warped. Panel 3-20-C also shows obvious damage in the weave in the upper right

hand corner (Figure 6). Significant thickness variations, noted in multiple panels can lead to inconsistencies in load/stress calculations.

Figure 5. Panel 5-7-C-1, dark areas correspond to less presence of matrix on the surface.

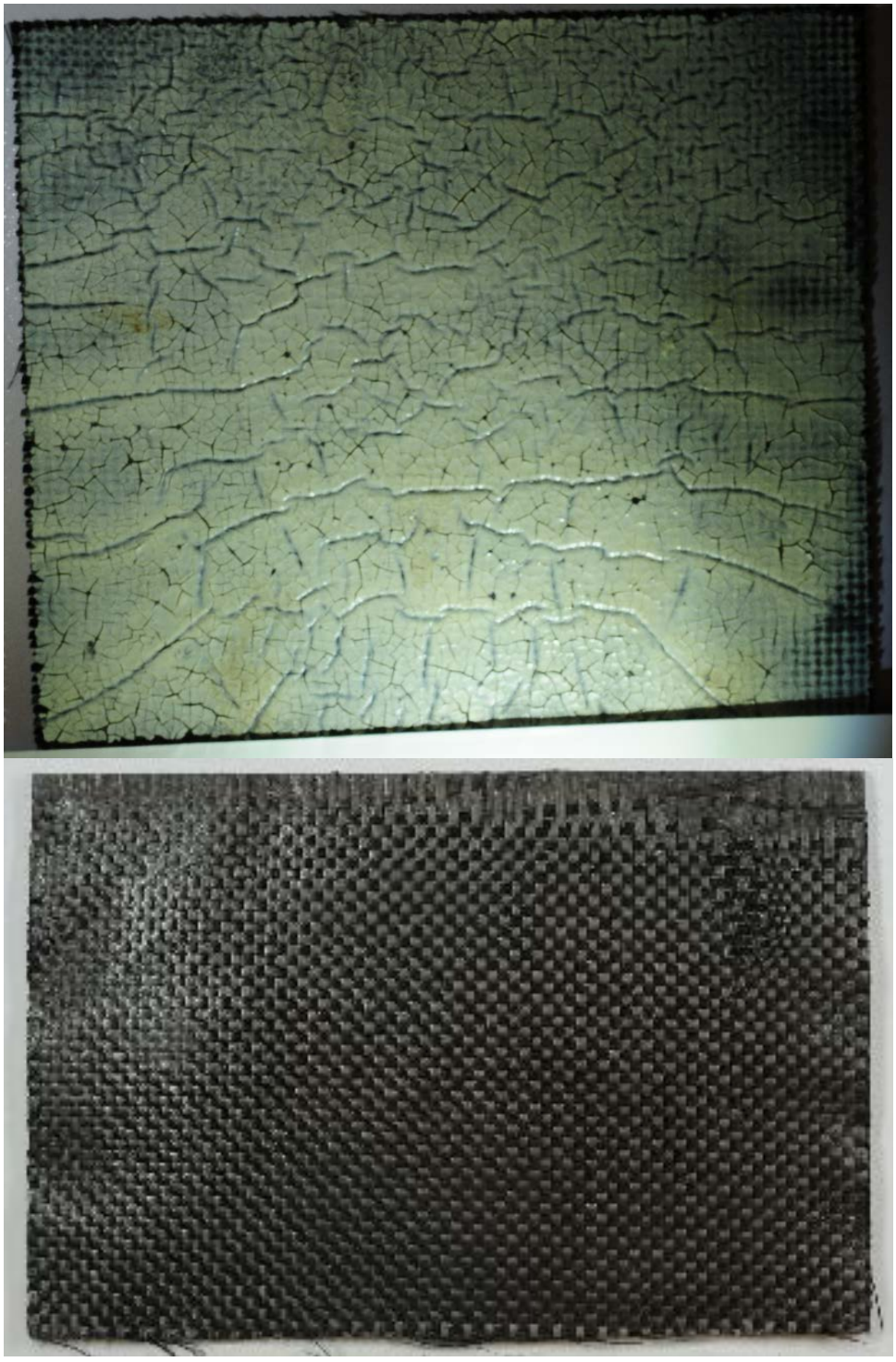

Figure 6. Surfaces of panels 3-14-C-1 (top) and 3-20-C (bottom)

Despite the surface flaws observed in composite panels, most of the specimens cut from the panels were determined to be suitable for testing in this pilot effort to characterize mechanical properties and behavior of this material system. However, material processing can definitely be improved for future work and evaluation of the material system.

3.2 Test Specimen Design and Preparation

Each composite panel was first cut into strips using a water-cooled diamond saw. A standard dog-bone shaped tensile specimen was cut from each strip using a diamond grinding bit. The drawing of the test specimen design is shown in Figure 7.

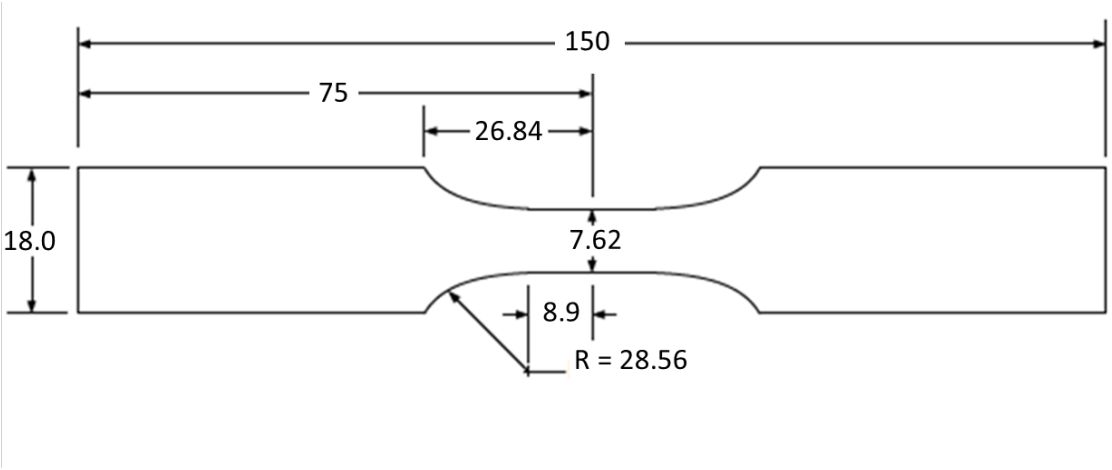

Figure 7. Dog bone shaped tensile specimen drawing, dimensions in mm.

After machining, large amounts of dust and multiple exposed fibers were noted the surface of the specimens (see Figure 8). Hence the specimens were handled using nitrile gloves, more for personal protection than for risk of contaminating the specimens. The specimens were brushed lightly to remove carbon fiber particles and set out on paper

towels to dry in the laboratory air. Width and thickness of the specimen gage section were measured using a Mityoyo CD-56”CT digital caliper. The thickness and width were used to calculate the cross-sectional area, needed for the load/engineering stress calculations.

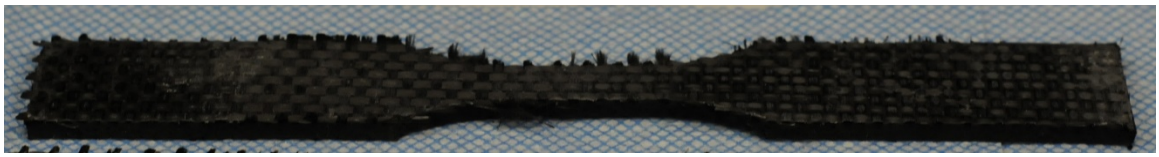

Figure 8. As-machined specimen from panel 3-20-C.

In preparation for testing, 38-45 mm x 16.5 mm x 0.9 mm fiberglass tabs were bonded to the gripping sections of the test specimens using M-Bond 200 adhesive. Fiberglass tabs protect the specimen from damage due to gripping and help distribute the gripping pressure. A test specimen with fiberglass tabs is shown in Figure 9.

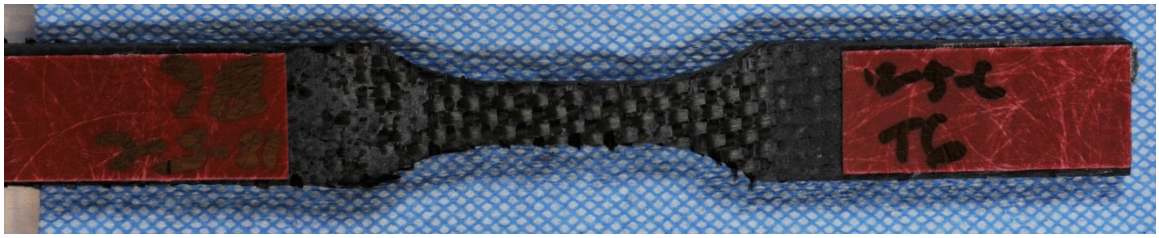

Figure 9. Test specimen with fiberglass tabs, from panel 12-5-C.

Most of the specimens were deemed to be suitable for testing. However, all specimens cut from panels 5-6-C-1 and 5-6-C-2 appeared to be “rubbery” and could be easily twisted by hand. Hence these specimens were not considered to be suitable for further testing. This behavior is likely due to having too few layers of carbon fiber along with poor matrix quality holding the fibers in place.

During testing at elevated temperature, some specimens were found to expand significantly in the thickness direction as the temperature was raised from 23°C to test temperature of 300°C. Such considerable thermal expansion is attributed to profuse cracking and dehydration of the geopolymer matrix. From then on, each specimen was weighed using a Voyager Pro model VP214CN scale before and after thermal exposure.

IV. Experimental Setup and Testing Procedures

This section first describes the experimental setup and procedures used for temperature calibration, and for performing tension and fatigue tests. Lastly, details are provided regarding the optical microscope used for the material characterization.

4.1 Experimental Equipment

All tests were performed using an 810 MTS servo-hydraulic testing machine with a 3-kip load capacity. The machine is equipped with water-cooled 528189-01 wedge grips. A Neslab RTE7 Chiller supplied 18.9℃ water to the wedge grips for cooling. Gripping pressure was set to 10 MPa for most tests. In tests, where a particularly high tensile load was anticipated, gripping pressure was increased to 11 MPa. Strain measurement was accomplished with an MTS model 632.53E-14 uniaxial high-temperature extensometer. An MTS 653.01A single-zone furnace equipped with an MTS 409.83 temperature controller was used to provide the elevated temperature environment for testing at 300℃. An MTS Flex Test 40 digital controller was used for input signal generation and data acquisition. In all tests strain, displacement, force, force command, temperature, and time data were collected. The extensometer is equipped with long ceramic rods to prevent damage from the furnace heat. The tips of the extensometer rods are conical in shape, as shown in Figure 10. The high-temperature setup is shown in Figure 11.

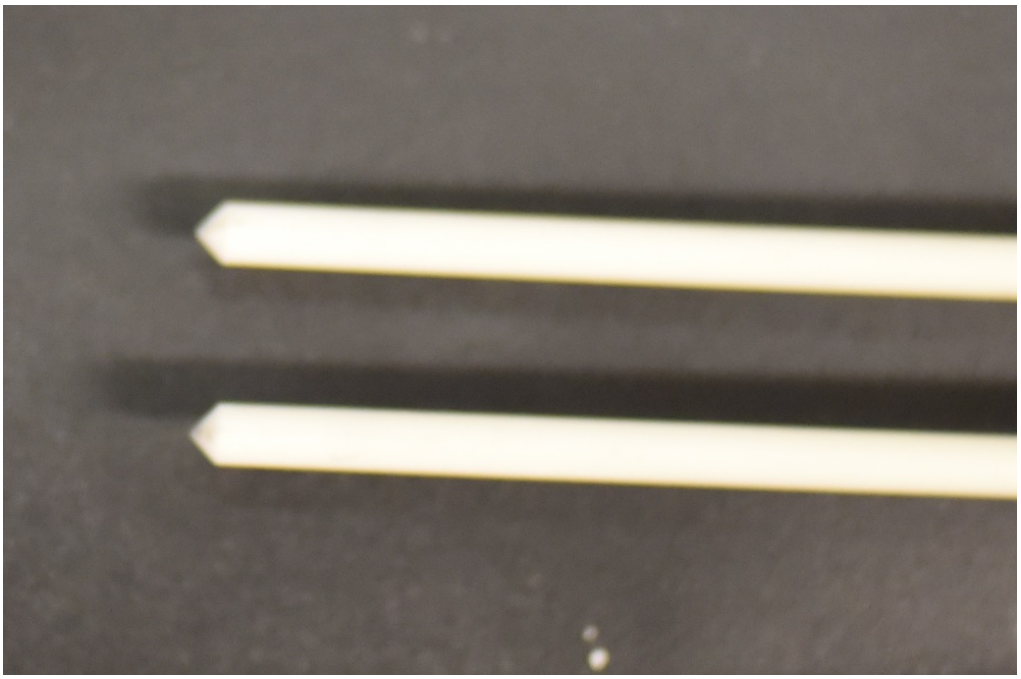

Figure 10. Contact end of ceramic high-temperature extensometer rods.

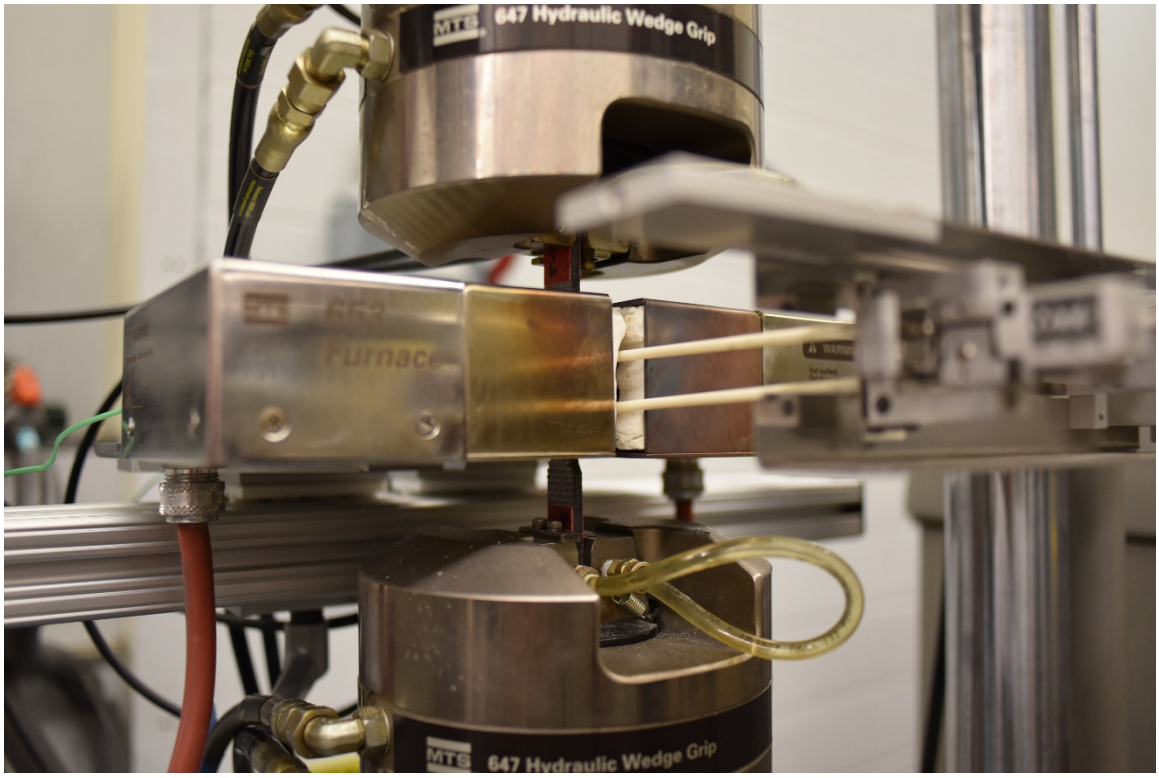

Figure 11. High-temperature test setup.

4.2 Temperature Calibration

A specimen cut from panel 5-9-C was selected for temperature calibration. This specimen was instrumented with two type K thermocouples in the specimen gage section, one on each side of the specimen. The thermocouples were secured by Kapton tape and copper wire similar to Wilkinson [12]. A hand-held Omega HH202A temperature sensor was used to display the temperature measured by the type K thermocouples. The specimen instrumented with thermocouples was mounted in the testing machine under load control. During temperature calibration, the load was held at zero to allow for thermal expansion of the calibration specimen. The furnace was closed and temperature controller setting corresponding to the specimen temperature of 300°C was recorded. Temperature was then maintained for approximately 3 h to ensure stability. The controller setting was verified by allowing the system to cool down, then commanding the temperature controller to increase temperature to the recorded set point at 2°C/min.

4.3 Mechanical Testing Procedures

4.3.1 Room Temperature Modulus Measurements

Except for couple preliminary tensile test specimens (Section 5.1), the elastic modulus of each specimen was measured at room temperature to assess specimen-to-specimen variability in mechanical properties. In order to measure the elastic modulus, test specimens were cycled between zero stress and 20 MPa 3 times at the loading/unloading rate of 1 MPa/s. The maximum stress of 20 MPa imposed during these tests is believed to be well within the elastic range for the composites studied. With this low stress, no damage is believed to occur during the modulus measurement tests. When

using an MTS high-temperature extensometry for strain measurement, it is recommended that small indentations (dimples) be placed on the side of the test specimen to ensure good contact with the extensometer extension rods (i.e. to prevent the rods from slipping) during the test. For the composite system studied, the rough surface nature and 90° fibers can secure the rods. As such, for the modulus measurement tests the specimens were not dimpled for extensometer placement.

4.3.2 Monotonic Tensile Tests

Tension tests to failure were conducted at 23 and 300°C. All monotonic tensile tests to failure were performed in displacement control with displacement rate of 0.025 mm/s. In most of the tension tests, the test specimens were dimpled for extensometer placement, as it was thought the extensometer was slipping during the extraneous strain behavior observed and described in Section 5.4. The dimples are created by using a punch-like tool with a broad “V” tip and a hammer, separated ~12.7 mm (0.5 inches) apart in the gage section.

4.3.3 Tension-tension Fatigue Tests

Tension-tension fatigue tests were performed in load control with the target R ratio of minimum to maximum stress of 0.1 with the frequency of 1 Hz. Fatigue run-out was set to $2x10^5$ cycles. A pilot tension-tension fatigue test was performed at room temperature, with the rest of the tension-tension fatigue tests conducted at 300°C. A screenshot of the MTS procedure used to conduct a tension-tension fatigue test at 300°C can be seen in Figure 12.

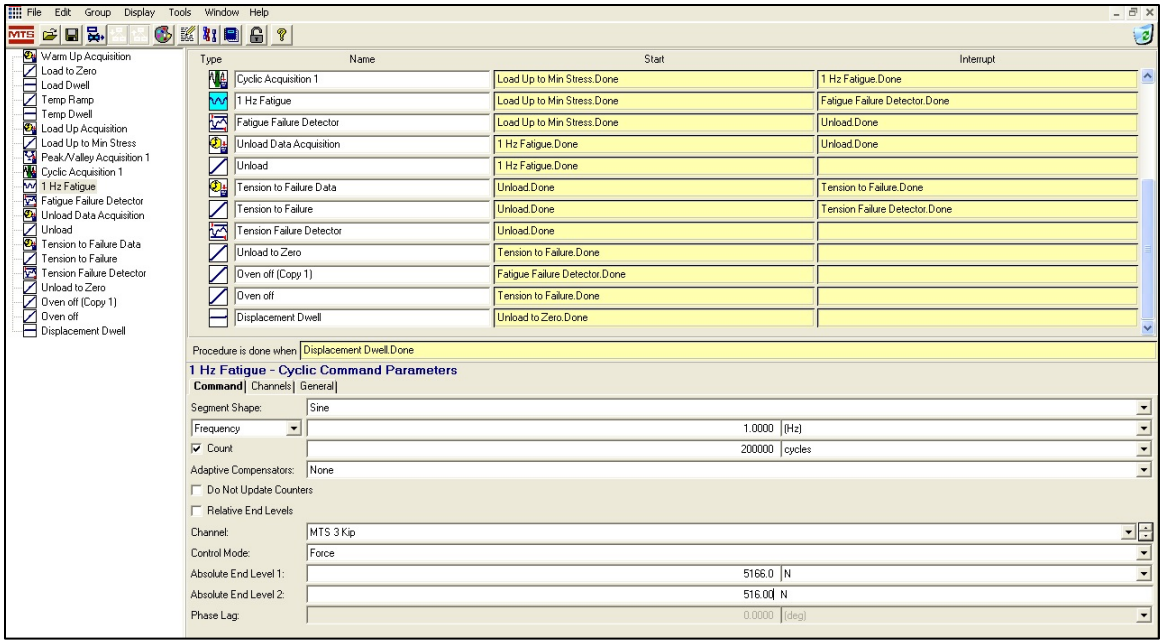

Figure 12. Tension-Tension Fatigue Test Procedure.

4.4 Material Characterization

Composite microstructure was examined before and after testing using a Zeiss Discover V12 stereoscopic optical microscope (Figure 13) equipped with a Zeiss AxioCam HRc digital camera. This was done to document the damage and failure modes of the testing specimens.

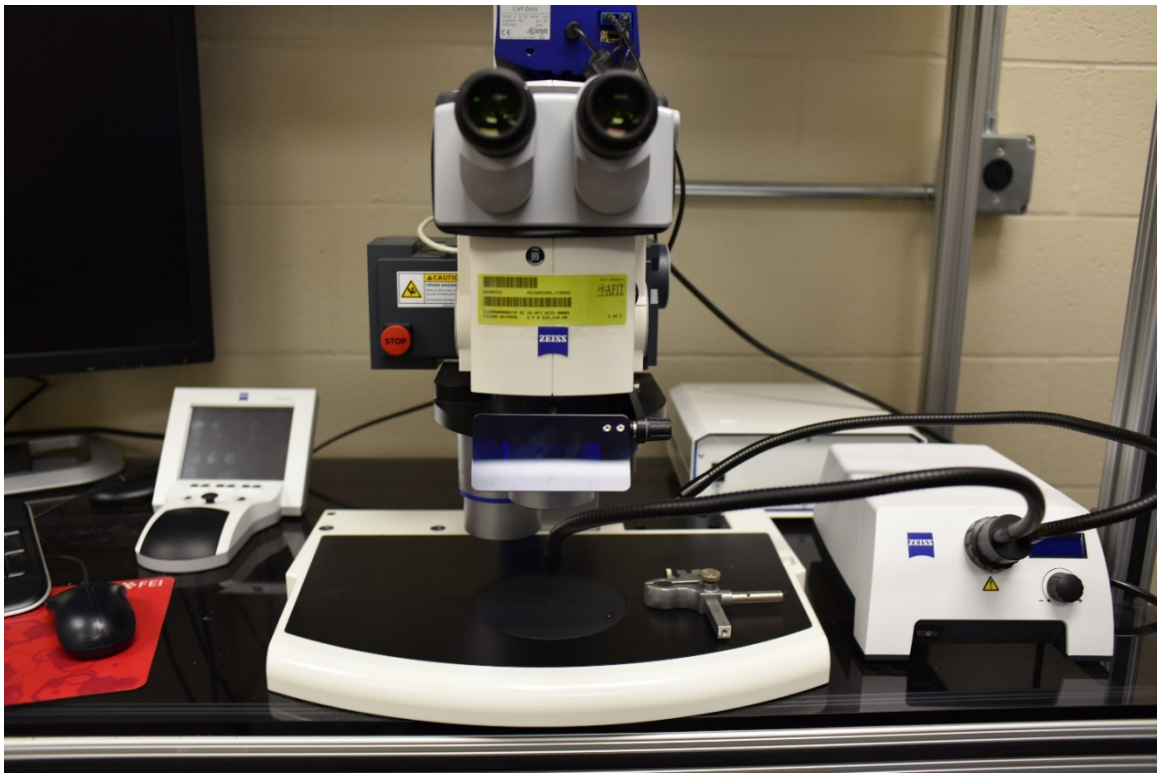

Figure 13. Zeiss Discover V12 Stereoscopic optical microscope.

V. Results and Discussion

5.1 Monotonic Tension at 23°C – Pilot Tests

Two monotonic tension tests to failure were conducted at room temperature (23°C) in laboratory air to measure the basic tensile properties and to gage whether the material should be studied further. These tests yielded promising results. The UTS values produced in these tests exceeded the UTS estimates provided by the composite manufacturer, as seen in Table 3.

Table 3. Tensile strength of geopolymer matrix/carbon fiber composites from pilot tests. Estimated strength is compared with the experimental UTS values.

Panel	Specimen	Geopolymer Matrix Type	UTS Estimate (MPa)	UTS (MPa)
5-10-C	5-10-C-1	1b (NaGP)	145	244
5-9-C	5-9-C-1	2 (KGP)	250	289

Tensile stress-strain curves obtained at 23°C are shown in Figure 14. The stress-strain curves initially exhibit linear elastic behavior. As the stress reaches 70-100 MPa, nonlinear behavior (likely due to matrix cracking) takes places. Then the stress-strain curve continues with a reduced slope.

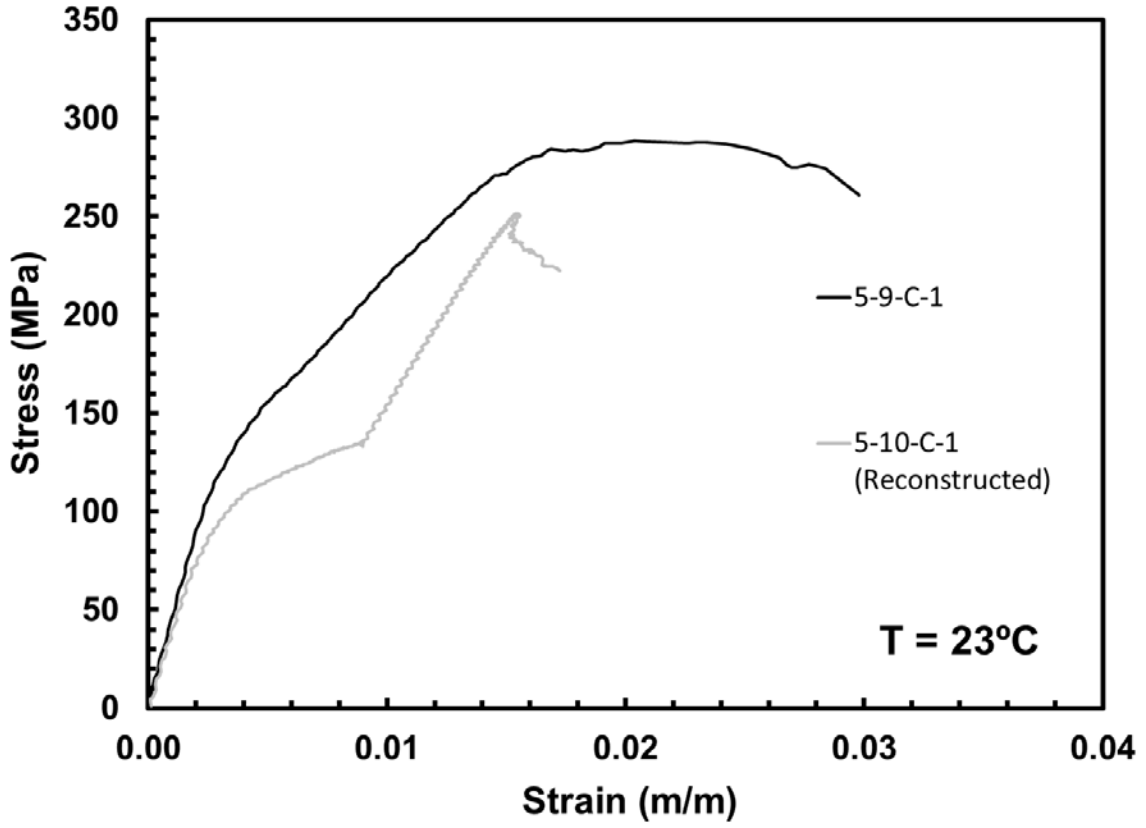

Figure 14. Tensile stress-strain curves obtained at 23°C for specimens from panels 5-9-C and 5-10-C.

The reason for the sharp bend in the 5-10-C-1 curve at around 0.95% strain is due to sliding in the grips. 5-10-C-1 was the first specimen tested, and the initial calculated gripping pressure was not working. The specimen was unloaded a couple times and the grip pressure adjusted before testing again, in order to reach the UTS. The curve can be justified to be reconstructed fairly well since it matches the 5-10-C-2 curve largely in behavior (Figure 15). If 5-10-C-1 had the correct initial pressure it would be expected for it to produce a smoother transition as exhibited in 5-10-C-2.

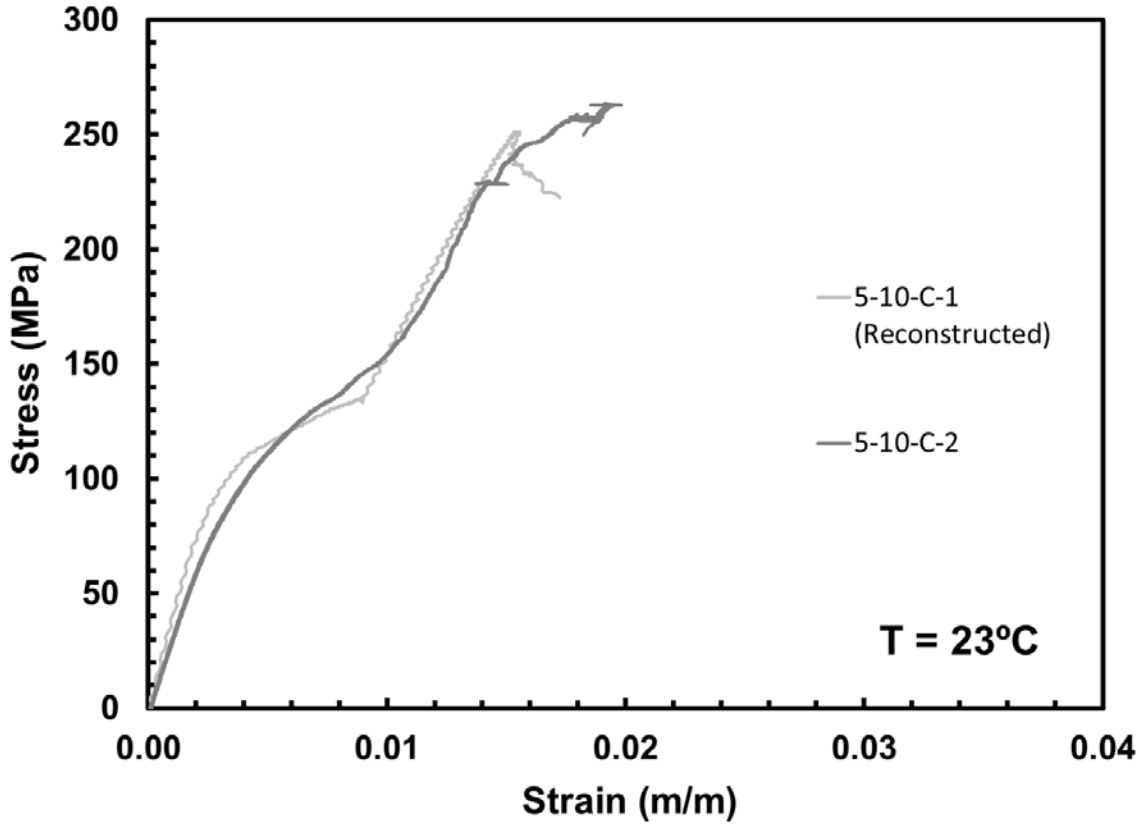

Figure 15. Reconstructed 5-10-C-1 curve compared with later 5-10-C-2- test.

Regardless of the validity of the reconstruction, because the UTS values produced in tension tests to failure significantly exceeded those estimated by the composite manufacturer, the material was viewed as promising. Further testing of the material was warranted. Room-temperature modulus testing would be the next step in the investigation.

5.2 Room-temperature Modulus Testing

Room-temperature elastic modulus was measured for all specimens with the exception of 5-10-C-1 and 5-9-C-1, since they were tested in the initial pilot tensile tests. A room-temperature elastic modulus represents an individual “signature” of the

specimen. Collection of elastic modulus data permits assessment of specimen-to-specimen variability for a particular material. Elastic modulus measurements are summarized in the Appendix. The average value of the elastic modulus was calculated for each panel. These average values are displayed in the Table 4.

Table 4. Average Values of elastic modulus obtained for composite panels at 23°C.

Panel	Geopolymer Matrix Type	Average Specimen Thickness (mm)	Average Thickness per Ply (mm/ply)	UTS Estimate (MPa)	Number of Specimens Tested	Average Modulus (GPa)	Standard Deviation (GPa)	Covariance (%)
3-14-C-1	1a (NaGP)	4.35	0.40	150-180	6	24.5	1.6	6.5
3-14-C-2	1a (NaGP)	3.91	0.36	150-180	6	26.2	1.7	6.5
3-20-C	1b (NaGP)	3.32	0.26	200	4	37.5	2.6	6.9
5-10-C	1b (NaGP)	4.80	0.34	145	6	40.2	1.4	3.4
5-7-C-1	2 (KGP)	3.78	0.27	300	6	47.5	1.5	3.2
5-7-C-2	2 (KGP)	4.20	0.30	200	6	40.4	2.4	5.9
5-9-C	2 (KGP)	3.83	0.27	250	7	42.6	2.0	4.6
12-C-3	2 (KGP)	4.17	0.30	250	6	34.9	5.4	15.3
12-5-C	2 (KGP)	4.68	0.33	250	7	33.0	7.2	21.7
13-1-C	2 (KGP)	4.88	0.35	250	7	29.6	2.7	9.3

The modulus values measured for several panels exhibit high covariance (>9%). This high covariance indicates high specimen-to-specimen variability in basic mechanical properties. Thus it is doubtful whether any individual specimen can be considered representative of the rest of the panel. Panels 12-C-3, 12-5-C, and 13-1-C were therefore deemed unsuitable for further investigation. Modulus values obtained for six panels showed better covariance (<9%). These panels thus became the focus of the experimental work. However, panel 3-20-C was not investigated further because of its low specimen count. Furthermore, specimens from panel 3-20-C produced lower modulus values than specimens from panel 5-10-C with the same Type 1 geopolymer matrix.

In the case of panels with the Type 1 geopolymer matrix, there is no apparent correlation between cross-sectional area of the specimen and its elastic modulus (see Figure 16). According to the information provided by Metna Co., these panels contain different number of carbon-fiber fabric plies. Panels 3-14-C-1 and 3-14-C-2 have 11 plies. Panels 3-20-C and 5-10-C have 13 and 14 plies, respectively. Results in Table 4 suggest a correlation between an average modulus and a number of carbon fiber fabric plies in a given panel. Tensile behavior of a 0/90 cross-ply is fiber-dominated. Hence it is not surprising that panels 3-14-C-1 and 3-14-C-2 with the lowest number of carbon-fiber fabric plies also have the lowest average modulus. Panels 3-20-C and 5-10-C have a higher ply count and consequent a higher average modulus.

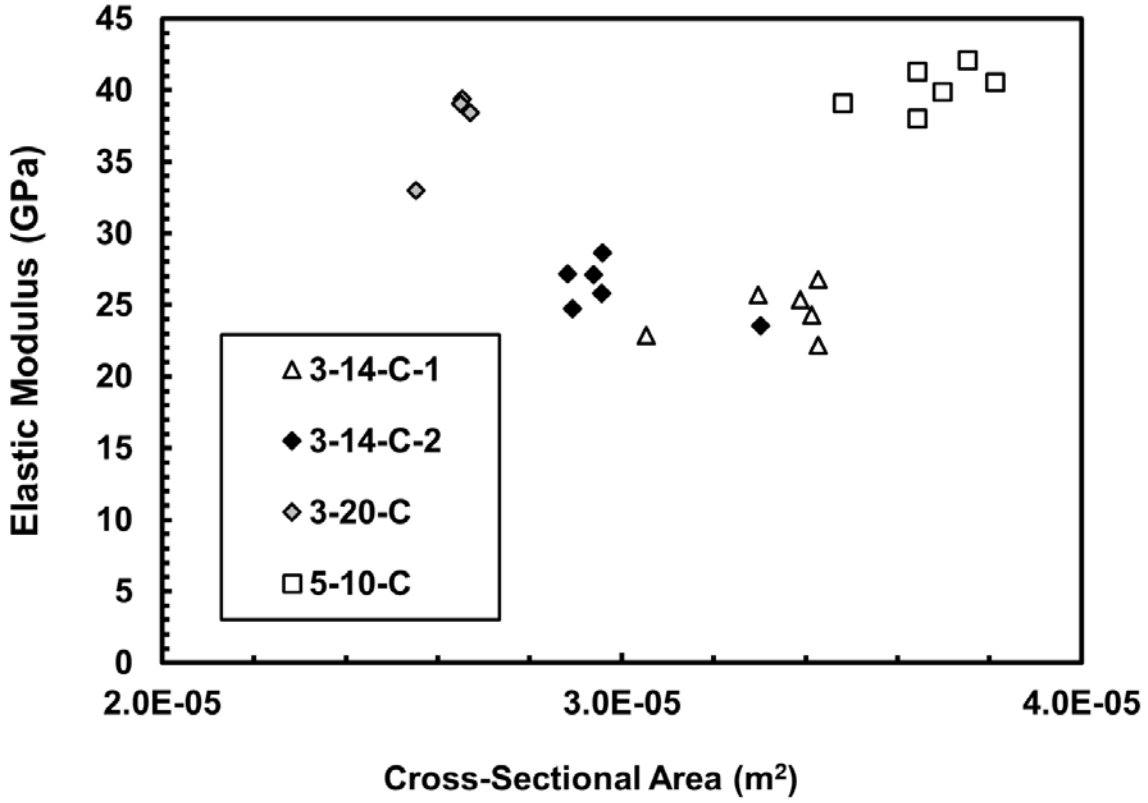

Figure 16. Elastic modulus vs cross-sectional area of Type 1 panels.

For the panels with Type 2 geopolymer matrix, there is a strong correlation between cross-sectional area of the specimen and its elastic modulus (see Figure 17). Note that all panels with Type 2 geopolymer matrix have 14 layers of reinforcing carbon fiber fabric. The results in Table 4 reveal that panels with the lowest cross-sectional area have the highest average stiffness.

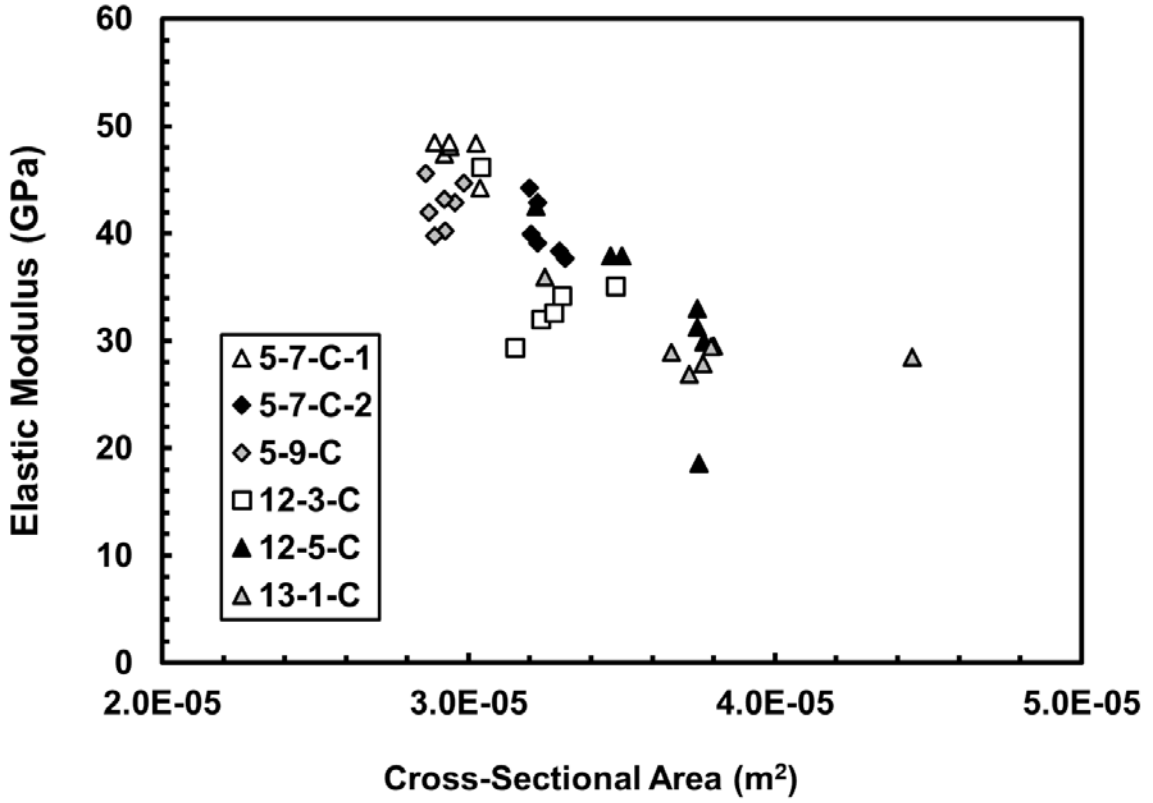

Figure 17. Elastic modulus vs cross-sectional area of Type 2 panels.

It is worth noting that in the case of the composite with Type 2 geopolymer matrix, there is a strong correlation between average elastic modulus and individual ply thickness. Because these panels all have the same number of reinforcing carbon-fiber fabric plies (14) increasing ply thickness indicates decreasing fiber volume fraction. Because tensile behavior of a 0/90 cross-ply is fiber-dominated, tensile modulus will decrease with decreasing fiber volume fraction. In our case, the elastic modulus should decrease with increasing ply thickness, as seen in Figure 18. Slight variations in this trend are likely be due to processing differences or fiber misalignment. Results in Figure 18 suggest that for the composites studied in this work, the optimal ply thickness would be ~0.3 mm or less if high stiffness is desired.

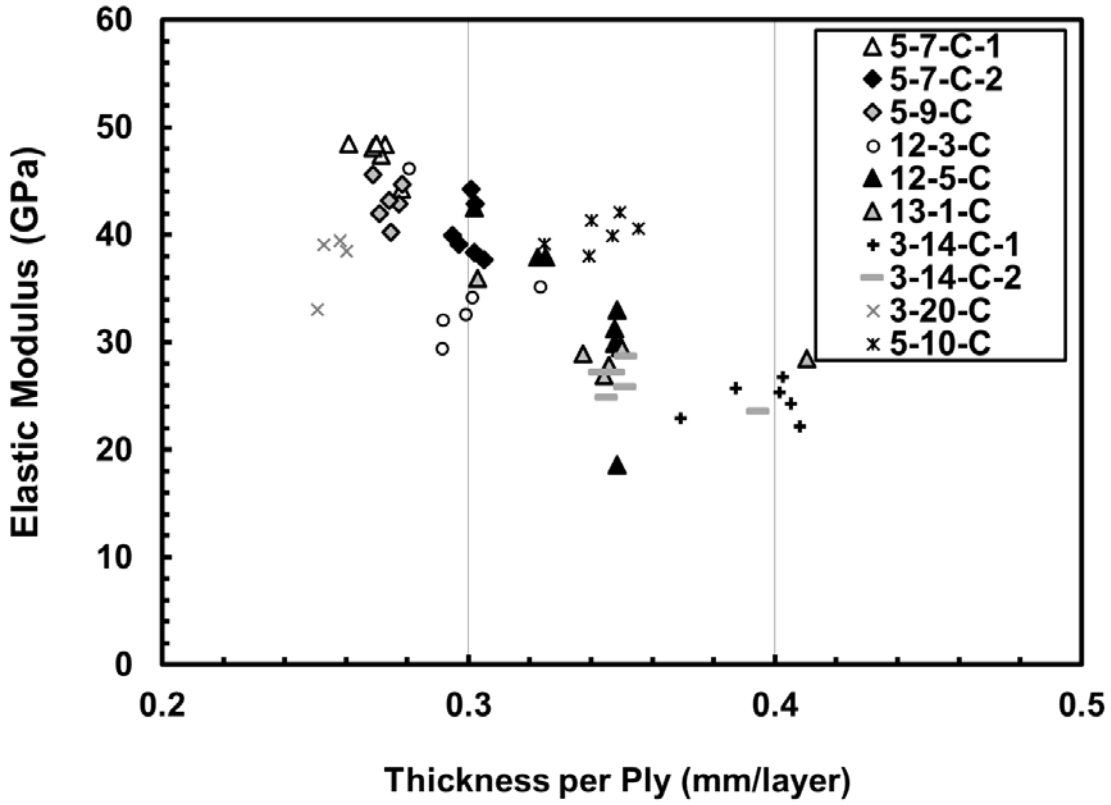

Figure 18. Elastic modulus vs thickness per ply of all panels tested.

5.3 Monotonic Tension at 23°C

Following room-temperature modulus, several tension tests to failure were performed at 23°C. Specimens of the composite with Type 2 geopolymer matrix from panels 5-9-C and 5-7-C-1 exhibit tensile stress-strain behavior typical for a 0/90 cross-ply (see Figure 19). The tensile stress-strain curves show initial linear elastic region with high elastic modulus, followed by nonlinear stress-strain behavior caused by matrix cracking. Some slight stiffening of the stress-strain curve obtained for specimen 5-7-1-3 is observed as stress exceeds 200 MPa, which is attributed to straightening of fibers and/or

to stress redistribution from matrix to fibers. Both stress-strain curves show fairly large failure strains, indicating that a large amount of progressive damage has occurred prior to ultimate composite failure.

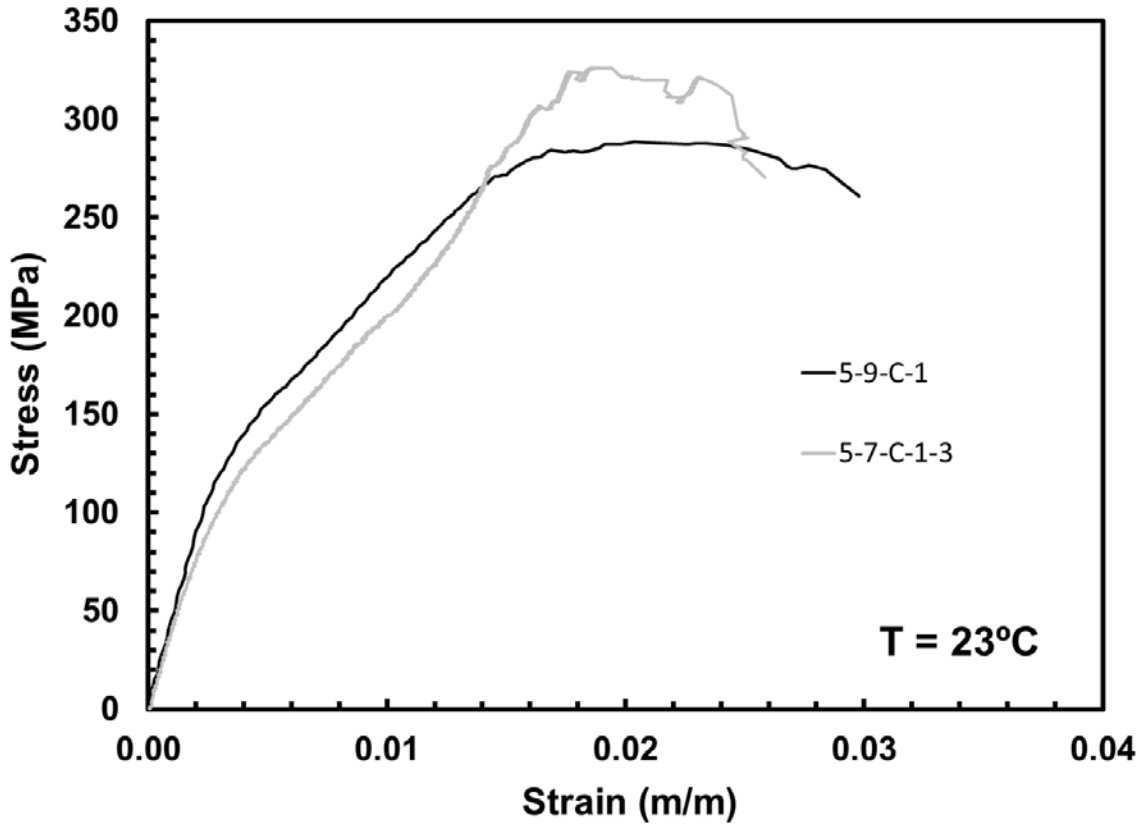

Figure 19. Tensile stress-strain curves obtained at 23°C for specimens 5-9-C-1 and 5-7-C-1-3 of the composite with Type 2 geopolymer matrix.

However, monotonic tensile tests of specimens of the composite with Type 2 geopolymer matrix from panel 5-7-C-2 suggest inferior material performance (see Figure 20). The elastic modulus is lower. Moreover, the stress-strain curve has a pronounced “S” shape. Finally, these specimens produced lower values of tensile strength and failure

strain. The arrow displays an estimated failure point for 5-7-C-2-2 due to the extensometer slipping during the test.

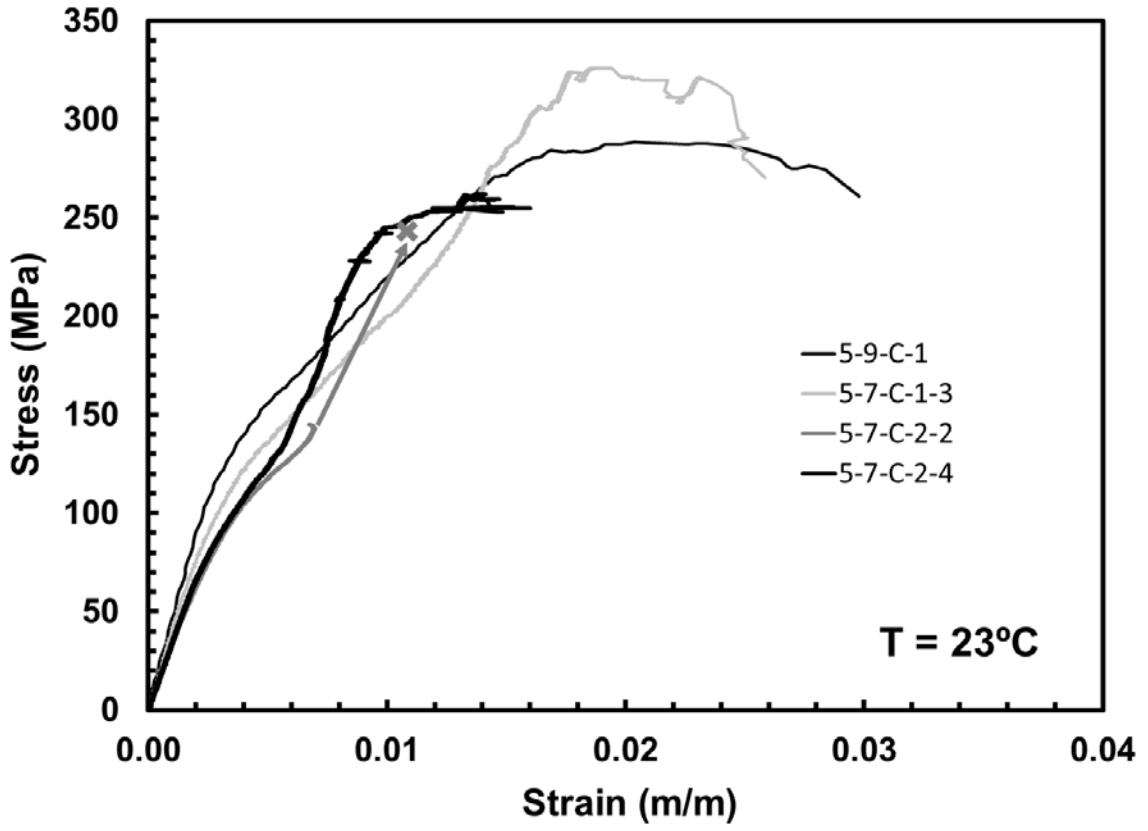

Figure 20. Tensile stress-strain curves obtained at 23°C for the composite with Type 2 geopolymer matrix.

Testing of specimens of the composite with Type 1 geopolymer matrix yielded surprising results (see Figure 21). Specimen 3-14-C-2-2 produced the highest UTS of 331 MPa. Recall that panel 3-14-C-2 exhibited a surface defect in a form of excess matrix on the surface resembling “elephant skin.” Specimen 3-14-C-1-1 also produced a reasonably high tensile strength. However, specimens from panels 3-14-C-1 and 3-14-C-2 produced poor elastic modulus. Yet specimen 3-14-C-2-2 does show the highest failure strain

obtained in tension tests at 23°C. It is recognized that deformation mechanism operating here is damage. Individual fibers in the composite fail progressively, then stress is redistributed to the remaining fibers causing them to deform further and so on.

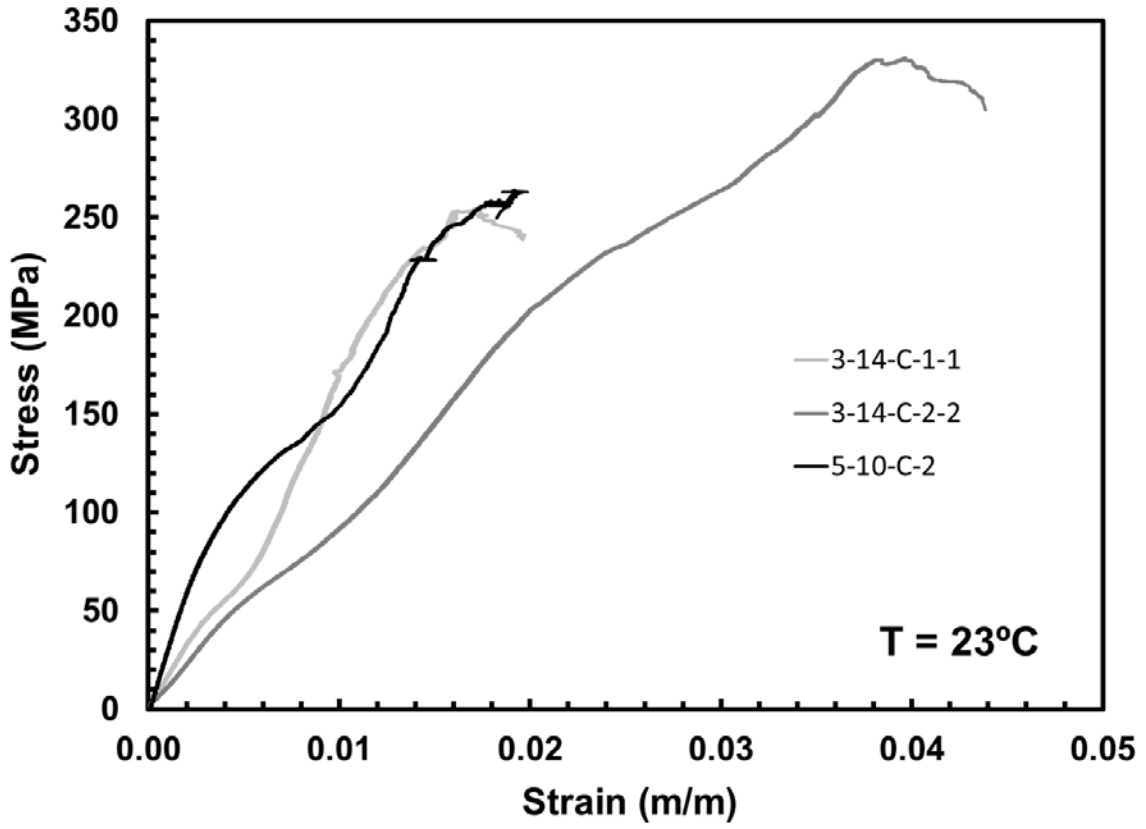

Figure 21. Tensile stress-strain curves obtained at 23°C for the composite with Type 1 geopolymer matrix.

Tensile properties obtained for geopolymer-matrix/carbon-fiber composites at 23°C in laboratory air are summarized in Table 5. Results in Table 5 reveal that specimens of the composite with Type 2 geopolymer matrix from panels 5-7-C-1 and 5-9-C offer the best performance overall. They produced high elastic modulus and high tensile strength. Specimen 3-14-C-2 has a high UTS as well, but its stiffness is less than

half the stiffness obtained for the composite with Type 2 geopolymer matrix. The data presented in Table 5 does not take into account the effect of dimpling the specimen for extensometer placement. Yet we believe that dimpling has negatively affected tensile properties of panels 3-14-C-1 and 3-14-C-2. These specimens were not dimpled for initial room-temperature modulus tests, where they still produced a low modulus.

Table 5. Tensile properties obtained for geopolymer-matrix/carbon-fiber composites at 23°C in laboratory air.

Panel	Geopolymer Matrix Type	Modulus E (GPa)	Tensile E (GPa)	UTS (MPa)
3-14-C-1	1a (NaGP)	24.5	18.0	262
3-14-C-2	1a (NaGP)	26.2	12.3	324
5-10-C	1b (NaGP)	40.2	35.3	264
5-7-C-1	2 (KGP)	47.5	42.8	326
5-7-C-2	2 (KGP)	40.4	35.5	253
5-9-C	2 (KGP)	42.6	44.0	288.6

Specimen failure in tension tests (manifested by the loss of load-carrying capacity) occurs much earlier than the separation of the specimen into two parts. Figure 22 shows considerable swelling and delamination in the specimen gage section. The geopolymer matrix cracks and fails to hold the composite together, causing the plies to delaminate and fail. As the displacement continues to increase, the specimen eventually separates into two parts. Careful examination of the failed specimens reveals no indication of a strong bond between the geopolymer matrix and the carbon fiber, with the matrix undergoing flaking off of the failed carbon fiber sections. A stronger, less fragile matrix or stronger fiber-matrix bond would likely yield a different failure mode and might also improve composite performance. A stronger matrix might also improve

handling qualities, which is why the blue tech towels are used because of the large amount of geopolymer debris and dust coming off the specimens from comminution.

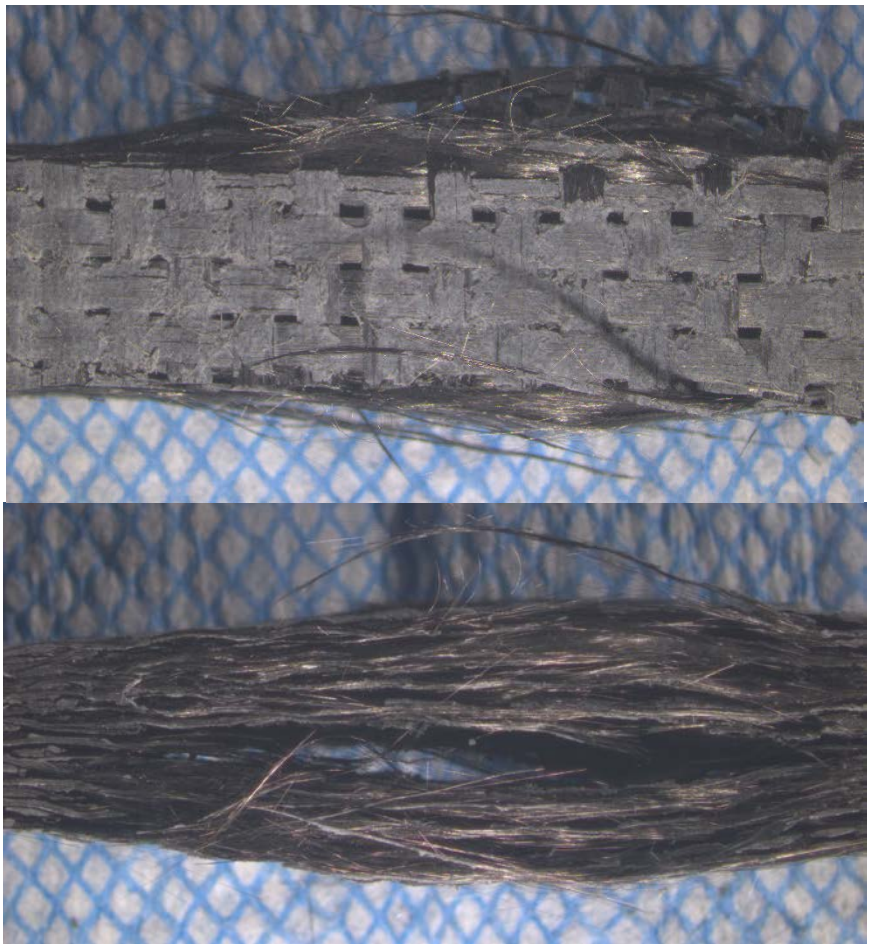

Figure 22. Specimen 5-7-C-1-3, failed in tension test at 23°C.

5.4 Thermal Exposure and Dimpling Effects

In order to conduct elevated temperature tests, one specimen (5-9-C-5) was instrumented with thermocouples for temperature calibration. This specimen followed the calibration procedure and the single zone furnace command of 262°C brought the best

results, with 300±10°C as measured on the specimen. Thus 262°C was chosen as the temperature controller set point for obtaining 300°C on the specimen. The first specimen to be tested at elevated temperature was specimen 5-9-C-7. During heat-up to test temperature of 300°C and prior to any mechanical loading being applied, it was discovered that the strain was not behaving as expected. Most materials undergo thermal expansion with increasing temperature. In contrast, specimen 5-9-C-7 appeared to produce negative strain as the temperature was increased from 23 to 300°C (see Figure 23).

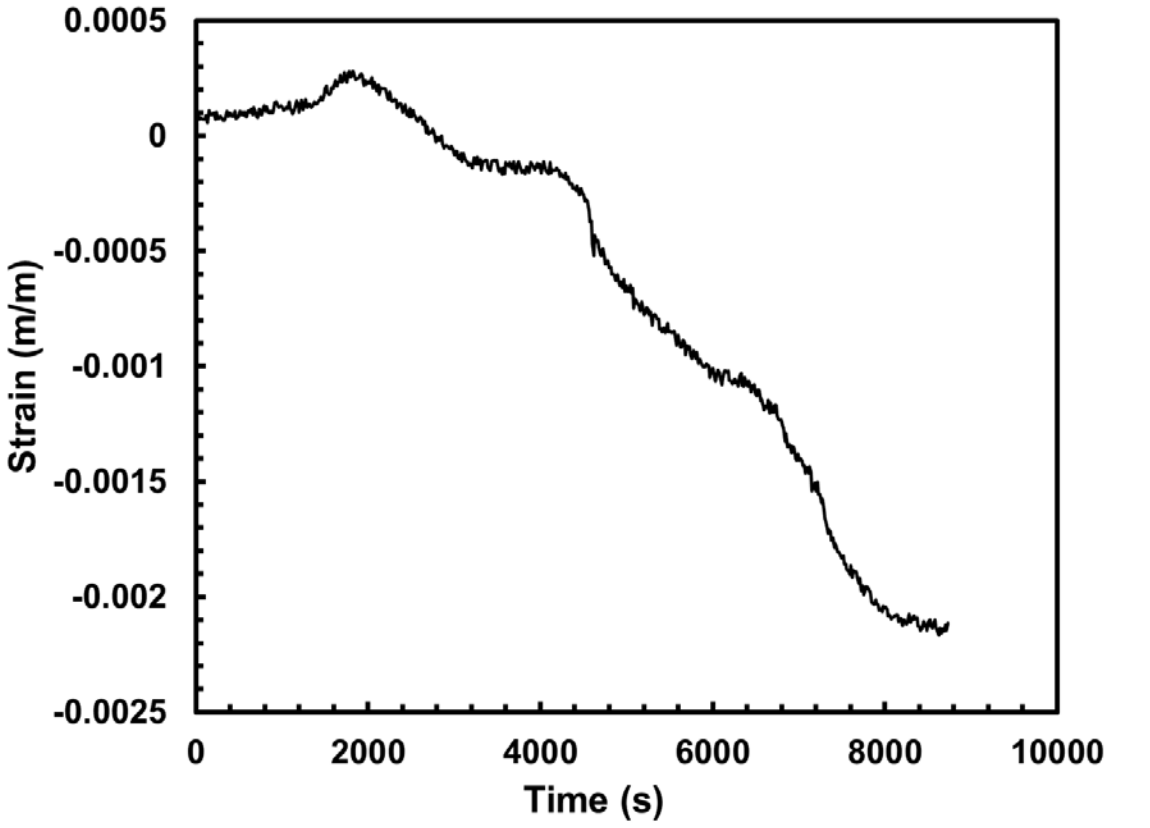

Figure 23. Strain vs. time curve obtained for specimen 5-9-C-7 during temperature increase from 23 to 300°C under zero load.

It was hypothesized that the rods might be slipping on the surface, because the surface might be more slippery or fragile at temperature. Thus the test was stopped and the furnace commanded off. To prevent the apparent extensometer slipping, it was decided to dimple test specimens prior to testing. It was also decided to start documenting before and after effects of thermal exposure to try and understand how the material is behaving in regards to the thermal environment which is causing this strain behavior. However, erratic strain behavior during heat up to test temperature was still observed in subsequent tests (see Figure 24). Because the specimens referred to in Figure 24 were dimpled, extensometer slipping was unlikely. We conclude that the erratic strain behavior was caused by other phenomena.

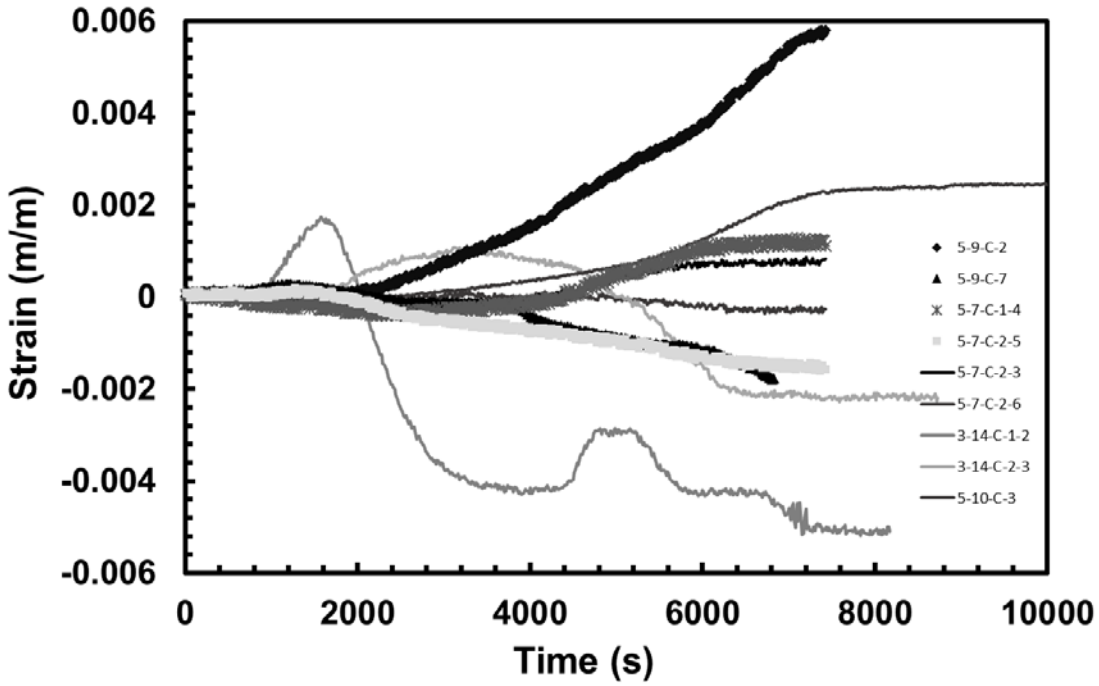

Figure 24. Strain vs. time behavior observed for geopolymer matrix composite specimens during temperature rise from 23 to 300°C under zero load. Strain behavior is erratic. Strain measurements vary widely even for specimens cut from the same composite panel.

Examination of the test specimens before and after thermal exposure (under zero load) with an optical microscope revealed extensive matrix cracking. The erratic formation and growth of matrix cracks during temperature rise is likely caused by dehydration of the geopolymer matrix. As a result, a reliable strain measurement cannot be obtained during heat-up to test temperature due to the cracking. Hence thermal strains could not be measured and linear thermal expansion coefficients could not be calculated in this work.

Once the test temperature of 300°C is reached, specimens are held at test temperature at zero load for at least 45 min prior to mechanical load being applied. During this dwell period, the strain appears to reach a relatively stable steady-state behavior, suggesting that progressive matrix cracking caused by dehydration due to the thermal exposure has stopped (or nearly stopped). Once this rapid damage growth in the geopolymer matrix stops and thermally-induced matrix cracking reaches a steady state, a more reliable strain measurement can be obtained. Hence we believe that strains measured during mechanical loading at 300°C provide useful information.

To confirm the findings discussed above, we examined the response to thermal exposure of specimens tested in fatigue at 300°C). Note that these specimens were not dimpled for extensometer placement in order not to cause damage to the matrix by dimpling. The strain vs. time response of specimens from panel 3-14-C-1 to temperature rise from 23 to 300°C is depicted in Figure 25. The strain behavior in Figure 25 is as erratic as that shown in Figure 24.

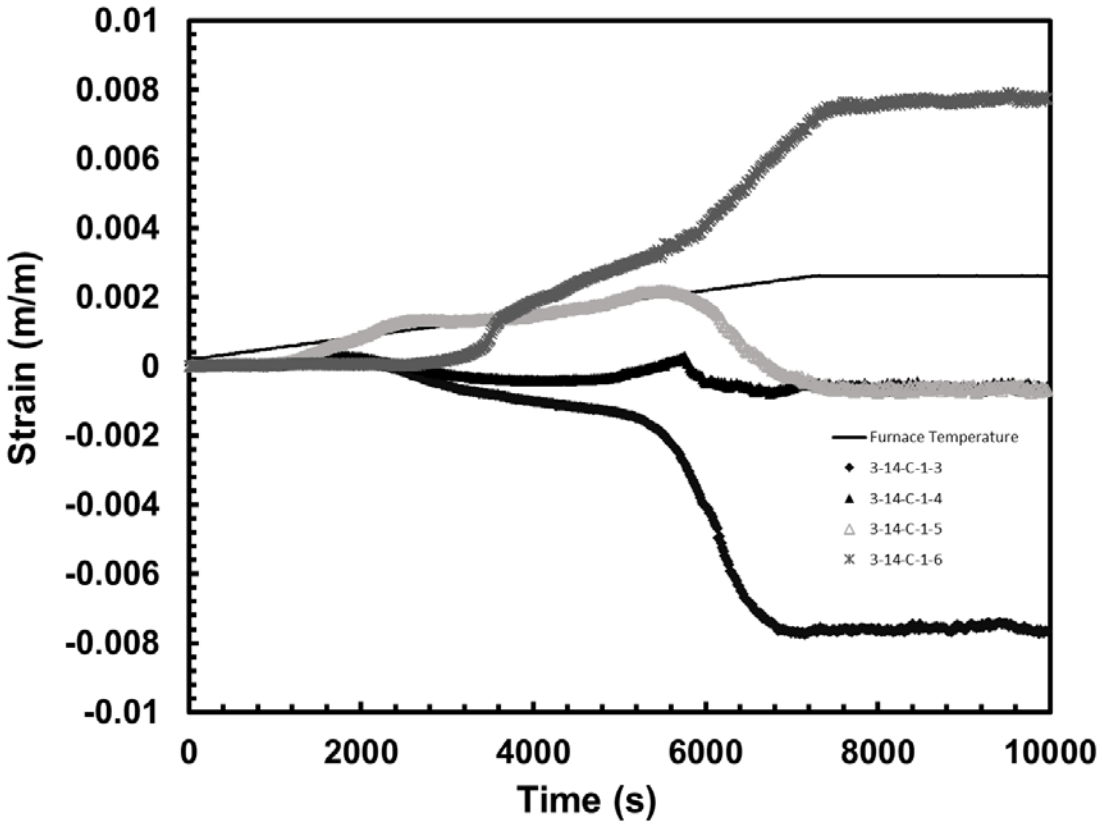

Figure 25. Strain vs. time behavior observed for geopolymer matrix composite specimens from panel 3-14-C-1 during temperature rise from 23 to 300°C under zero load. Specimens were not dimpled prior to thermal exposure.

The results in Figure 25 reveal an interesting trend. As exposure time approaches 5600 s, many of the specimens appear to take a sudden curve towards their end state. 5600 seconds roughly corresponds to a furnace command signal of 206.5°C, which corresponds to a specimen temperature of ≈ 245°C. It is recognized that geopolymers undergo dehydration during heating. The dehydration process can be divided into three phases: (1) the loss of physically bonded water as temperature increases to 100°C, (2) the loss of chemically bonded water as temperature increases from 100 to 300°C, and (3) the dehydroxylation of OH as temperature exceeds 300°C [5]. Typically, most of the water loss occurs during Phase 1 as the temperature rises to 100°C as the physically bonded

water evaporates [5]. Phase 1 of the dehydration process causes little damage to the material [5]. The thermal exposure plots suggest that considerable shrinkage and microcracking must be due to the loss of chemically bonded water as the temperature rises from 100 to 300°C.

To achieve a better understanding of the material response to thermal exposure, specimens were first examined with an optical microscope, then subjected to temperature increase to 300°C followed by a 45-min dwell at 300°C (the first thermal exposure), and finally cooled down to room temperature and once again examined with an optical microscope. The strain measurements obtained during this process were analyzed as discussed before. The effect of thermal exposure on composite microstructure can be clearly seen in the micrographs, with Figure 26 showing a severe case of matrix cracking and thickness swelling due to thermal exposure. For Type 1b and Type 2 geopolymer matrix materials this behavior was less pronounced and harder to detect on the thickness view, but looking at the specimen surface there are still signs of dehydration and microcracking of the matrix (Figure 27).

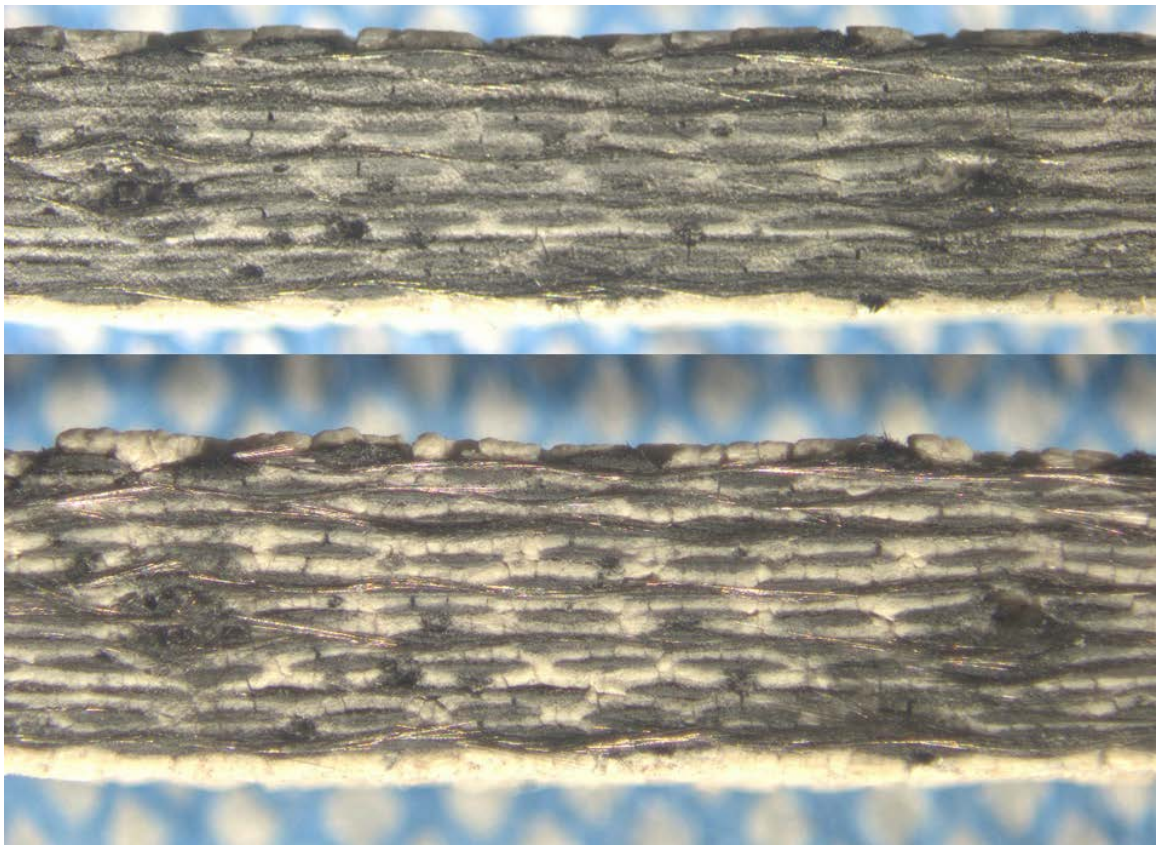

Figure 26. 3-14-C-1-2 gage section before thermal exposure (top) and after thermal exposure (bottom). Dimples (dark depressions) can be seen on left and right hand side of frame.

Figure 27. Microcracking of matrix on surface of 5-7-C-14 Type 2 geopolymer matrix specimen before thermal exposure (left) and after (right).

After the first exposure and micrographs were taken, the specimens were ready for mechanical testing at 300°C. Following the test procedure developed in this work, test specimens were once again heated under zero load to 300°C at the commanded rate of 2°C/min to the set point, allowed to thermally equilibrate for at least 45 min at 300°C (the second thermal exposure), then subjected to a desired mechanical loading. Hence the tensile test specimens experienced two thermal exposures in the course of their history.

We note significant changes in the strain vs. time behavior produced during the second thermal exposure compared to that produced during the first thermal exposure. During the second thermal exposure, an initial decrease in strain is still observed (see Figures 28 and 29). However, this change in strain is an order of magnitude less than the change observed during the first thermal exposure. Overall, strain changes little during the secondary thermal exposure, indicting the damage state of the matrix (i. e. matrix microcracking caused by temperature increase) has stabilized.

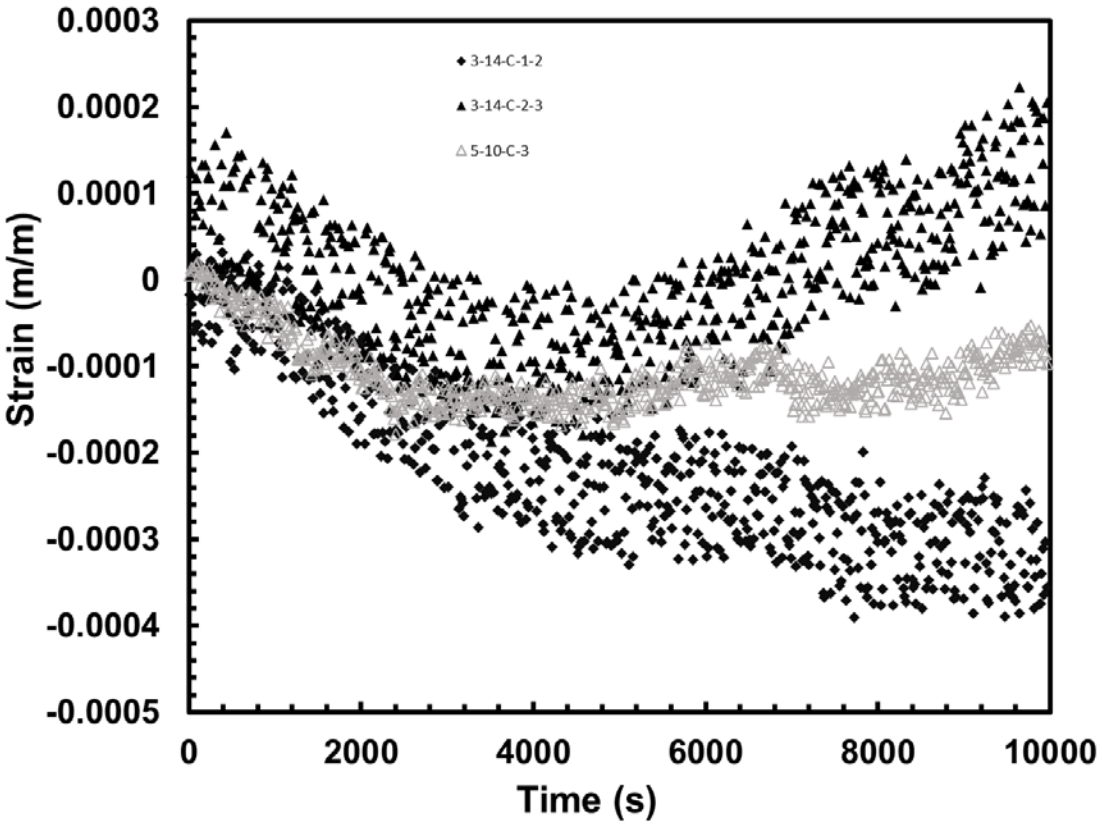

Figure 28. Strain vs. time behavior observed for composite specimens with geopolymer matrix of Type 1 during second temperature exposure.

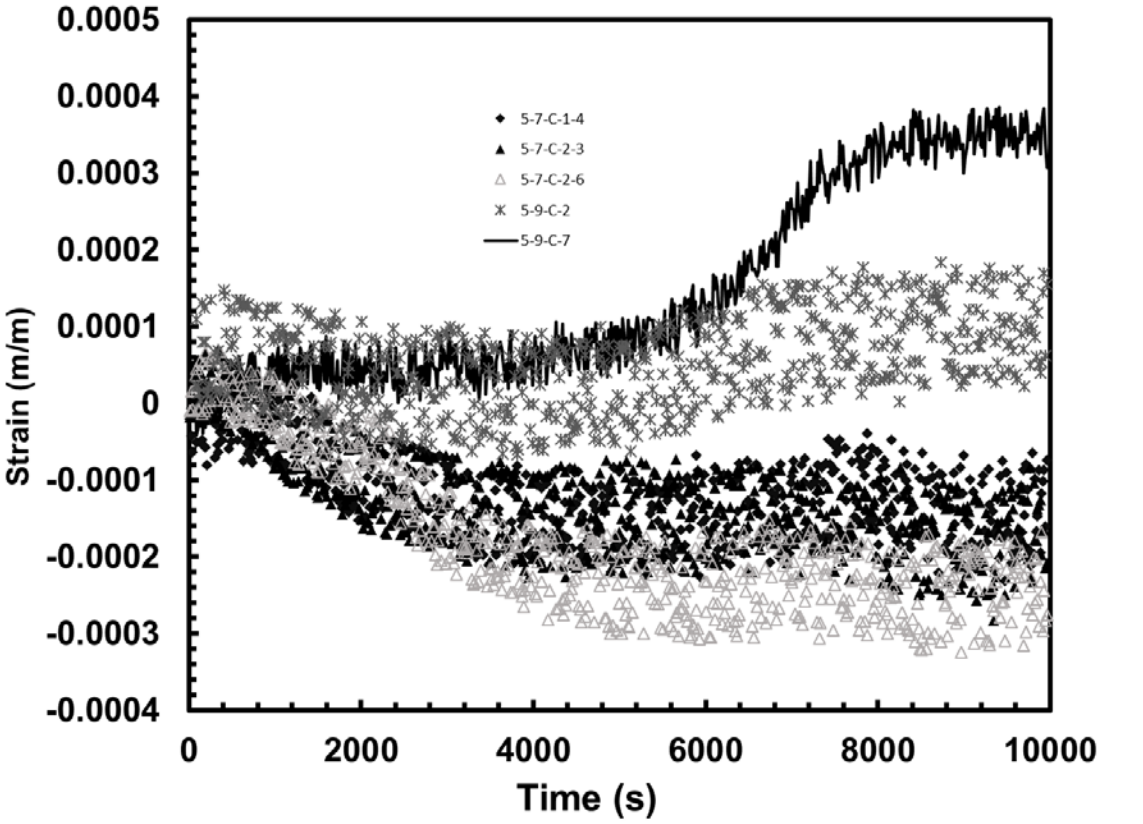

Figure 29. Strain vs. time behavior observed for composite specimens with geopolymer matrix of Type 2 during second temperature exposure.

Another important observation was made when specimens was observed before and after thermal exposure. Noticeable through-thickness swelling in the specimen gage section occurred during thermal exposure. Additionally, thermal exposure resulted in significant mass loss likely due to the dehydration of the geopolymer matrix. The through-thickness swelling measurements and mass loss are summarized in Table 6.

The data in Table 6 may not be statistically significant, with only 1-3 specimens from each panel being considered. Nonetheless the results in Table 6 reveal a large difference in swelling observed for the composite with Type 1 geopolymer matrix and that observed for the composite with Type 2 geopolymer matrix. The composite with

Type 1 matrix experiences considerably greater swelling than the composite with Type 2 matrix. Panels 5-7-C-1 and 5-7-C-2 of the composite with Type 2 matrix had negligible dimensional changes. Whereas panel 5-9-C of the composite with Type 2 matrix exhibited some swelling, is was still significantly less than the swelling observed for panels of the composite with Type 1 matrix. Such significant differences in the behavior of the composites with Type 1 and Type 2 geopolymer matrices are likely due to differences in processing and chemistry. Mass loss seems to be consistent at 2-3% across all composite panels. It should be noted that the mass measurements were obtained by weighing each specimen in whole, including the tabs, so the mass loss is not truly representative of what the composite suffers in mass loss in the test gage section. However, the relative consistency of the mass loss measurements provide evidence of a similar dehydration behavior between the panels.

Table 6. Through-thickness swelling and mass loss due to thermal exposure.

Panel	Geopolymer Matrix Type	Swelling %	Mass loss %	Sample Size
3-14-C-1	Type 1a (NaGP)	15.9	-3.1	1
3-14-C-2	Type 1a (NaGP)	17.1	-2.4	1
5-10-C	Type 1b (NaGP)	17.4	-1.7	1
5-7-C-1	Type 2 (KGP)	0.7	-	1
5-7-C-2	Type 2 (KGP)	-0.5	-2.3	3
5-9-C	Type 2 (KGP)	5.2	-	1

Examination of the test specimens with an optical microscope also revealed that dimpling the specimen for extensometer placement causes appreciable matrix cracking (Figure 30). This practice was also found to reduce the initial stiffness of the materials without reducing the strength. Recognizing that dimpling of the specimen causes damage to the geopolymer matrix, the remaining specimens were not dimpled.

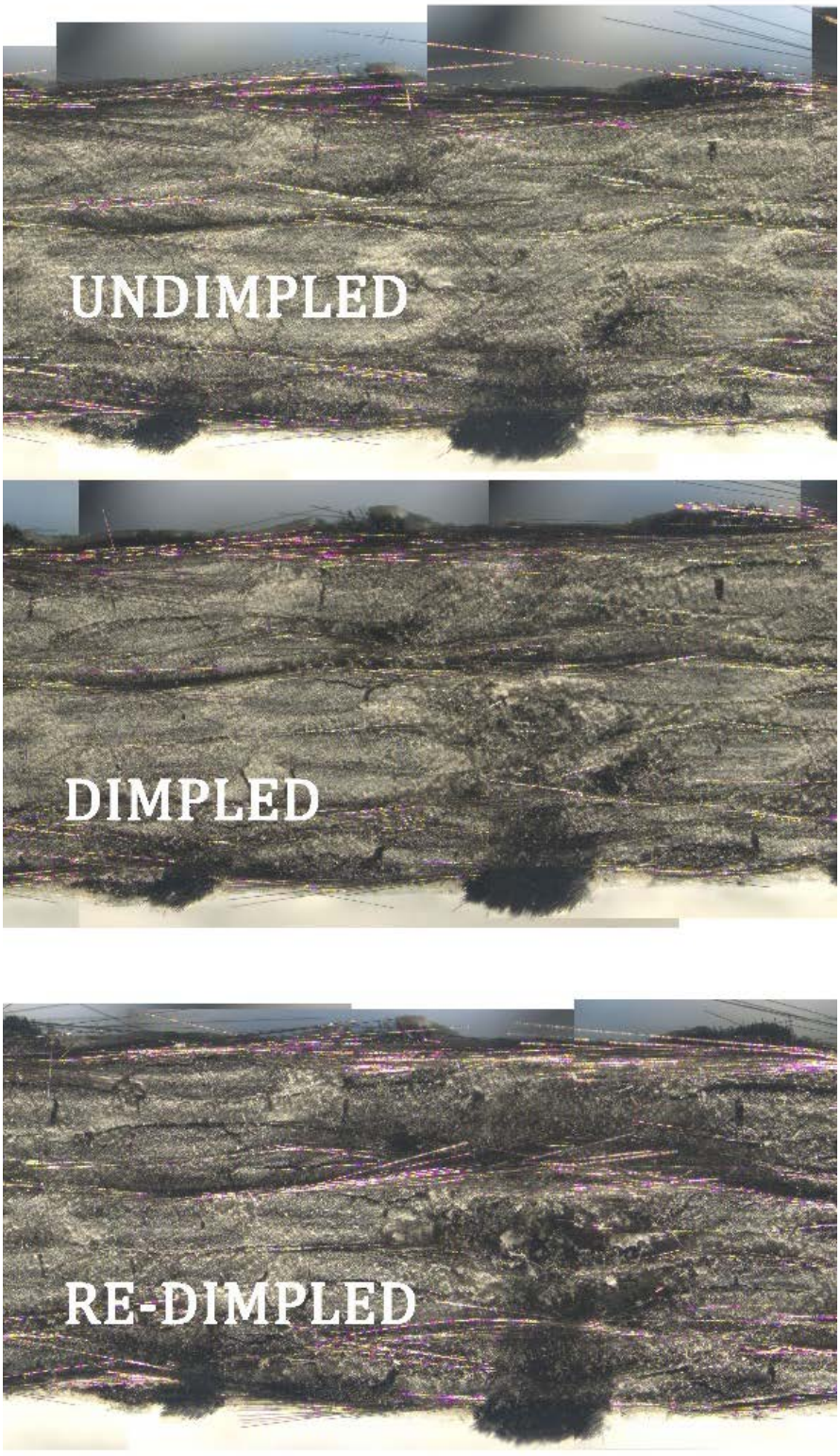

Figure 30. Cracks on the side of a specimen appear from dimpling and grow from re-dimpling.

5.5 Monotonic Tension at 300°C

Tension tests to failure were performed at 300°C according to the test procedure described in Section 4.3.2. As expected, the modulus and tensile strength decreased with increasing temperature. The tensile stress-strain curve obtained for specimen 5-9-C-7 of the composite with Type 2 geopolymer matrix is shown in Figure 31. The "S" shape of the stress-strain curve in Figure 31 can be attributed to "stiffening" of carbon fibers with increasing strain. The carbon fibers are likely straightening (see schematic in Figure 32) as matrix cracking progresses, resulting in increase in stiffness. The UTS obtained in this test at 300°C (240 MPa) was 17% lower than the UTS obtained for this composite panel at 23°C. This high strength retention is due to the carbon fibers playing a dominant role in the composite performance.

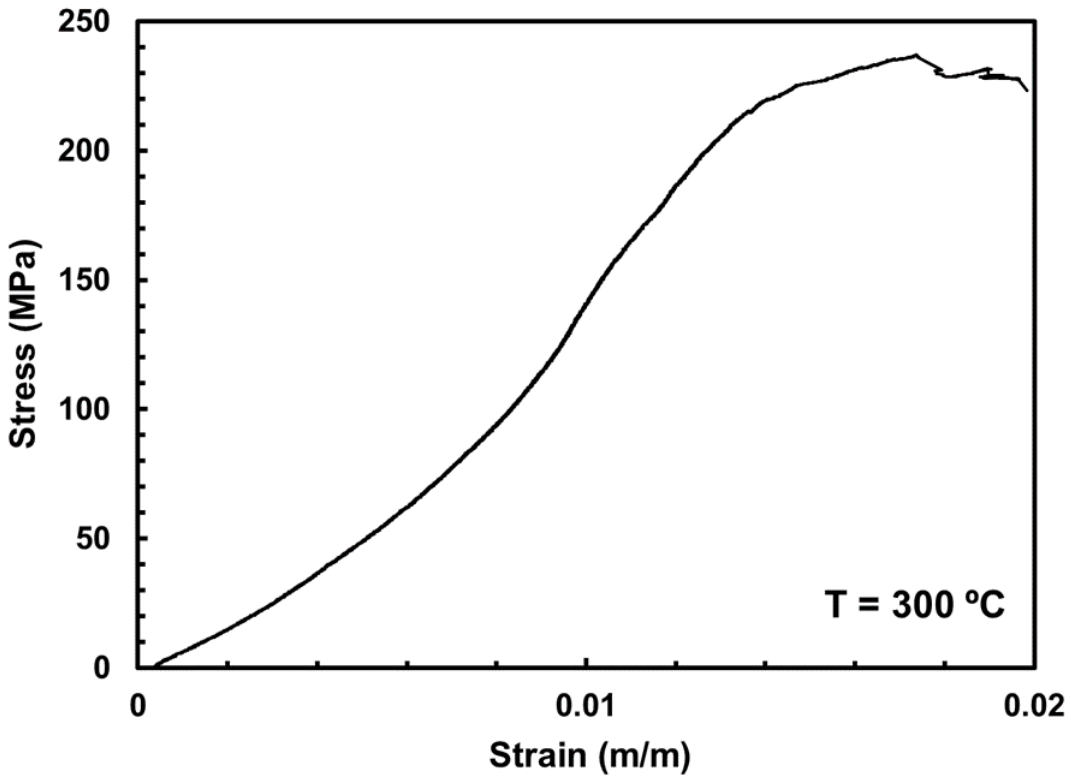

Figure 31. Tensile stress-strain curve obtained at 300°C for specimen 5-9-C-7 of the composite with Type 2 geopolymer matrix.

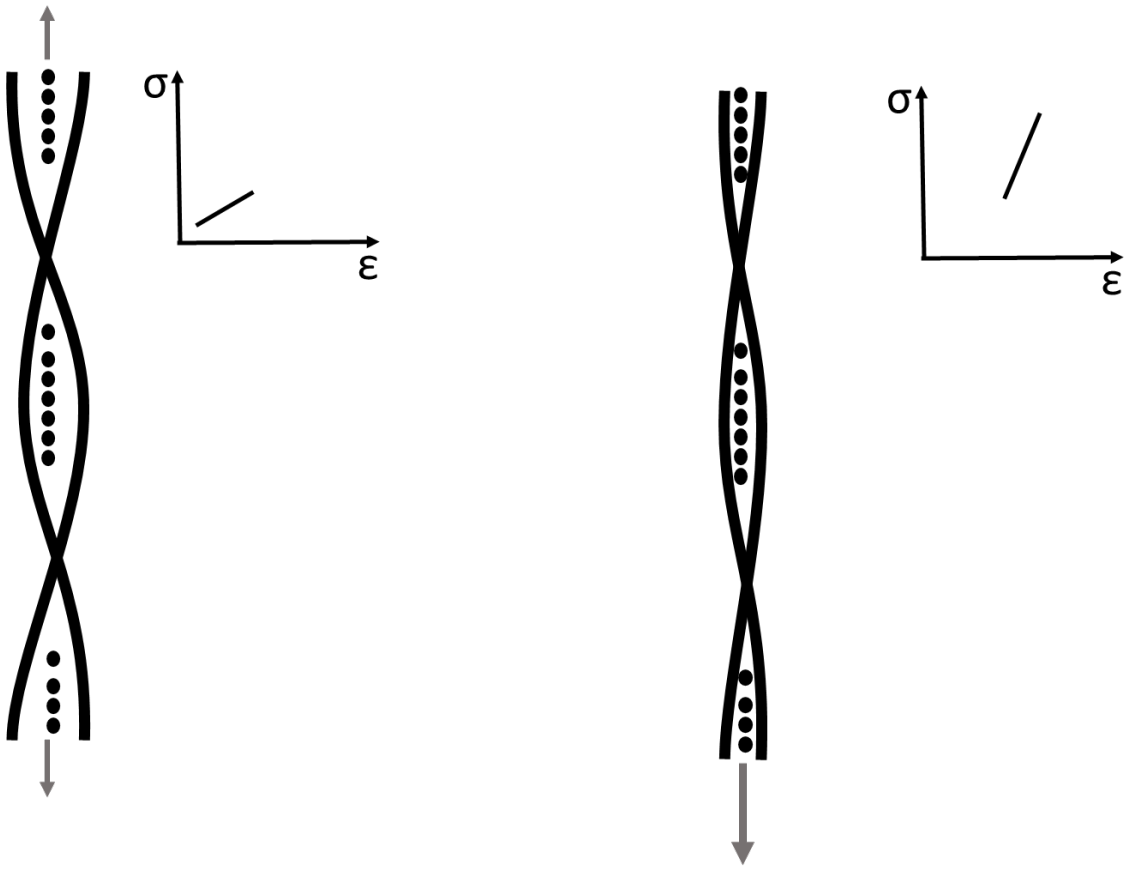

Figure 32. Schematic depicting straightening of reinforcing fibers with increasing strain.

The tensile stress-strain curve obtained for specimen 5-9-C-2 of the composite with Type 2 geopolymer matrix at 300°C is shown in Figure 33 together with the stress-strain curve obtained for specimen 5-9-C-7. Although the two specimens were cut from the same panel, the stress-strain curve obtained for specimen 5-9-C-2 does not exhibit early stiffening noted for specimen 5-9-C-7. During the loading there was a spike in the displacement which caused the spike/dip in the stress around 0.8% strain. Instead of continuing with the stiffening behavior of 5-9-C-7, this spike must have caused enough damage to accelerate the progressive failure of the 0° fibers, causing a loss of stiffness.

This accelerated fiber failure might have a minor effect on the loss of UTS when compared to the other test, but the two results are relatively similar with UTS of 239.9 and 218 MPa, within 10% of each other for a low population sample size.

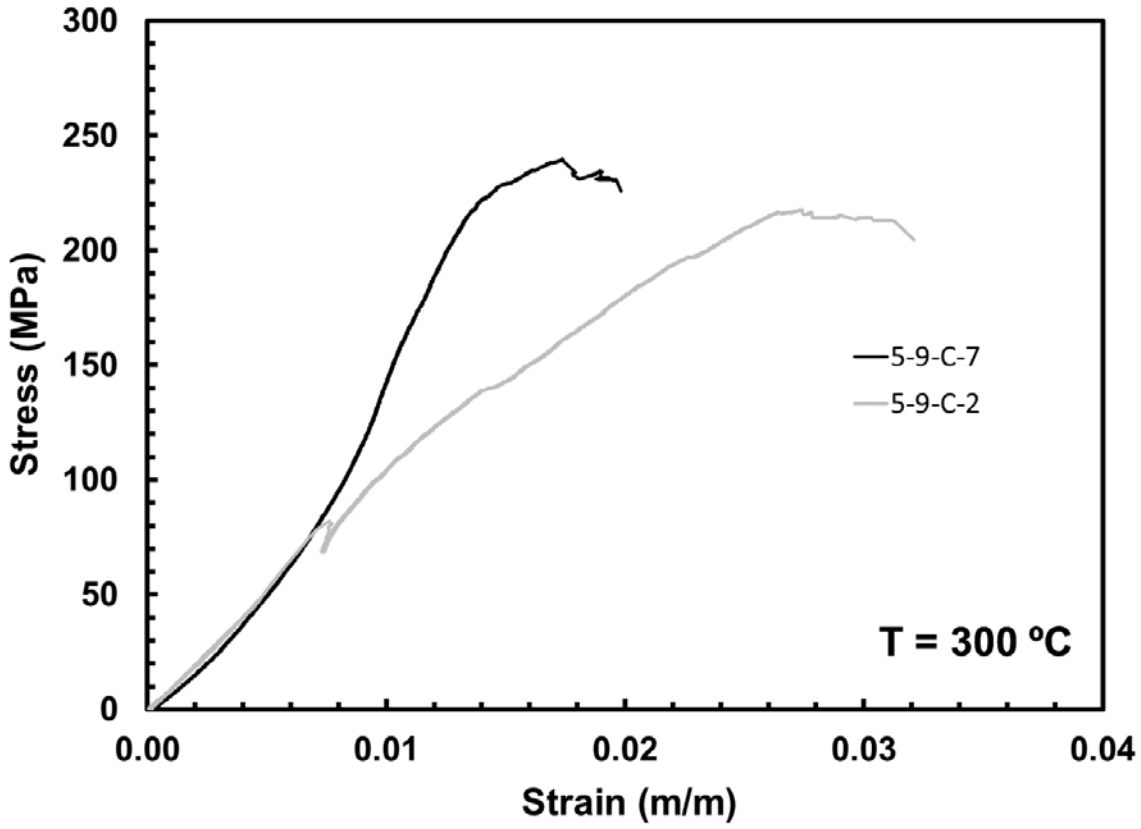

Figure 33. Tensile stress-strain curved obtained at 300°C for specimen 5-9-C-7 and 5-9-C-2 of the composite with Type 2 geopolymer matrix.

Further tensile testing of Type 2 geopolymer matrix produced different stress-strain behavior than that obtained for specimens from panel 5-9-C (Figure 34). The tensile stress-strain curve obtained for specimen 5-7-C-1-4 is nearly linear up to the UTS. In contrast, the stress-strain curves obtained for specimens from panel 5-7-C-2 have a pronounced “S” shape with an initial linear region for stresses up to ~25 MPa. Yet the

initial modulus obtained for specimens from panel 5-7-C-2 is close to that produced by specimen 5-7-C-1-4. Note that the stress-strain response of specimens from panel 5-7-C-2 is likely affected by multiple voids seen under optical microscope prior to testing (Figure 35).

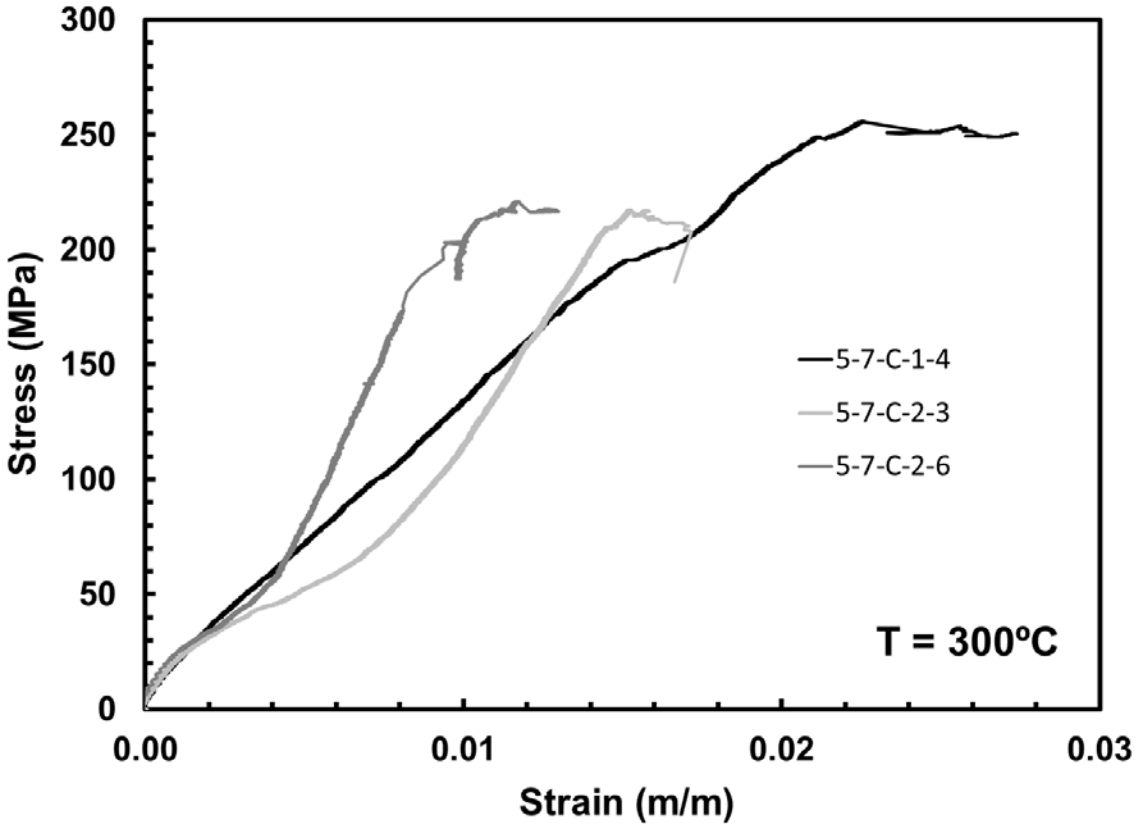

Figure 34. Tensile stress-strain curved obtained at 300°C for composite panels 5-7-C-1 and 5-7-C-2 with Type 2 geopolymer matrix.

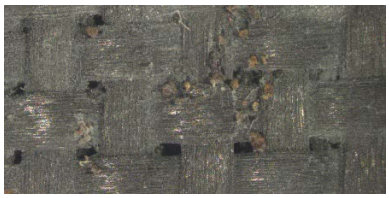

Figure 35. Voids in the matrix located at fiber cross-overs on the surface of the composite specimen 5-7-C-2-3 with Type 2 geopolymer matrix.

The tensile stress-strain curves obtained for composite with Type 1 geopolymer matrix at 300°C are shown in Figure 36. The stress-strain curves obtained for panels 3-14-C-1 and 3-14-C-2 have a pronounced "S" shape with a short initial linear region. In contrast, the stress-strain curve obtained for specimen from panel 5-10-C is nearly linear up to the UTS.

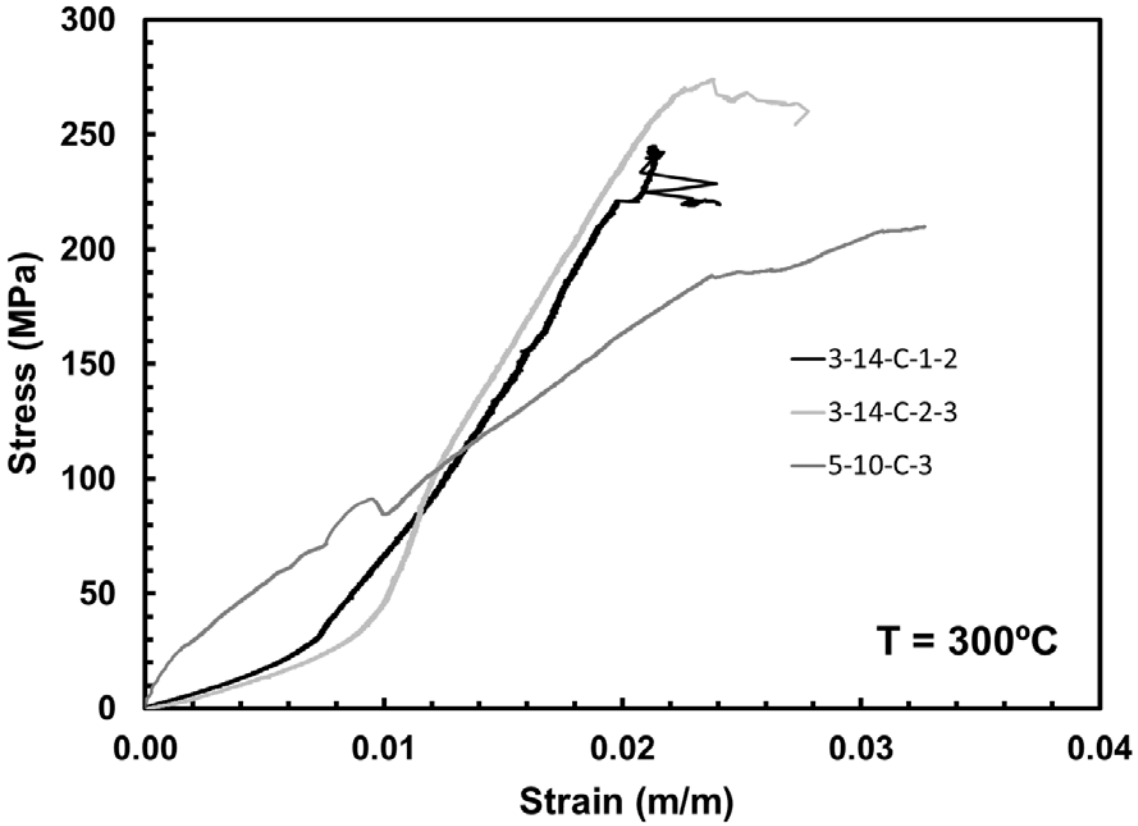

Figure 36. Tensile stress-strain curved obtained at 300°C for composite with Type 1 geopolymer matrix.

5.6 Tension-Tension Fatigue at 23°C

An exploratory tension-tension fatigue test was performed at 23°C for composite specimen 3-14-C-2-4 with Type 1 geopolymer matrix. The maximum fatigue stress was set to 194 MPa, which represents 60% of the average UTS obtained for this composite at 23°C. The specimen achieved fatigue run-out defined as 200,000 cycles. Failure of specimen did not occur when the test was terminated after 210,000 cycles. Figure 37 shows evolution of the stress-strain hysteresis behavior observed in this test. The stress-strain curve produced during the first cycle reflects significant matrix degradation. The stress-strain curves produced during subsequent cycles exhibit considerably less hysteresis. Swelling of the specimens was observed during the loading portion of the fatigue cycle, similar to observations reported by Wilkinson [12]. Such swelling of the specimens is likely due to the straightening of the fibers, which bulge out due to the cracked matrix material between the plies when under increasing load.

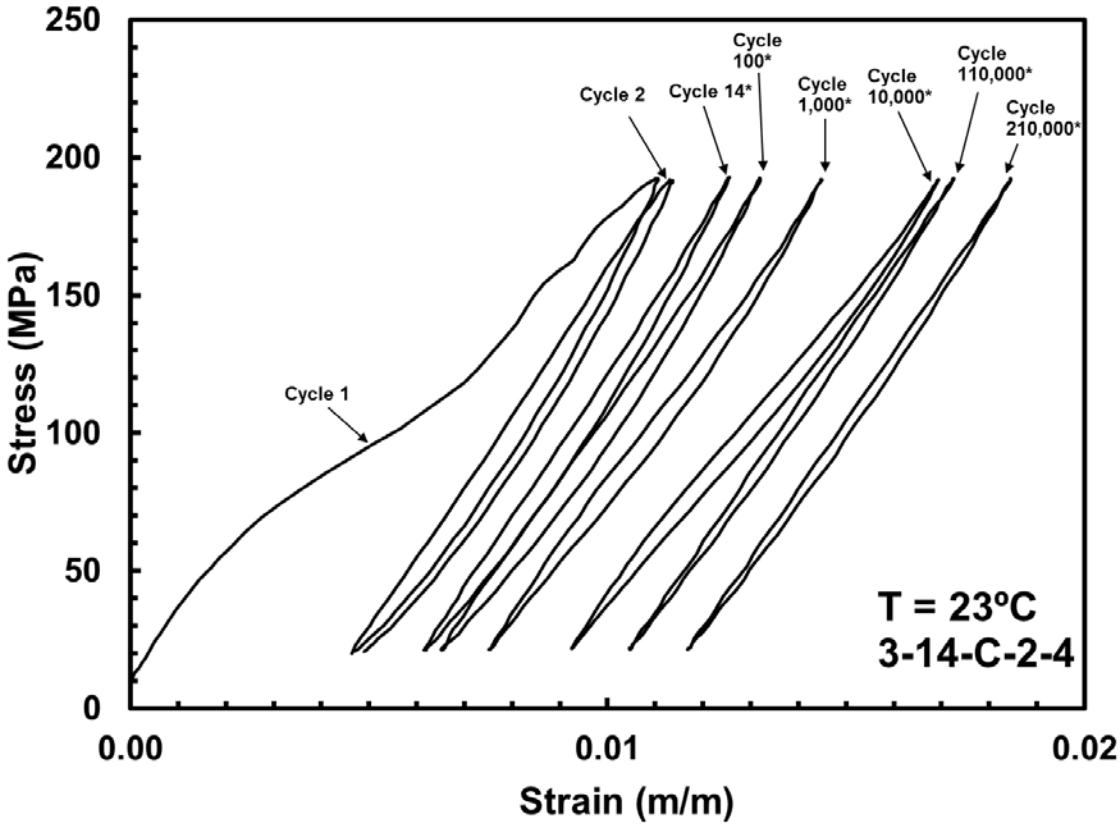

Figure 37. Stress-strain hysteresis response of composite specimen 3-14-C-2-4 with Type 1 geopolymer matrix in a tension-tension fatigue test performed at 23°C. Due to extensometer slippage, the cycles with an asterisk (*) are separated arbitrarily to show hysteresis curve evolution.

Recall that failure of specimen did not occur when the test was terminated after 210,000 cycles. Upon reaching 210,000 cycles the specimen was unloaded to a low positive load to avoid compression. Then tension test to failure was performed to measure the retained properties. The tensile stress-strain curve obtained for this pre-fatigued specimen (Figure 38) is nearly linear to failure, suggesting that 0° fibers carry the load. The retained tensile strength was 314 MPa. The UTS values obtained for this composite at 23°C were 317 and 331 MPa. It appears that the composite retains nearly 100% of its

tensile strength. Of course, this result may be an artifact of considerable data scatter exhibited by the composites studied in this work.

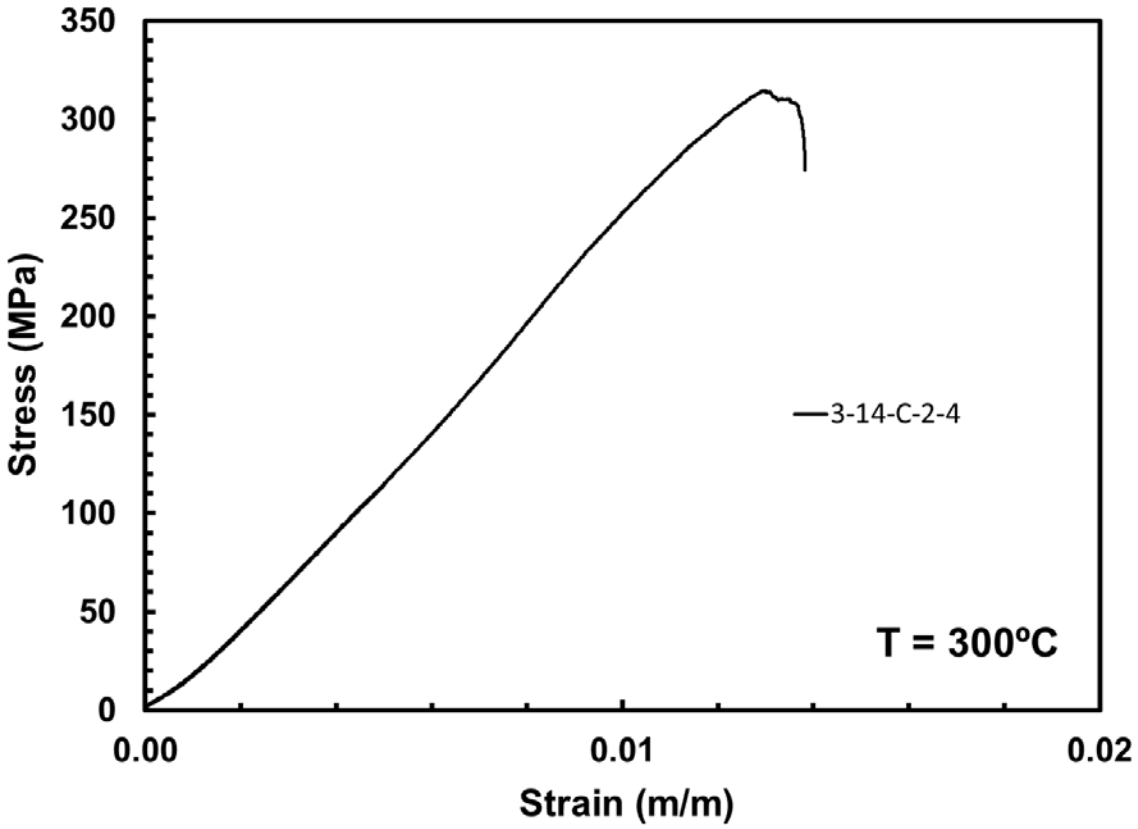

Figure 38. Tensile stress-strain curve obtained for composite specimen 3-14-C-2-4 with Type 1 geopolymer matrix following 210,000 tension-tension fatigue cycles at 23°C.

5.7 Tension-Tension Fatigue at 300°C

Tension-tension fatigue tests were performed at 300°C according to the procedure outlined in Section 4.3.3. Results are summarized in Table 7.

Table 7. Summary of fatigue results obtained for geopolymer matrix composites at 23 and 300°C in laboratory air.

Specimen	Geopolymer Matrix Type	Temperature (°C)	Peak Stress (MPa)	Cycles to Failure (N)
3-14-C-1-3	1a (NaGP)	300	104.8	58,393
3-14-C-1-4	1a (NaGP)	300	131	28,312
3-14-C-1-5	1a (NaGP)	300	157.2	12,590
3-14-C-1-6	1a (NaGP)	300	183.75	1,876
3-14-C-2-1	1a (NaGP)	300	194.4	4,708
3-14-C-2-4	1a (NaGP)	23	194.4	210,000+
5-10-c-4	1b (NaGP)	300	122	77,006
5-10-C-5	1b (NaGP)	300	78.74	200,000+
5-10-C-6	1b (NaGP)	300	98.5	120,148
5-10-C-7	1b (NaGP)	300	183	6,798
5-9-C-3	2 (KGP)	300	144.3	24,415
5-9-C-4	2 (KGP)	300	173.16	3,403
5-9-C-6	2 (KGP)	300	86.58	200,000+
5-9-C-8	2 (KGP)	300	115	71,402
5-7-C-1-1	2 (KGP)	300	244.5	50
5-7-C-1-2	2 (KGP)	300	97.8	200,000+
5-7-C-1-5	2 (KGP)	300	195.6	17,225
5-7-C-1-6	2 (KGP)	300	130.4	114,050

Specimen 3-14-C-2-1 with Type 1 geopolymer matrix was tested at 300°C with the maximum fatigue stress of 194 MPa. Recall that specimen 3-14-C-2-4 was subjected to the same peak stress at 23°C. Results presented in Table 8 demonstrate that temperature increase from 23 to 300°C significantly degrades fatigue performance of the

composite with Type 1 geopolymer matrix. For a given maximum stress level, the cyclic life at 300°C was nearly two orders of magnitude lower than that at 23°C. The degradation of the fatigue performance at 300°C is likely accelerated by rapid damage development in the matrix, leading to composite delamination early in cyclic life.

Table 8. Comparison of 3-14-C-2 specimens subject to tension-tension fatigue.

Specimen	Peak Stress (MPa)	Test Temperature (°C)	Tensile Strength % After Test	Cycles to Failure
3-14-C-2-4	194.4	23	~95%	210,000+ (runout)
3-14-C-2-1	194.4	300	N/A	4707

Figure 39 shows evolution of the stress-strain hysteresis behavior obtained for specimen 3-14-C-2-1 at 300°C. The stress-strain curve produced during the first cycle reflects considerable damage occurring to the matrix as the load increases to reach maximum fatigue stress. The stress-strain hysteresis loops produced in subsequent cycles reflect nearly linear behavior throughout the load cycle. This result suggests that once extensive damage occurs to the matrix during the first cycle, the load is transferred to carbon fibers. Afterwards the response of the composite is controlled by the fibers with minimal contribution from the matrix. The results in Figure 39 also indicate that strain ratcheting (progressive strain accumulation with fatigue cycles) takes place.

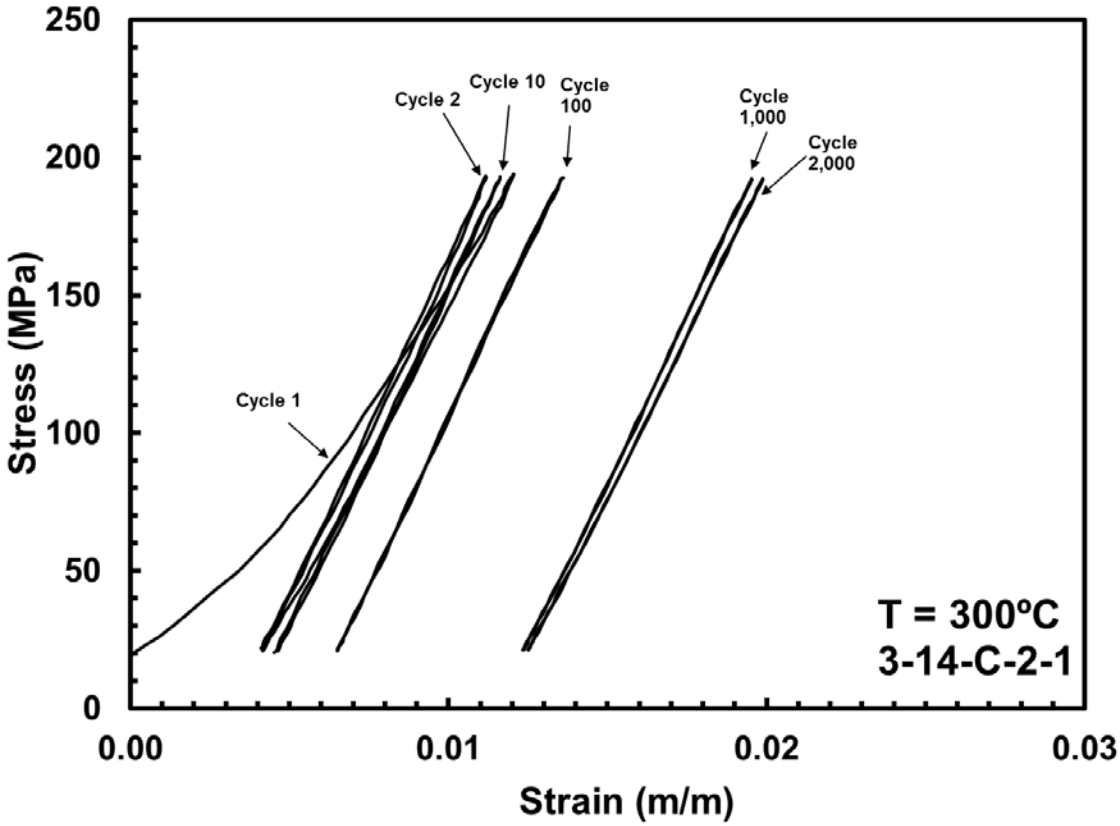

Figure 39. Evolution of stress-strain hysteresis response of specimen 3-14-C-2-1 with Type 1 geopolymer matrix in a tension-tension fatigue test performed at 300°C.

Results of all tension-tension fatigue tests performed in this work at 300°C are shown in Figure 40 as maximum stress vs. cycles to failure (S-N) curves. Results in Figure 40 show that composite specimen 5-7-C-1 with Type 2 geopolymer matrix produced the best fatigue performance, while composite specimen 3-14-C-1 with Type 1 geopolymer matrix produced the worst fatigue performance. It is also seen that specimens from panel 5-7-C-1 perform better than specimens cut from other panels. Some panels were observed to bulge or swell when under loading as observed in Section 5.6, but this was difficult to observe with the furnace halves being in the way of direct observation.

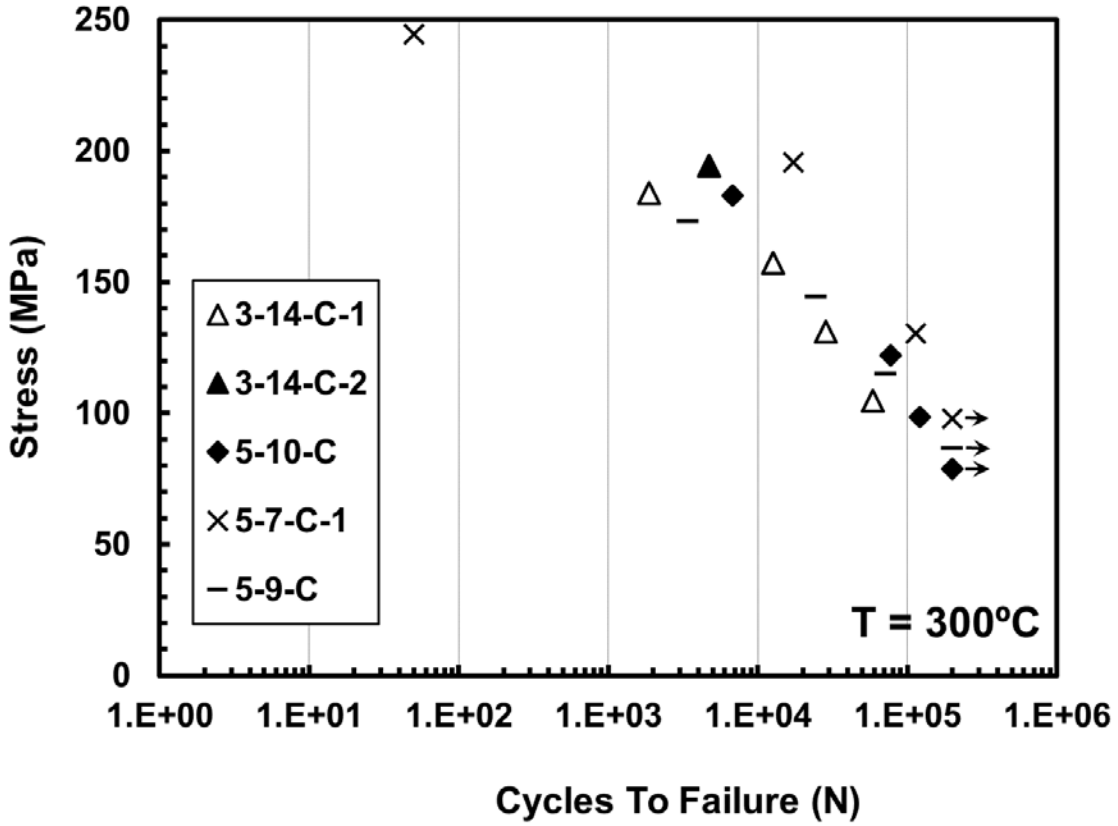

Figure 40. Maximum stress vs. cycles to failure (S-N) curves obtained for geopolymer matrix composites in tension-tension fatigue tests at 300°C.

The maximum stress vs. cycles to failure (S-N) curves obtained for composite specimens with Type 1 geopolymer matrix are also shown in Figure 41. It appears that the higher ply count for panel 5-10-C does help for lower stresses, where there is a noticeable advantage over 3-14-C-1. Runout was not achieved for 3-14-C-1 and 3-14-C-2 at 300°C. Fatigue run-out of 200,000 cycles was achieved for a specimen from composite panel 5-10-C tested with a low maximum stress of 78.7 MPa. The points on the left hand side of the plot represent the 300°C tensile test results.

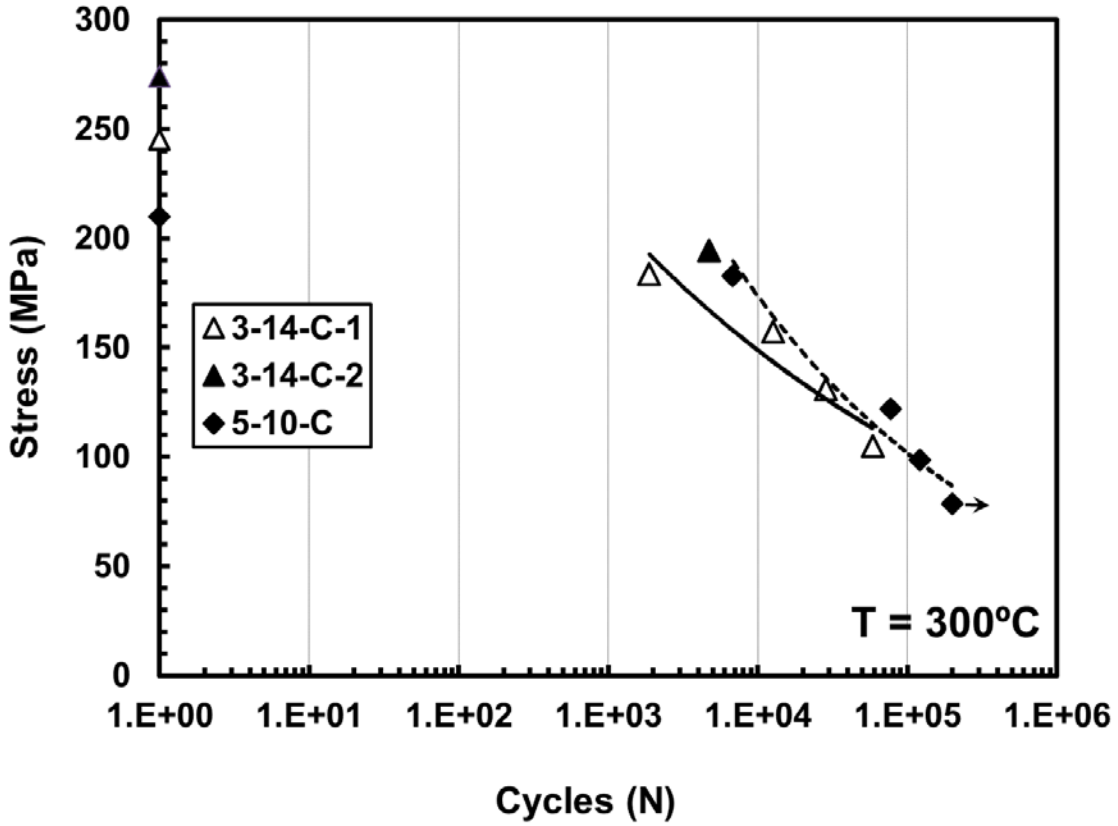

Figure 41. Maximum stress vs. cycles to failure (S-N) curves obtained for composites with Type 1 geopolymer matrix in tension-tension fatigue tests at 300°C. There is no trend line for 3-14-C-2 due to only one data point.

The maximum stress vs. cycles to failure (S-N) curves obtained for composite specimens with Type 2 geopolymer matrix are shown in Figure 42. Results in Figure show clearly that specimens from 5-7-C-1 produced better fatigue performance than those from panel 5-9-C. Fatigue runout was achieved for both composite panels in tests performed with maximum fatigue stresses of 86.6 MPa and 97.8 MPa. Note that these stress levels represent 30% of the room-temperature UTS obtained for a given composite panel. The points on the left hand side of the plot represent the 300°C tensile test results.

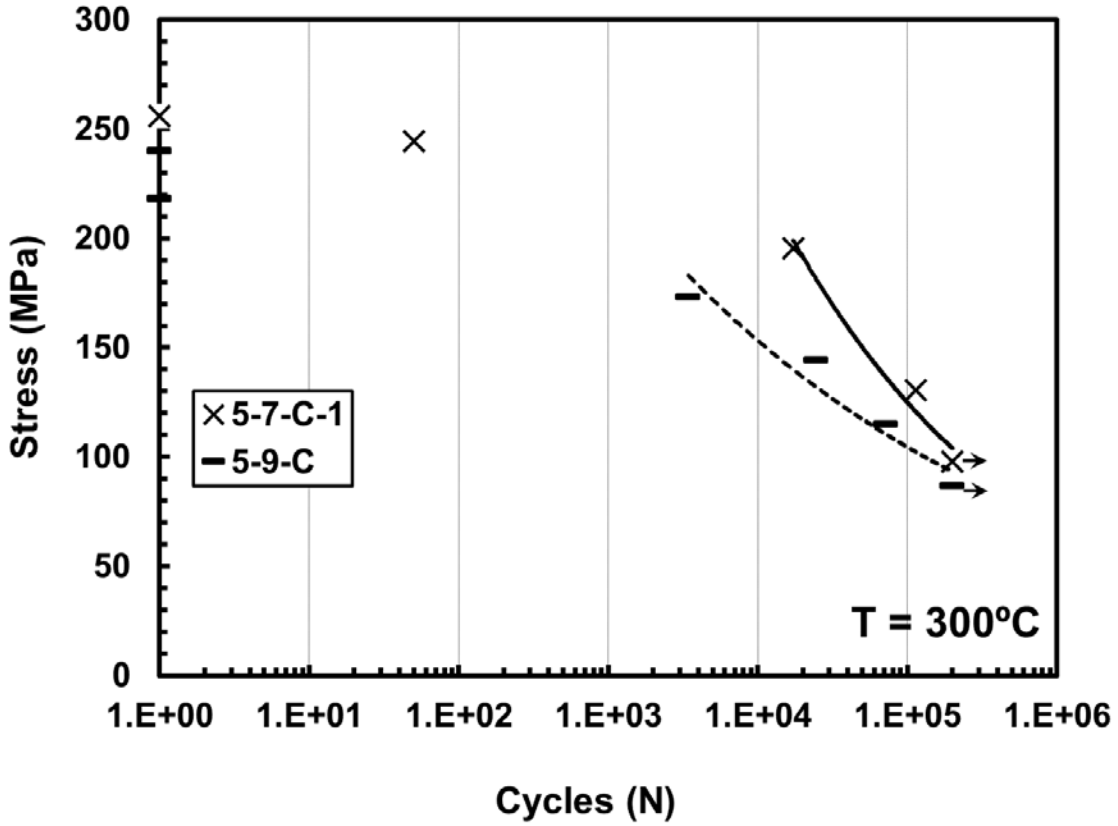

Figure 42. Maximum stress vs. cycles to failure (S-N) curves obtained for composites with Type 2 geopolymer matrix in tension-tension fatigue tests at 300°C. Trend line for 5-7-C-1 does not account for the specimen which failed at 50 cycles.

Figure 43 shows the stress-strain hysteresis loops obtained for specimen 5-7-C-1-1 tested with a high maximum stress of 245 MPa, which corresponds to 75% of the room-temperature UTS for this composite. This specimen survived only 49 cycles, creating audible snaps on the first cycle. The stress-strain hysteresis loops obtained for cycles 2-20 exhibit a typical hysteresis curve shape. The stress-strain hysteresis loop obtained for cycle 49 is considerably wider suggesting impending failure. Indeed, the specimen failed shortly after reaching the peak stress for cycle 50.

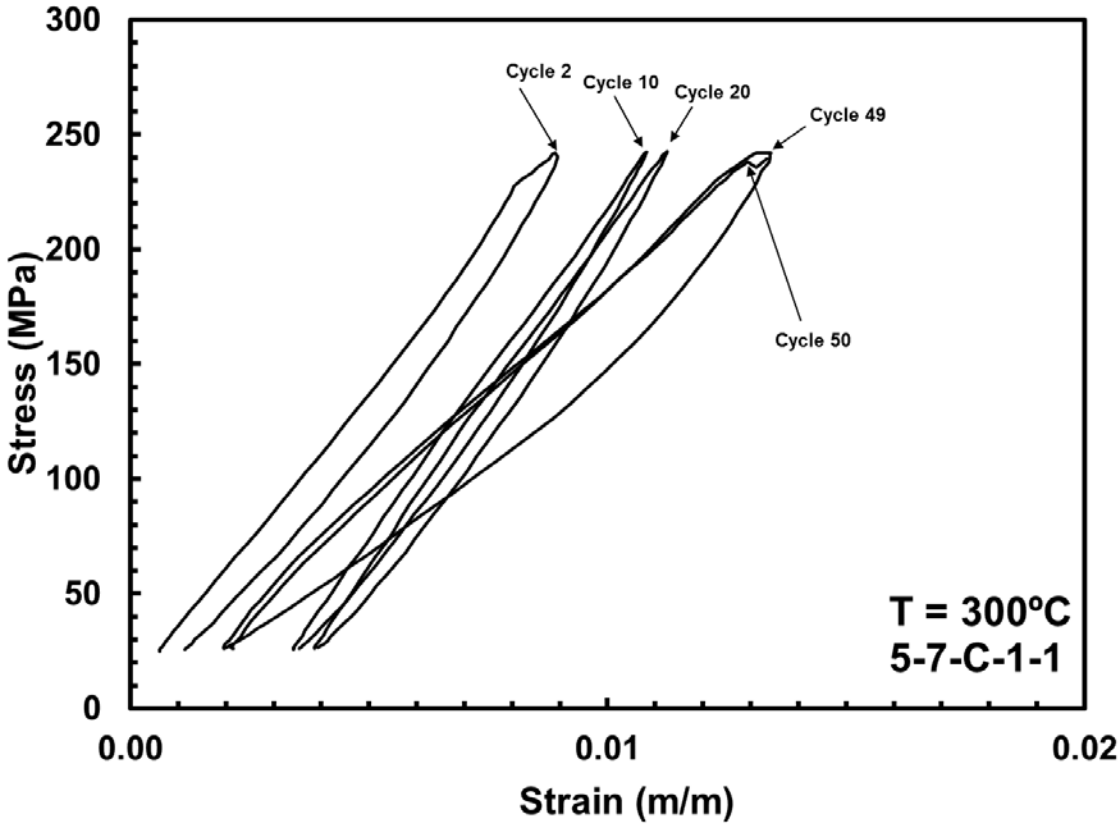

Figure 43. Evolution of stress-strain hysteresis response of composite specimen 5-7-C-1-1 with Type 2 geopolymer matrix in a tension-tension fatigue test performed at 300°C.

Figure 44 shows the stress-strain hysteresis loops obtained for specimen 5-7-C-1-6 tested with a lower maximum stress of 130 MPa, which corresponds to 40% of the room-temperature UTS for this composite. Again, significant damage occurs to the matrix during the first cycle. The stress-strain hysteresis loops produced in subsequent cycles reflect nearly linear behavior throughout the load cycle. This result suggests that once extensive damage occurs to the matrix during the first cycle, the load is transferred to carbon fibers. Afterwards the response of the composite is controlled by the fibers with minimal contribution from the matrix. The results in Figure 44 also indicate that strain

ratcheting takes place. There is a noticeable decrease in in the 100,000 cycles hysteresis loop when compared to the others, where it fails soon after at 114,050 cycles.

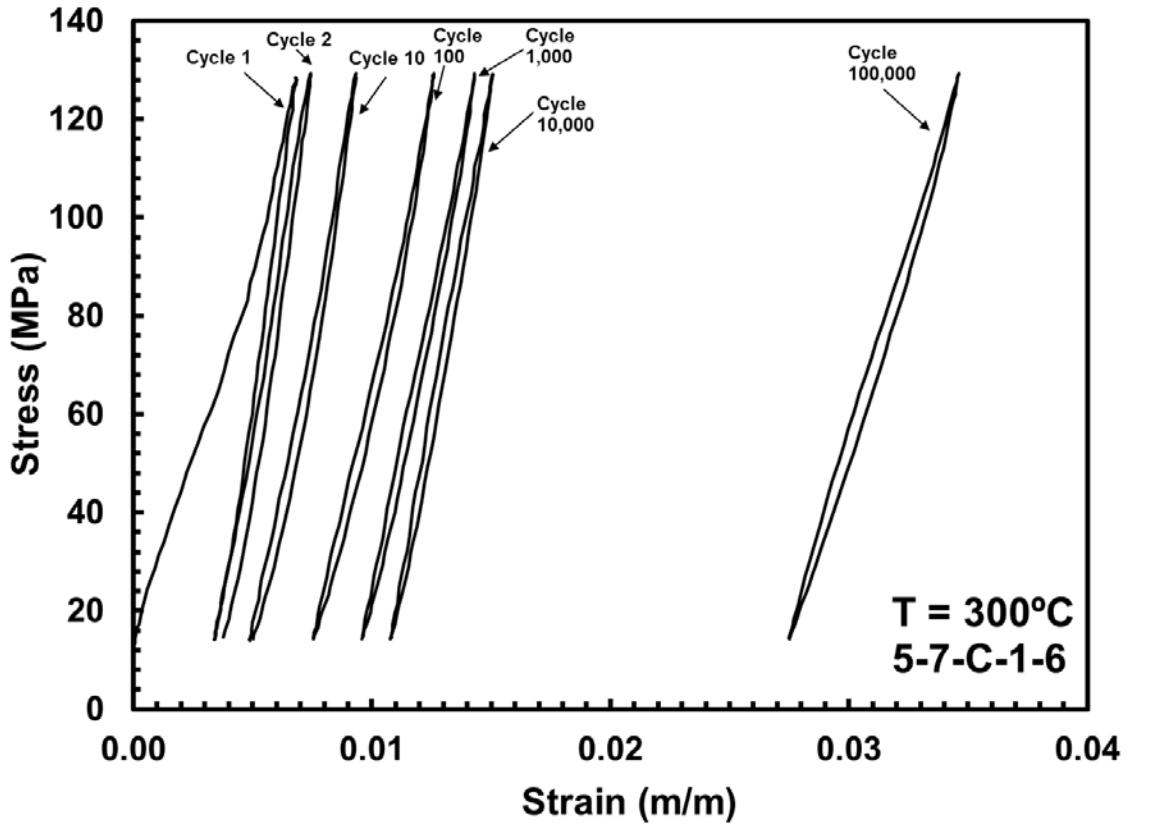

Figure 44. Evolution of stress-strain hysteresis response of composite specimen 5-7-C-1-6 with Type 2 geopolymer matrix in a tension-tension fatigue test performed at 300°C.

Figure 45 shows the hysteresis evolution of specimen 5-7-C-1-2, which achieved runout. Strain ratcheting is clearly observed as seen in other specimens. There is no significant loss of stiffness when the fatigue testing is stopped at 200,000 cycles, but there is a clear evolution towards less hysteresis. This evolution could be due to finer and finer matrix damage allowing the carbon fibers to become straighter under load.

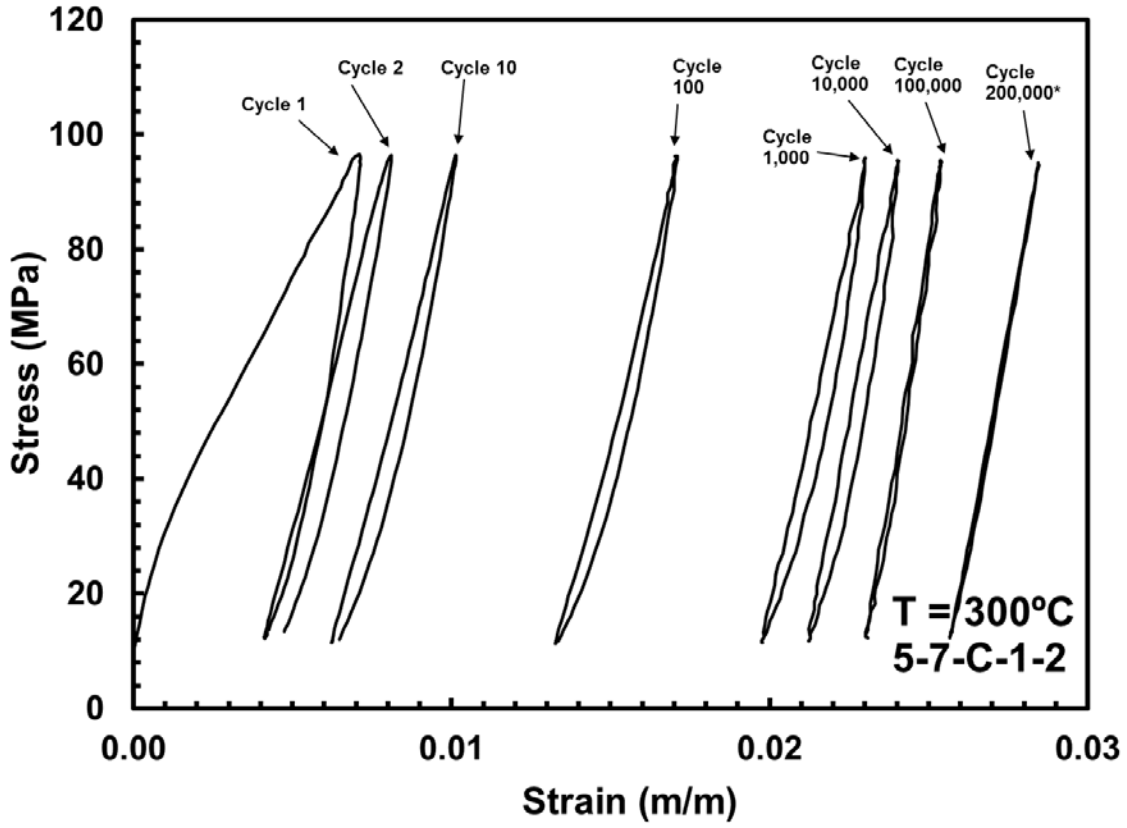

Figure 45. Evolution of stress-strain hysteresis response of composite specimen 5-7-C-1-2 with Type 2 geopolymer matrix in a tension-tension fatigue test performed at 300°C. Cycle 200,000 with the asterisk is arbitrarily shifted right due to extensometer slipping.

The experimental results presented here indicate that in all fatigue tests performed at 300°C, significant damage occurs to the geopolymer matrix during the first load cycle. Afterwards the load is transferred to fibers, which are the dominant factor in the fatigue performance of the composite. To better understand the contribution of the carbon fibers to the fatigue performance, we analyze the fatigue data obtained in this work using a loading metric, N_{x_max}, which represents the maximum load per unit length carried by a carbon fabric ply. We also assume that the geopolymer matrix is degraded and is no longer carrying load. The quantity N_{x_max} is defined by Equation 1.

$$N_{x\_\max} = \frac{\sigma_{\max} t}{n} \quad (1)$$

Where N_{x_max} is the maximum load per unit length per ply, σ_{max} is the maximum stress in a fatigue load cycle, t is the composite specimen thickness, and n is the number of composite plies. The fatigue data obtained at 300°C are plotted as N_{x_max} vs. cycles to failure in Figure 46.

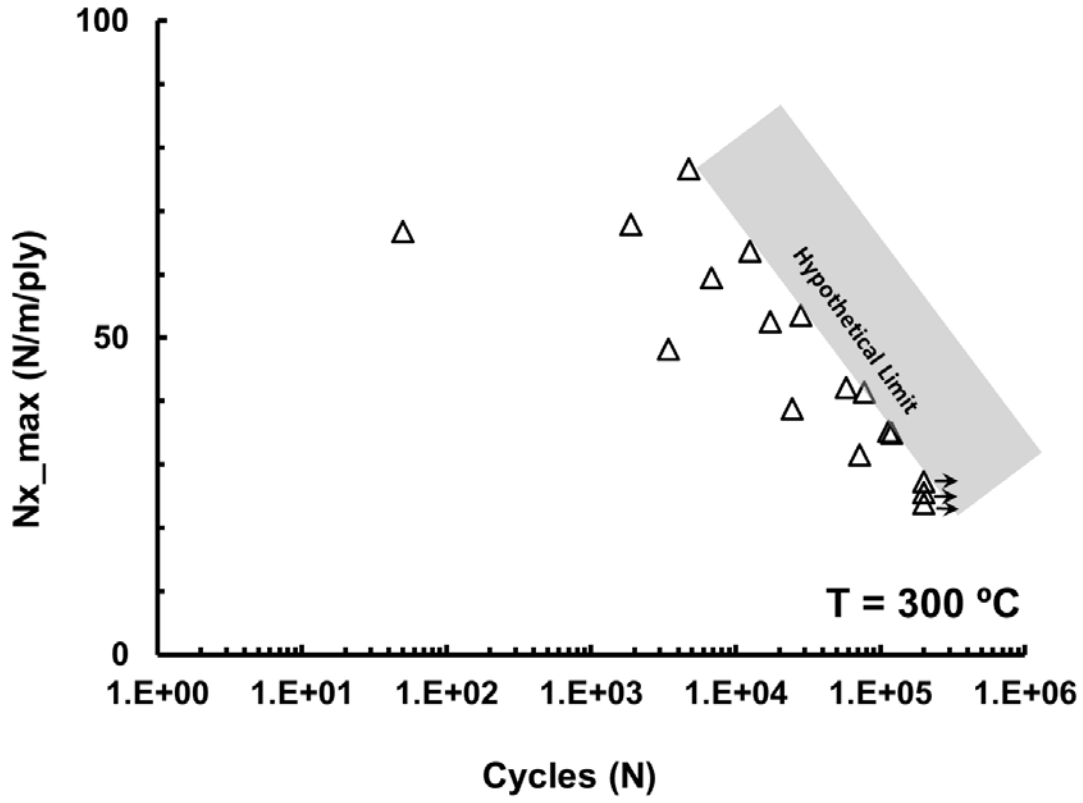

Figure 46. Maximum load per unit length per ply vs. cycles to failure obtained at 300°C.

The limited data appears to indicate a “hypothetical limit” of sorts, at least with the current quality and processing of the material. Plotting this normalized value versus cycles to failure is a piece of evidence that confirms the carbon fiber dominance in the

behavior of the composite in tension-tension fatigue, with the matrix playing the role of just being “good” enough to hold the fibers up to the limit. Earlier versions of this plot were used during the experiment planning to predict the maximum cycles a specimen was expected to endure, with reasonable success.

Specimens which achieved fatigue run-out of 200,000 cycles were tested in tension to failure at 300°C to determine the retained tensile properties. Evaluation of retained properties is useful in assessing the damage state of the composite subjected to prior fatigue loading. Full retention of tensile strength would suggest that no fatigue damage occurred to the fibers. However, evidence of damage to the fibers is present as the tensile strength of these run-out specimens was degraded, as seen in Table 9. The tensile stress-strain curves obtained for the pre-fatigued specimens with Type 1 and Type 2 geopolymer matrices are shown in Figure 47. The results clearly show the specimen from 5-7-C-1 to have the best performance. An example of a failed specimen is seen in Figure 48.

Table 9. Retained properties of the geopolymer-matrix composite specimens subjected to prior fatigue in laboratory air at 300°C.

Panel	Geopolymer Matrix Type	Fatigue Stress (MPa)	Retained Strength (Mpa)	Strength Retention (%)
5-10-C-5	1b (NaGP)	78.7	130.5	62.2
5-7-C-1-2	2 (KGP)	97.8	191.4	74.8
5-9-C-6	2 (KGP)	86.6	125.7	54.9

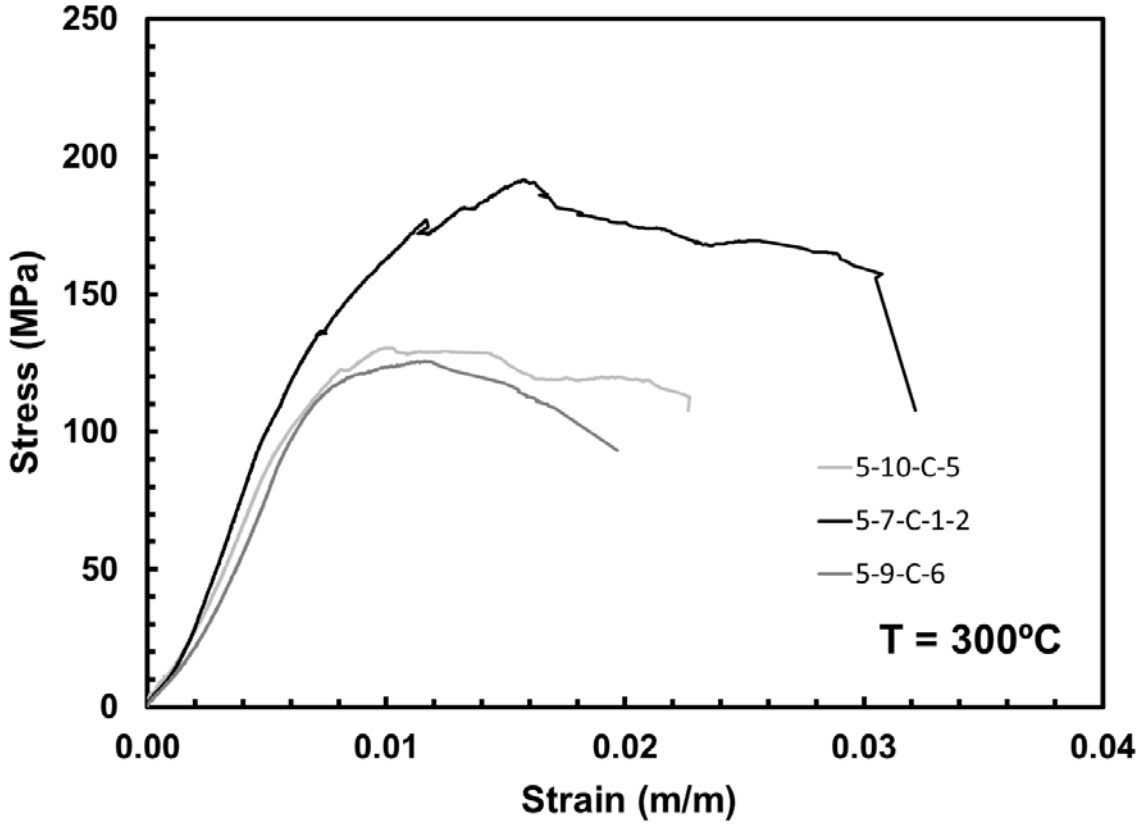

Figure 47. Tensile stress-strain curve obtained at 300°C for composite specimens achieving runout condition of 200,000 cycles at 300°C.

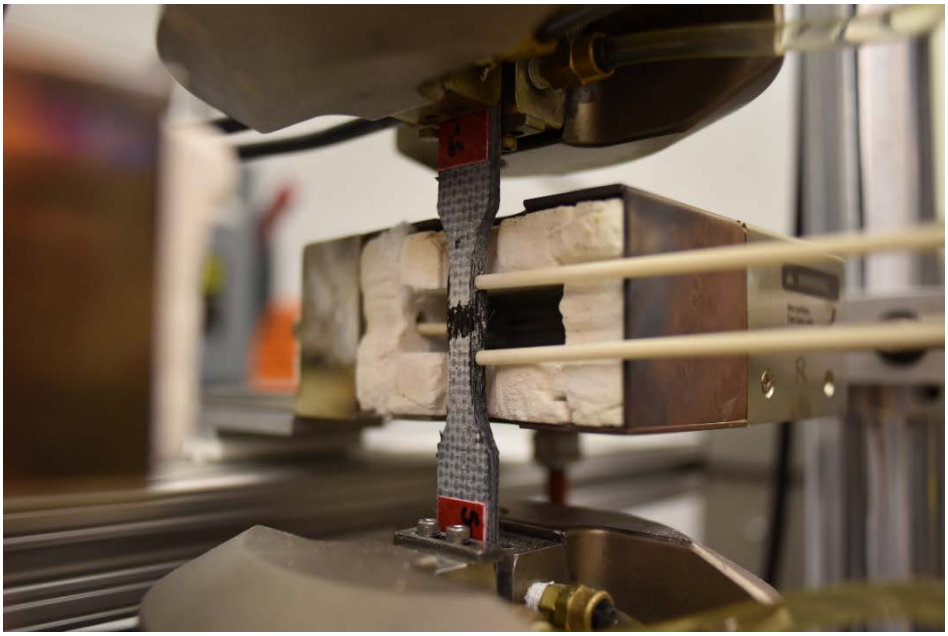

Figure 48. Failed fatigue runout specimen from tension testing.

R values for the fatigue testing remained around 0.11 on average instead of the target 0.10. Due to a short number of specimens, a specimen was not used to tune the MTS controller, but the results were found acceptable to continue testing. The difference of R between 0.10 and 0.11 is small enough to not make a large difference in cyclic testing, especially in these exploratory tests.

VI. Conclusions and Recommendations

Tension-tension fatigue of geopolymer matrix composites was studied in this work. Tensile stress-strain behavior was also examined and tensile properties were measured at 23 and 300°C. Several variants of the composite material were studied.

The experimental results revealed significant differences in mechanical properties from panel-to-panel, and significant variability between the specimen-to-specimen within a panel. Room temperature tests showed promising performance with conventional composite behavior. Tests at 300°C revealed that thermal exposure under zero load caused considerable damage to the geopolymer matrix. As a result, for many specimens the mechanical response of the composite in the 300°C tests was dominated by carbon fibers with minimal contribution from the geopolymer matrix once it is damaged.

It appears that processing of the composite panels was not carefully controlled. Due to small amount of test material and large scatter of experimental data obtained for each composite panel, it is difficult to form definitive conclusions regarding the mechanical properties and behavior of the composite variants examined in this work. However, we note that the composite panel 5-7-C-1 with Type 2 geopolymer matrix appears to offer a high modulus, the second highest UTS at 300°C, and the best fatigue performance at 300°C. The geopolymer chemistry and the processing method used to fabricate the composite panel 5-7-C-1 may serve as the best foundation for further development of this material system.

Both Type 1 and Type 2 geopolymer matrix materials experienced considerable damage during thermal exposure under zero load. This result does not bode well for a matrix material to be used in a high-temperature composite. Further improvement to

chemistry and processing of both Type 1 and Type 2 geopolymer matrix materials should be explored. Additionally, examination of the test materials under an optical microscope revealed poor infiltration of the matrix into the composite. Improving matrix distribution throughout the composite may improve composite machinability as well as composite properties. From the modulus results, to duplicate the high stiffness seen in some of the panels, a ply thickness of 0.3 mm or less should be used when fabricating the material. It is possible that heat treating the composite panels at 40-100°C may cause the dehydration of the geopolymer to occur in a slow and controlled manner, resulting in less mass loss and matrix cracking during subsequent mechanical loading at elevated temperature.

Appendix

PANEL 3-14-C-1		
Specimen	Average Area (m^2)	Average Area RT E (GPa)
1	3.38906E-05	25.4
2	3.29582E-05	25.7
3	3.42624E-05	26.8
4	3.42737E-05	22.2
5	3.41232E-05	24.3
6	3.05312E-05	22.9
	AVERAGE	24.5
	ST DEV	1.6
	COVARIANCE	6.5
PANEL 3-14-C-2		
Specimen	Average Area (m^2)	Average Area RT E (GPa)
1	3.30129E-05	23.5
2	2.88283E-05	27.2
3	2.93887E-05	27.1
4	0.00002958	28.7
5	2.95571E-05	25.8
6	2.89306E-05	24.8
	AVERAGE	26.2
	ST DEV	1.7
	COVARIANCE	6.5
PANEL 3-20-C		
Specimen	Average Area (m^2)	Average Area RT E (GPa)
1	2.55258E-05	33.0
2	2.67058E-05	38.5
3	2.65289E-05	39.4
4	2.64905E-05	39.1
	AVERAGE	37.5
	ST DEV	2.6
	COVARIANCE	6.9
PANEL 5-10-C		
Specimen	Average Area (m^2)	Average Area RT E (GPa)
1		-
2	3.64299E-05	41.3
3	3.75226E-05	42.1
4	3.64167E-05	38.0
5	3.69754E-05	39.9
6	3.81213E-05	40.6
7	3.47972E-05	39.1
	AVERAGE	40.2
	ST DEV	1.4
	COVARIANCE	3.4

Figure 49. Modulus results for Type 1 geopolymer matrix specimens.

PANEL 5-7-C-1		
Specimen	Average Area	Average Area RT E (GPa)
1	3.02417E-05	48.4
2	2.88979E-05	48.4
3	3.0381E-05	44.2
4	2.91967E-05	47.4
5	2.94042E-05	48.1
6	2.93699E-05	48.5
	AVERAGE	47.5
	ST DEV	1.5
	COVARIANCE	3.2
PANEL 5-7-C-2		
Specimen	Average Area	Average Area RT E (GPa)
1	3.19932E-05	44.3
2	3.29539E-05	38.4
3	3.20367E-05	40.0
4	3.22557E-05	39.1
5	3.22467E-05	42.9
6	3.31637E-05	37.7
	AVERAGE	40.4
	ST DEV	2.4
	COVARIANCE	5.9
PANEL 5-9-C		
Specimen	Average Area (m^2)	Average Area RT E (GPa)
1	2.91452E-05	-
2	2.87029E-05	41.9
3	2.86139E-05	45.6
4	2.98355E-05	44.7
5	2.95522E-05	42.9
6	2.92347E-05	40.3
7	2.9197E-05	43.2
8	2.888E-05	39.8
	AVERAGE	42.6
	ST DEV	2.0
	COVARIANCE	4.6

Figure 50. Modulus results for Type 2 geopolymer matrix specimens (continued next page).

PANEL 12-3-C		
Specimen	Average Area (m^2)	Average Area RT E (GPa)
1	3.04055E-05	46.2
2	3.15112E-05	29.4
3	3.30446E-05	34.2
4	3.47799E-05	35.1
5	3.23536E-05	32.0
6	3.27816E-05	32.6
	AVERAGE	34.9
	ST DEV	5.4
	COVARIANCE	15.32093734
PANEL 12-5-C		
Specimen	Average Area (m^2)	Average Area RT E (GPa)
1	3.5E-05	37.9
2	0.000037668	29.9
3	3.46428E-05	37.9
4	3.75109E-05	18.6
5	3.22072E-05	42.5
6	3.74571E-05	31.3
7	3.74621E-05	33.0
	AVERAGE	33.0
	ST DEV	7.2
	COVARIANCE	21.7
PANEL 13-1-C		
Specimen	Average Area (m^2)	Average Area RT E (GPa)
1	3.79886E-05	29.5
2	3.24925E-05	36.0
3	0.000037926	29.4
4	3.76391E-05	27.9
5	3.66058E-05	28.9
6	3.71943E-05	26.9
7	4.44792E-05	28.5
	AVERAGE	29.6
	ST DEV	2.7
	COVARIANCE	9.252253134

Figure 51. Modulus results for Type 2 geopolymer matrix specimens (continued).

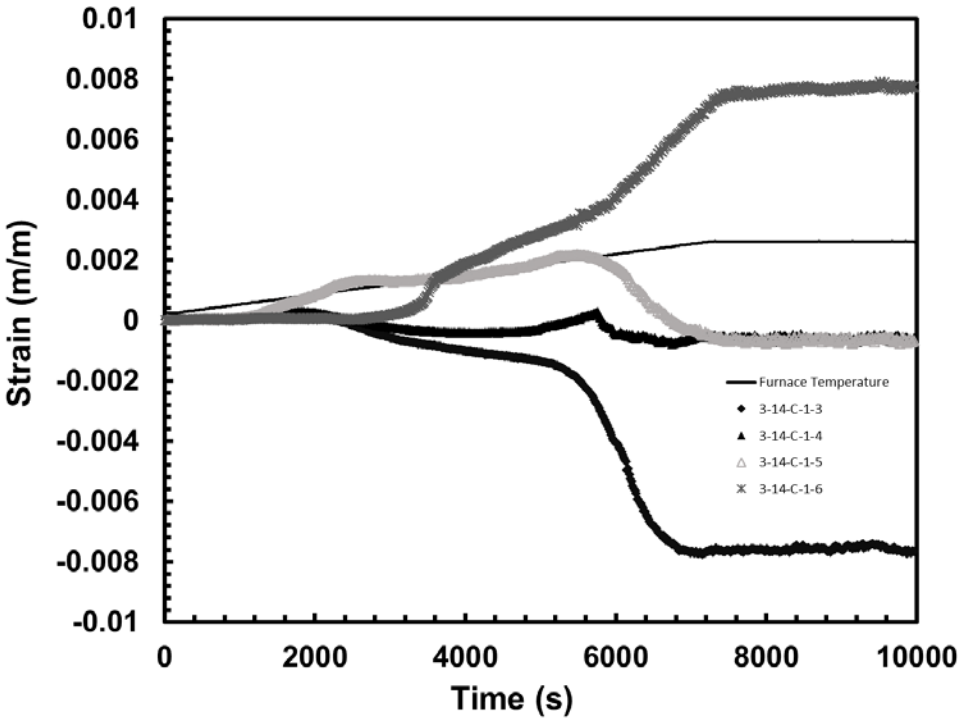

Figure 52. Initial exposure of 3-14-C-1 specimens.

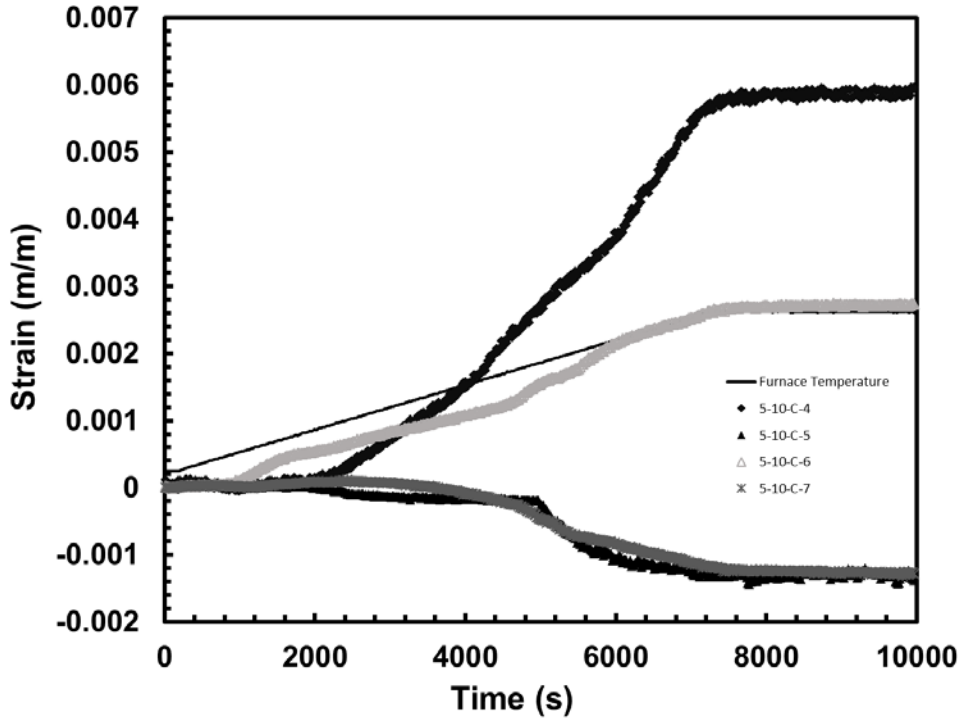

Figure 53. Initial thermal exposure of 5-10-C fatigue specimens.

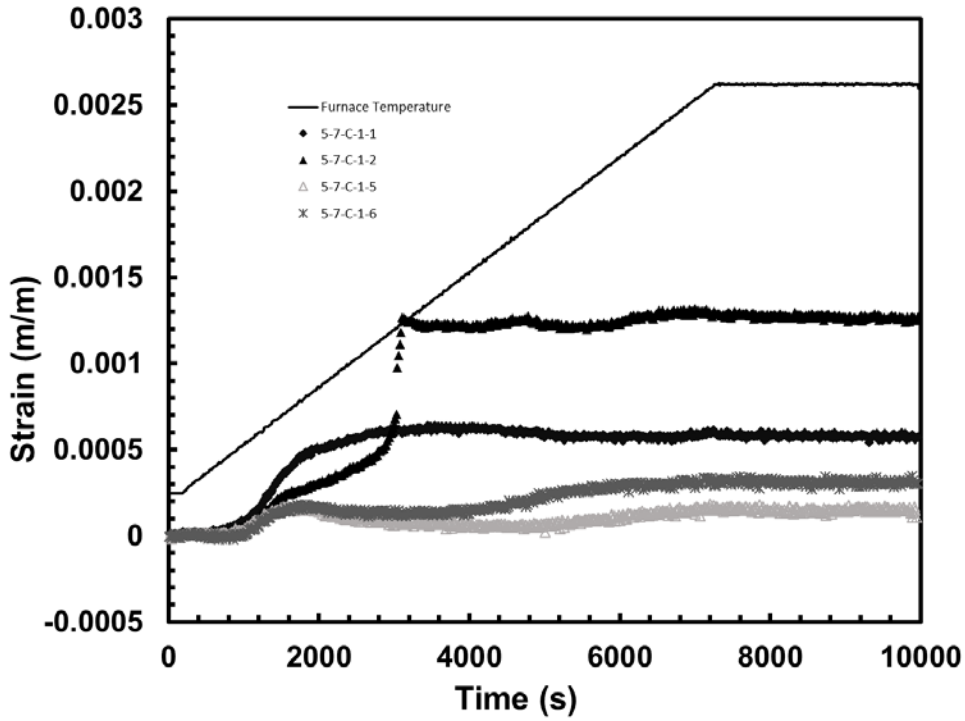

Figure 54. Initial thermal exposure of 5-7-C-1 fatigue specimens.

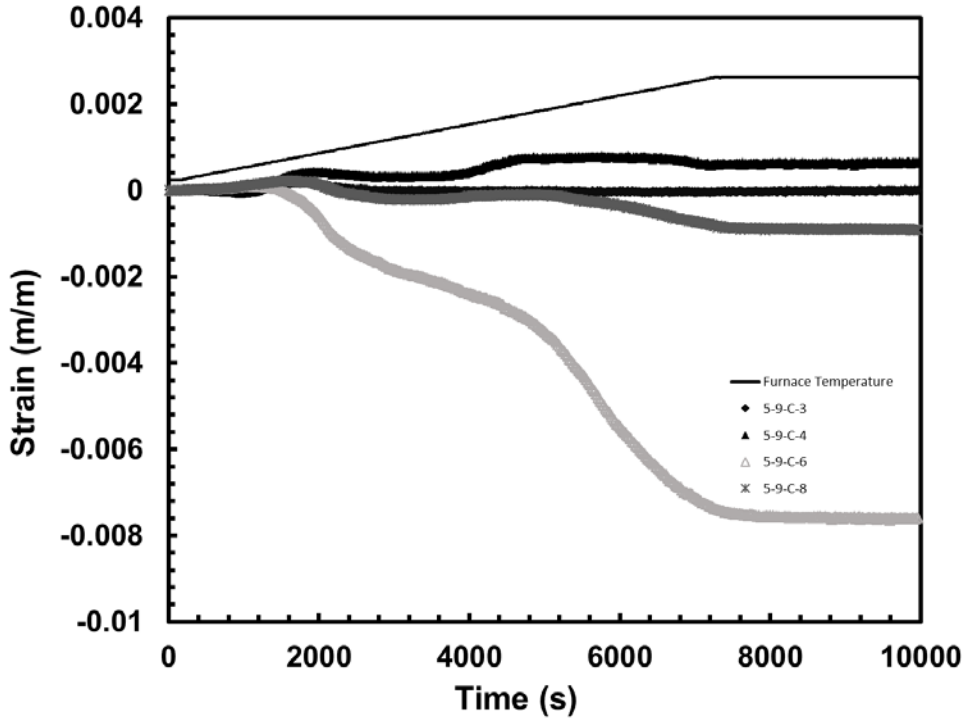

Figure 55. Initial thermal exposure of 5-9-C fatigue specimens.

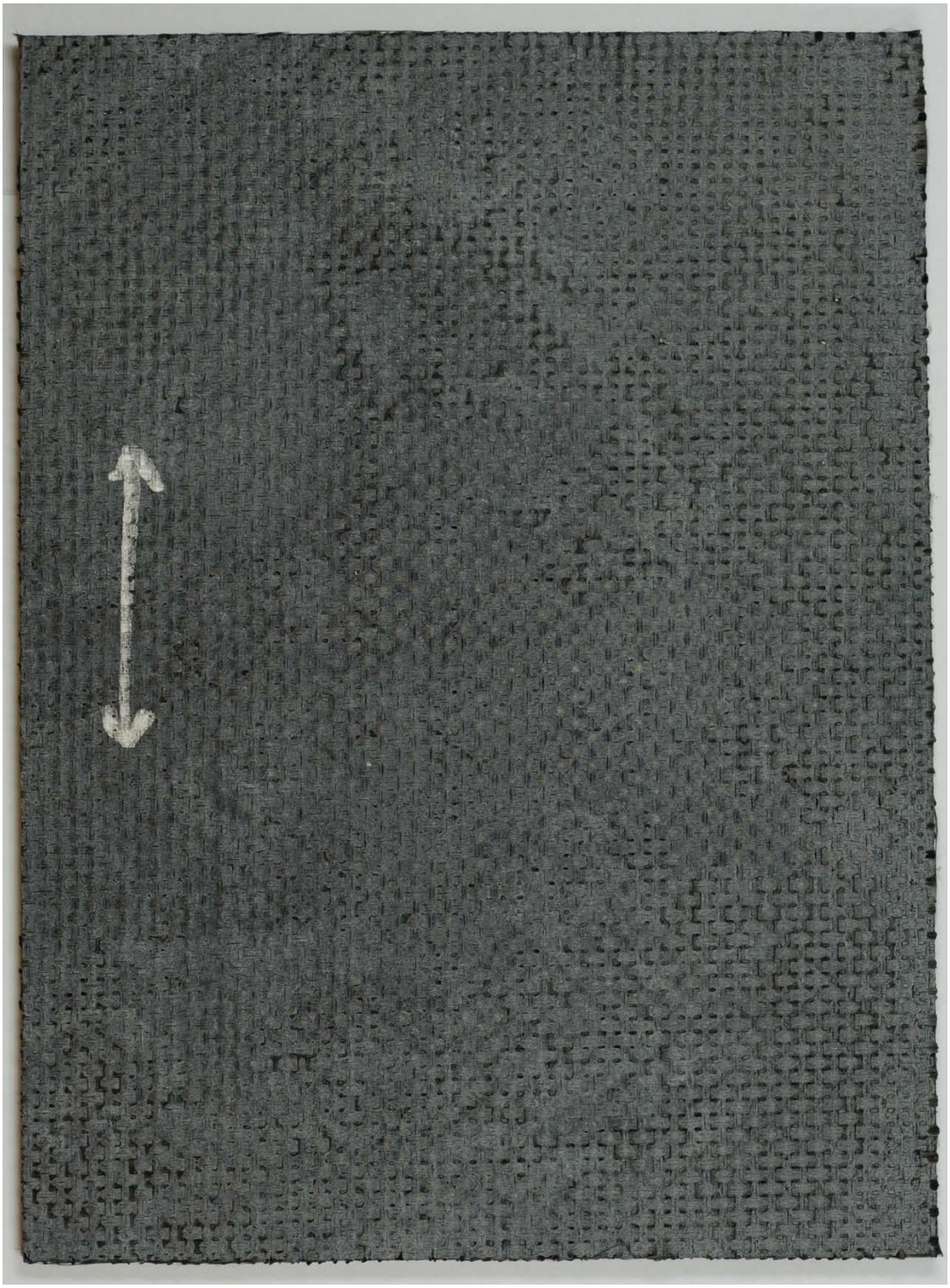

Figure 56. "Front" side of panel 5-7-C-1.

Figure 57. "Back" side of panel 5-7-C-1.

Bibliography

[1] Ahci, E. and R. Talreja. “Characterization of viscoelasticity and damage in high temperature polymer matrix composites.” *Composites Science and Technology*, 66: 2506-2519 (3 April 2006).

[2] Odegard G. and M. Kumosa. “Elastic-plastic and failure properties of a unidirectional carbon/PMR-15 composite at room and elevated temperatures.” *Composites Science and Technology*, 60: 2979-2988 (2000).

[3] Gentz, M., D. Armentrout, P. Rupnowski, L. Kumosa, E. Shin, J.K. Sutter and M. Kumosa. “In-plane shear testing of medium and high modulus woven graphite fiber reinforced/polyimide composites.” *Composites Science and Technology*, 664: 203-220 (2004).

[4] Xu, Y., Peeyush Bhargava and Alan Zehnder. “Time and temperature dependent mechanical behavior of HFPE-II-52 polyimide at high temperature.” *Mechanics of Materials*, 100: 86-95 (2016).

[5] Davidovits, Joseph. *Geopolymer Chemistry and Applications.* France: Institut Géopolymère, 2015.

[6] Lyon, Richard. *Fire response of geopolymer structural composites.* DOT/FAA/AR-TN95/22. Atlantic City International Airport NJ: FAA Technical Center, January 1996.

[7] Musil, Sean S., Greg Kutyla and W. M. Kriven. “The Effect of Basalt Chopped Fiber Reinforcement on the Mechanical Properties of Potassium Based Geopolymer,” Urbana IL: Department of Material Science and Engineering, University of Illinois at Urbana-Champaign (2012).

[8] Meng, Weina and Kamal H. Khayat. “Mechanical properties of ultra-high-performance concrete enhanced with graphite nanoplatelets and carbon nanofibers,” *Composites Part B*, 107: 113-122 (2016).

[9] Lorenza C, Manzi S. and Maria Chiara Bignozzi. “Superplasticizer Addition to Carbon Fly Ash Geopolymers Activated at Room Temperature.” *Materials*, 9: 586 (18 July 2016).

[10] Antoni, Wijaya S.W., Satira J. Sugiarto A. and D. Hardjito. “The use of borax in deterring flash setting of high calcium fly ash based geopolymer.” *Materials Science Forum*, 857: 416-420 (2016).

[11] Gadow, R. and P. Weichand. “Novel Intermediate Temperature Ceramic Composites, Materials and Processing for Siloxane Based Basalt Fiber Composites,” *Key Engineering Materials 2014*, 611-612: 382-390 (2015).

[12] Wilkinson, Michael P. *Mechanical Properties and Fatigue Behavior of Unitized Composite Airframe Structures at Elevated Temperature.* MS thesis, AFIT-ENY-14-M-51. School of Engineering and Management, Air Force Institute of Technology (AU), Wright-Patterson AFB OH, March 2014 (AD-A610904).

[13] Michael, Lee. *Fatigue Behavior of an Advanced SiC/SiC Composite in Air and Steam.* MS thesis, AFIT-ENY-MS-16-M-223. School of Engineering and Management, Air Force Institute of Technology (AU), Wright-Patterson AFB OH, March 2016.

[14] Boucher, Nicholas. *Fatigue Behavior of an Advanced Melt-Infiltrated SiC/SiC composite at 1200°C in Air and in Steam.* MS thesis, AFIT-ENY-MS-17-M-242. School of Engineering and Management, Air Force Institute of Technology (AU), Wright-Patterson AFB OH, March 2017.

[15] Schmidt, S., S. Beyer, H. Knabe, H. Immich, R. Meistring and A. Gessler. “Advanced Ceramic Matrix Composite Materials for Current and Future Propulsion Technology Applications.” Acta Astronautica, 55:409 – 420 (2004).

[16] Musil, Sean S. *Novel High-Temperature Inorganic Composites Using Porous Alkali Activated Aluminosilicate Binders.* Ph.D. dissertation. University of Illinois at Urbana-Champaign, Urbana IL, 2014.

[17] Lukey, G.C., J.S.J. van Deventer, J.L. Provis and P. Duxson. *Design of geopolymeric materials based on nanostructural characterization and modeling.* AOARD-054025. The US Research Laboratory. 2006.

[18] Barbosa, Valeria F.F., K.J.D. MacKenzie and Cleilio Thaumaturgo. “Synthesis and characterization of materials based on inorganic polymers of alumina and silica: sodium polysialate polymers.” International Journal of Inorganic Materials, 2:309 – 317 (2000).

[19] Papakonstantinou, Christos G. and Perumalsamy N. Balaguru. “Fatigue Behavior of high Temperature Inorganic Matrix Composites.” *Journal of Materials in Civil Engineering*, 19: 321-328 (2007).

[20] Lyon R.E., Foden A.J., Balagurur P.N., Davidovits J. and Davidovics M. “Fire Resistant Aluminosilicate Composites.” *Fire and Materials*, 21: 67-73 (1997).

REPORT DOCUMENTATION PAGE

Form Approved
OMB No. 0704-0188

PLEASE DO NOT RETURN YOUR FORM TO THE ABOVE ADDRESS.

1. REPORT DATE *(DD-MM-YYYY)*	2. REPORT TYPE	3. DATES COVERED *(From - To)*
23-03-2018	Master's Thesis	Sept 2016 - Mar 2018

4. TITLE AND SUBTITLE

Tensile Properties and Fatigue Behavior of Geopolymer Matrix Composites with Carbon Fiber Reinforcement at Elevated Temperature

5a. CONTRACT NUMBER

5b. GRANT NUMBER

5c. PROGRAM ELEMENT NUMBER

6. AUTHOR(S)

Wilcox, Steffan M.L., Capt

5d. PROJECT NUMBER

5e. TASK NUMBER

5f. WORK UNIT NUMBER

7. PERFORMING ORGANIZATION NAME(S) AND ADDRESS(ES)

Air Force Institute of Technology
Graduate School of Engineering and Management (AFIT/EN)
2950 Hobson Way
Wright-Patterson AFB OH 45433-7765

8. PERFORMING ORGANIZATION REPORT NUMBER

AFIT-ENY-MS-18-M-304

9. SPONSORING/MONITORING AGENCY NAME(S) AND ADDRESS(ES)

Air Force Research Laboratory Aerospace Systems Directorate
Mr. Michael Falugi
Bldg 65
2790 D Street
Wright-Patterson AFB OH 45433

10. SPONSOR/MONITOR'S ACRONYM(S)

AFRL/RQVS

11. SPONSOR/MONITOR'S REPORT NUMBER(S)

12. DISTRIBUTION/AVAILABILITY STATEMENT

Distribution Statement A.
Approved for Public Release; Distribution Unlimited.

13. SUPPLEMENTARY NOTES

This material is declared a work of the U.S. Government and is not subject to copyright protection in the United States.

14. ABSTRACT

The tensile stress-strain and tension-tension fatigue behavior of geopolymer matrix composites reinforced with 0/90 carbon fibers was investigated at 23 and 300°C in laboratory air. The relative ease of synthesis and low processing temperatures, along with fire resistance make geopolymers an attractive choice as a matrix material for composite materials for use at elevated temperature. Currently, geopolymer matrix composites are being considered as possible replacements for ceramic matrix composites and high-temperature polymer matrix composites. In this work composites with two different types of geopolymer matrix were evaluated: (1) composite with a sodium-based geopolymer matrix (NaGP) and (2) composite with a potassium-based geopolymer matrix (KGP). Experimental results revealed a degrading effect of elevated temperature on tensile stress-strain behavior and tensile properties. Fatigue run-out was set to 2x105 cycles., with fatigue run-out only achieved at a low maximum stress of 30% UTS. Test specimens were examined before and after testing using an optical microscope, revealing profuse cracking of the geopolymer matrix occurred early in all tests. As a result further mechanical response of the composite was governed by the carbon fibers. The best mechanical performance was obtained from a panel of the KGP-matrix composite.

15. SUBJECT TERMS

geopolymer, tensile, fatigue, 300°C, geopolymer matrix composite, inorganic matrix composite

16. SECURITY CLASSIFICATION OF:			17. LIMITATION OF ABSTRACT	18. NUMBER OF PAGES	19a. NAME OF RESPONSIBLE PERSON
a. REPORT	b. ABSTRACT	c. THIS PAGE			Dr. Marina Ruggles-Wrenn, AFIT/ENY
U	U	U	UU	99	19b. TELEPHONE NUMBER *(Include area code)* (937) 255-3636 ext.4641, marina.ruggles-wrenn@us.af.mil

Reset

Standard Form 298 (Rev. 8/98)
Prescribed by ANSI Std. Z39.18